University of Nevada, Reno

Modeling water temperature dynamics at Shasta Lake, California under the drought conditions of 2015

A thesis submitted in partial fulfillment of the requirements for the degree of Master of Science in Hydrogeology

by
Rachel Melissa Hallnan
Dr. Laurel Saito/Thesis Advisor
Dr. Scott Tyler/Thesis Co-Advisor

August 2017

THE GRADUATE SCHOOL

We recommend that the thesis
prepared under our supervision by

RACHEL HALLNAN

Entitled

Modeling water temperature dynamics at Shasta Lake, California under the drought conditions of 2015

be accepted in partial fulfillment of the
requirements for the degree of

MASTER OF SCIENCE

Laurel Saito, Advisor

Scott Tyler (Co-Advisor) , Committee Member

Eric Danner, Committee Member

Mark Hausner, Graduate School Representative

David W. Zeh, Ph. D., Dean, Graduate School

August, 2017

Abstract

Reservoir managers at Shasta Dam in northern California are mandated to provide cold discharge temperatures for endangered Chinook salmon in the downstream Sacramento River. Hydrodynamic modeling of reservoir temperatures has been used to assess reservoir operations at Shasta Reservoir in the past, and can provide insight into reservoir conditions expected in the future. In this study, a CE-QUAL-W2 model of Shasta Reservoir is used to model reservoir temperature conditions under two projected climate change emissions scenarios, and to examine possible reservoir operations that may improve conditions in drought years. The record high air temperature year of 2015 was used as a baseline for simulations. Findings suggest that reservoir water temperatures will be higher under climate change, and that the duration of stratification will increase. Simulated reservoir operations aimed at providing cold discharge temperatures in the drought conditions of 2015 indicate that only extreme reductions in reservoir discharge during springtime resulted in substantial improvements to conditions during the fall of 2015. However, low resolution along the depth profile of the reservoir results in uncertainty in estimates of cold pool volume in the reservoir, a key metric used by reservoir managers in their decision making. High-resolution distributed temperature sensing data collected in 2015/2016 were used to evaluate the ability of increased bathymetric resolution of CE-QUAL-W2 to simulate 2015/2016 temperature conditions in the reservoir. The updated model resolution provided a better estimate of the amount of cold water in the reservoir throughout the year, and can be used in the future to inform decision making at Shasta Dam focused on sustaining Chinook salmon populations.

Table of Contents

List of Tables

List of Figures

Chapter 1: General Introduction

Project Background

The widespread construction of dams across the United States has resulted in changes in river habitats (Collier et al. 1996, Graf 2006). For example, construction of dams along California's Sacramento River blocked access to spawning habitat for native Chinook salmon, resulting in population declines (Yates et al. 2008) that led to listing of winter-run Chinook salmon in the Sacramento River as endangered under the Endangered Species Act in 1993 (NMFS 2011). Dam operations such as altered release schedules and selective withdrawals can be used to improve downstream flow regimes and water quality for aquatic communities including anadromous fish, improving fish populations (Collier et al. 1996, Poff et al. 1997, Bartholow et al. 2001, Sapin et al. 2017, Mateus and Tullos 2017). For example, Shasta Dam on the Sacramento River has a temperature control device (TCD) that allows for selective withdrawals while still generating power through penstock discharges to enable dam managers to control discharge temperatures to help downstream Chinook salmon populations (Hanna et al. 1999, Bartholow et al. 2001).

Salmon populations face additional stress associated with climate change, such as increased drought frequency and reduction of summer tributary flows, which threaten to further increase river and reservoir temperatures throughout California (Brekke et al. 2009). Climate models predict that low and mid-latitude areas such as northern California may experience increased drying associated with higher greenhouse gas concentrations, and thus more frequent and intense droughts (AghaKouchak et al. 2014). Elevated air temperatures associated with global warming will likely increase the rate of drying experienced during droughts, causing droughts to form more quickly and at a greater intensity (Trenberth et al. 2014).

Reservoir operations will likely play a key role in sustaining fish populations during drought and climate change conditions. However, uncertainty remains regarding the most effective operations scenarios during such conditions. Previous work has shown that droughts that last multiple years decrease the TCD's ability to meet downstream temperature thresholds set for Chinook salmon while still maintaining a cold pool of water in Shasta Reservoir (Sapin et al. 2017). Recent drought in California between 2012 and 2015 provides an example of reservoir conditions after multiple drought years, and of what future reservoir conditions might look like if climate change does induce more frequent and intense droughts. The lowest water year precipitation totals over the observational climate occurred during this time, and 2015 was the warmest year on global record (Griffin and Anchukaitis 2014, Joyce 2016).

Hydrodynamic modeling is useful for examining possible reservoir operations focused on maintaining downstream salmon habitat and cold pool reservoir storage (Sapin et al. 2017). The drought year of 2015 provides a valuable dataset for hydrodynamic modeling of reservoir temperatures that represents reservoir conditions after multiple years of drought, and may be representative of conditions expected in the future. However, low resolution modeling may not be adequate to capture a complete picture of likely changes associated with climate change (Sapin et al. 2017). This may result in more uncertainty in assessment of reservoir conditions such as cold-pool storage and duration of stratification.

Methods Development

This project combines previously developed hydrodynamic modeling methods with newly collected high-resolution temperature data at Lake Shasta. Modeling efforts

have been completed at Shasta Reservoir using CE-QUAL-W2 (W2), a two-dimensional hydrodynamic model developed by the U.S. Army Corp of Engineers (Cole and Wells 2011). Hanna et al. (1999) investigated the impact of the TCD on changes in reservoir water temperature patterns. The study found large changes in outflow temperature between pre-TCD to post-TCD operations due to the ability of the TCD to withdraw water from different and deeper elevations. In general, the study found that the deep hypolimnion experienced the largest temperature changes as a result of the TCD, because such deep withdrawals were not possible prior to the TCD installation (Hanna et al. 1999). Bartholow et al. (2001) also used W2 to examine dissolved oxygen, nitrate-nitrate, ammonium, soluble reactive phosphorus, phytoplankton, dissolved organic matter, sediment, and total inorganic carbon patterns within the reservoir. The study found that TCD operations did not have as much impact on the reservoir's dynamics as compared to hydrology and meteorology (Bartholow et al. 2001). The W2 model was additionally coupled with bioenergetics (Hanna et al. 1999) and food web models (Saito et al. 2001) that showed reservoir operations did not have a significant impact on reservoir fisheries because the fish primarily inhabit the epilimnion.

More recent applications of W2 included assessment of head-of-reservoir conditions for juvenile fish collection in Lake Shasta's tributaries (Clancey et al. in press), and modeling of reservoir operations under extreme climatic conditions (Sapin et al. 2017). Both studies suggested that a higher resolution W2 model would have been beneficial to modeling efforts. Sapin et al. (2017) found that during extreme wet and dry years, in-reservoir cold pool storage was depleted and target discharge temperatures were exceeded during the critical period for winter-run Chinook salmon rearing, and

recommended further examination of managing reservoir elevations and releases in extreme wet and dry years. Sapin et al. (2017) also involved reservoir managers who suggested that modeling temperature conditions after multiple drought years would be a useful tool for informing operations.

For this study, the CE-QUAL-W2 model of Shasta Reservoir was used to examine reservoir conditions under climate change emissions scenarios and in the drought year of 2015. Air and stream temperature increases projected for 2100 for both low and high carbon emissions scenarios were applied to meteorological and tributary data for Lake Shasta in 2015. The W2 model was used to simulate reservoir discharge temperatures and cold pool storage under these climate change scenarios. W2 was also used to simulate various operations during 2015 that conserve water during the spring to maximize the volume of cold pool for the rest of the year. Additionally, higher initial reservoir levels on January 1 were simulated to investigate the impact of storage conservation for the previous year focused on cold pool and discharge temperatures. However, the coarse resolution of the original W2 model for Shasta Reservoir used in this analysis resulted in uncertainty in calculations of cold pool storage and the onset date and duration of reservoir stratification. This uncertainty provided motivation to increase the Lake Shasta W2 model resolution to improve model estimates of cold pool and reservoir stratification.

High-resolution temperature profile data collected during 2015 and 2016 were used to inform the development and performance of a Lake Shasta W2 model with increased resolution along the depth profile of the reservoir. In late summer of 2015, NOAA Fisheries contracted the Center for Transformative Environmental Monitoring

Programs (CTEMPS) at the University of Nevada, Reno to deploy a distributed temperature sensing (DTS) fiber optic cable system in Shasta Reservoir. Between August of 2015 and August of 2016, the DTS provided high spatial (every 0.125 meter) and temporal (every 15 minutes) resolution temperature data of the top 90 meters of the water profile just upstream of Shasta Dam. The high-resolution data were used to compare the temperature profile adjacent to the dam modeled by the original W2 model of Shasta Reservoir with two alternative W2 models of the reservoir with higher bathymetric resolution in the depth profile. Each model was evaluated based on how closely cold pool volume estimates and stratification estimates matched the DTS data collected between August 2015 and July 2016.

Thesis Overview

This thesis is presented in four chapters. The first chapter (this chapter) provides an introduction to the project motivation and methods development. The second chapter is a manuscript describing modeled climate change scenarios and alternative reservoir operations for the drought year of 2015. The third chapter is a manuscript describing the DTS deployment at Shasta Reservoir and the high-resolution data collected, and its use in developing and evaluating new model resolution for the W2 hydrodynamic model of Shasta Reservoir. The final chapter describes the main conclusions from the work presented in the second and third chapters, and recommendations for future work. Appendices are included at the end of this thesis and describe additional details of completed work.

References

AghaKouchak, A., L. Cheng, O. Mazdiyasni, and A. Farahmand. 2014. Global warming and changes in risk of concurrent climate extremes: Insights from the 2014 California drought. Geophysical Research Letters 41:8847–8852.

Bartholow, J. M., R. B. Hanna, L. Saito, D. Lieberman, and M. Horn. 2001. Simulated limnological effects of the Shasta Lake temperature control device. Environmental Management 27:609–626.

Brekke, L. D., E. P. Maurer, J. D. Anderson, M. D. Dettinger, E. S. Townsley, A. Harrison, and T. Pruitt. 2009. Assessing reservoir operations risk under climate change. Water Resources Research 45:1–16.

Clancey, K., L. Saito, K. Hellmann, C. Svoboda, J. Hannon, and R. Bechwith. (in press). Evaluating head-of-reservoir water temperature for juvenile Chinook Salmon and Steelhead at Shasta Lake with modeled temperature curtains. Accepted to North American Journal of Fisheries Management.

Cole, T., and S. Wells. 2011. CE-QUAL-W2: A two-dimensional, laterally averaged, hydrodynamic and water quality model, version 3.7. User Manual. Instruction Report EL-11-1. US Army Corps of Engineers, Washington (DC).

Collier, M., R. H. Webb, and J. C. Schmidt. 1996. Dams and Rivers - A primer on the Downstream Effects of Dams. U.S. Geological Survey. Denver, CO.

Graf, W. L. 2006. Downstream hydrologic and geomorphic effects of large dams on American rivers. Geomorphology 79:336–360.

Griffin, D., and K. J. Anchukaitis. 2014. How unusual is the 2012 – 2014 California drought ? Geophysical Research Letters 41:9017–9023.

Hanna, R. B., L. Saito, and J. M. Bartholow. 1999. Results of Simulated Temperature Control Device Operations on In-Reservoir and Discharge Water Temperatures Using CE-QUAL-W2. Lake and Reservoir Management 15:87–102.

Joyce, E. 2016, January 21. "California Drought Improves; 2015 Warmest Year On Record". Capital Public Radio. Date Accessed: May 14 2017. http://www.capradio.org/articles/

Mateus, M. C., and D. Tullos. 2017. Reliability, Sensitivity, and Vulnerability of Reservoir Operations under Climate Change. Journal of Water Resources Planning and Management 143(4):4016085.

NMFS, National Marine Fisheries Service. 2011. 5-Year Review: Summary and Evaluation of Sacramento River Winter-run Chinook Salmon ESU. Long Beach.

Poff, N. L., J. D. Allan, M. B. Bain, J. R. Karr, K. L. Prestegaard, B. D. Richter, R. E. Sparks, and J. C. Stromberg. 1997. The Natural Flow Regime: A paradigm for river conservation and restoration. BioScience 47:769–784.

Saito, L., B. M. Johnson, J. M. Bartholow, and R. B. Hanna. 2001. Assessing ecosystem effects of reservoir operations using food web-energy transfer and water quality models. Ecosystems 4:105–125.

Sapin, J. R., L. Saito, A. Dai, B. Rajagopalan, and R. B. Hanna. (2017). Demonstration of Integrated Reservoir Operations and Extreme Hydroclimate Modeling of Water Temperatures for Fish Sustainability below Shasta Lake. Journal of Water Resources Planning and Management 143(10), 04017062. DOI:10.1061/(ASCE)WR.1943-5452.0000834.

Trenberth, K. E., A. Dai, G. Van Der Schrier, P. D. Jones, J. Barichivich, K. R. Briffa, and J. Sheffield. 2014. Global warming and changes in drought. Nature Climate Change 4:17–22.

Yates, D., H. Galbraith, D. Purkey, and B. Joyce. 2008. Climate warming, water storage, and Chinook salmon in California's Sacramento Valley. Climate Change 91:335–350.

Chapter 2: Modeling reservoir operations at Lake Shasta, California for the 2015 drought and climate change

Rachel Hallnan[a], Laurel Saito[b], David Busby[c], Eric Danner[d], Miles Daniels[e], and Scott Tyler[f]

[a]Graduate Research Assistant
Graduate Program of Hydrologic Sciences,
University of Nevada – Reno
Reno, NV, 89557 USA
Email: rhallnan@nevada.unr.edu

[b]Corresponding Author
Nevada Water Program Director
The Nature Conservancy
1 East First Street, Suite 1007, Reno, NV 89501 USA
Email: laurel.saito@tnc.org

[c]Undergraduate Research Assistant
Department of Geography & Environmental Sciences,
SUNY College at Oneonta
108 Ravine Pkwy, Oneonta, NY, 13820 USA
Email: dmbusby71@gmail.com

[d]Research Ecologist
NOAA Fisheries
110 Shaffer Rd, Santa Cruz, CA 95060 USA
Email: eric.danner@noaa.gov

[e]Associate Specialist
University of California, Santa Cruz
Institute of Marine Sciences
1156 High Street, Santa Cruz, CA 95064 USA
Email: miles.daniels@noaa.gov

[f]Professor
Department of Geological Sciences and Engineering
University of Nevada – Reno, Mail Stop 172
Reno, NV 89557 USA
styler@unr.edu

Abstract

Stress on California's salmon fisheries drives a need for effective temperature management in California's Sacramento River. Cold temperatures in the Sacramento River downstream of Shasta Dam are required for Chinook salmon spawning and rearing. The dam is equipped with a temperature control device that enables managers to provide cold discharge temperatures to downstream Chinook salmon populations. California experienced its worst drought in a century beginning in 2012 and extending throughout 2015, which provides insight into potential future reservoir conditions as climate change predictions suggest droughts will occur more frequently and with higher intensity. In this study, a two-dimensional hydrodynamic model of Shasta Lake is used to simulate 1) reservoir temperature conditions under potential climate change emissions scenarios, and 2) alternative reservoir operations during 2015 aimed at sustaining cold pool volume in the reservoir through November, a critical time for endangered winter-run Chinook salmon rearing. The results suggest that reservoir managers at Shasta Lake will have an increasingly difficult time maintaining adequate cold pool volume in the reservoir until November under climate change, and even extreme reductions in reservoir outflows may not be enough to mitigate this result.

Keywords: CE-QUAL-W2, Climate Change, Reservoir Temperatures, Chinook salmon, Hydrodynamic Modeling

Introduction

Population expansion and development in the western United States emphasize the need to sustainably manage the freshwater resources in this region. Drought and rising air temperatures associated with climate change continue to increase stress on existing water resources. In California, the Central Valley Project exists to provide water storage, irrigation releases, salinity controls for the San Francisco Bay Delta, flood control, and power generation (Stene 1996). Included in the project is Shasta Dam in northern California, which provides 5.61 billion cubic-meters (4.55 million acre-feet) of water storage, downstream flood control on the Sacramento River, and power generation (USBR 2015). However, Shasta Dam blocks access of Chinook salmon to their native spawning and rearing habitat in the tributaries above the dam (Saito et al. 2001). Salmon are anadromous fish that spend part of their adult life in the ocean and return to the fresh headwater streams to spawn and rear. For spawning and rearing to be successful, salmon require cold waters such as those found in upstream headwaters (Mills et al. 1997). Elevated water temperatures downstream of Shasta Dam have caused population declines, particularly for the winter-run Chinook salmon, which were listed as endangered under the Endangered Species Act (ESA) in 1993 (NMFS 2011).

As mandated by the ESA, focus has been placed on providing Chinook salmon spawning and rearing habitat conditions downstream of Shasta Dam (Mills et al. 1997). Mandated temperature thresholds have been set downstream of Shasta Dam during the summer and fall, including a threshold of 13.3°C (56°F) for the 100 km (62 mile) reach of river between Keswick Dam and Red Bluff, California (Nickel et al. 2004). This is a

spatially moving temperature target, where the specific target location can be adjusted up- or downstream during the summer and fall as needed based on river conditions. The goal of these temperature thresholds is to minimize thermal habitat loss for Chinook salmon (McCullough 1999) .

To help managers meet downstream temperature thresholds, a selective withdrawal structure called a temperature control device (TCD) was installed at Shasta Dam in 1997 (Figure 1). The TCD has intake gates at four different elevations, and allows managers to pull warm water from the surface of the reservoir, or cold water from the reservoir's depth. This allows managers to help mitigate Chinook salmon population declines by controlling discharge temperatures while still generating hydropower (Bartholow et al. 2001).

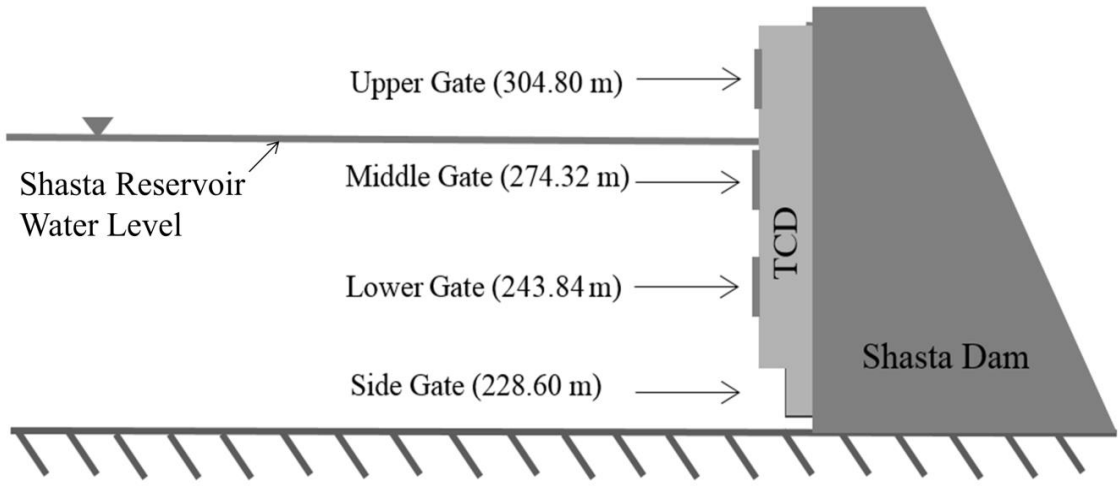

Figure 1. Schematic of the TCD at Shasta Dam.

Selective withdrawals from the near-surface occur during the winter and spring, while colder water at depth is conserved for release during the summer and fall

(Bartholow et al. 2001). This strategy aims to provide adequate downstream temperatures for spawning and rearing of Chinook salmon by taking advantage of density-driven temperature stratification within the reservoir. Managers use different target discharge temperatures below Shasta Dam with the goal of meeting the mandated thresholds, and conserving enough cold water to last through the fall (Hanna et al. 1999). Target temperatures vary throughout the year based on season, and change slightly based on whether it is a wet or dry year (USBR 2008). Winter-run Chinook salmon spawn in the river during summer, and the eggs develop into the fall. Because the egg life stage is the most temperature sensitive (McCullough 1999), the late summer/fall period marks the most critical time for managers to provide cold discharge temperatures for winter-run Chinook salmon.

Recent studies suggest that climate change will result in more climate extremes, including more intense droughts and higher air temperatures (AghaKouchak et al. 2014). This could result in warmer water temperatures that could be harmful to salmon populations. More specifically, climate models predict that low and mid-latitude areas may experience increased drying associated with higher greenhouse gas concentrations. Elevated air temperatures associated with global warming will likely increase the rate of drying experienced during droughts, causing droughts to form more quickly and at a greater intensity (Trenberth et al. 2014). Thus, increases in river and reservoir temperatures likely will occur, and could amplify salmon population declines (Brekke et al. 2009).

California experienced its most severe drought in a century from 2012-2015. The lowest water year precipitation totals over the observational climate record as well as record high temperatures were observed during this time (Griffin and Anchukaitis 2014). The 12-month accumulated precipitation for 2013 was less than 34% of the statewide annual average (Swain et al. 2014). Subsequently, 2015 was the warmest year on record globally, and the second warmest ever recorded in California (Joyce 2016). The drought resulted in lower snowpack, streamflows, and reservoir levels throughout California (Griffin and Anchukaitis 2014).

The low rainfall and warm air temperatures associated with this drought impacted the health of fisheries and aquatic ecosystems across California (Swain et al. 2014), and warrant concern for the declining winter-run Chinook salmon populations. Reservoirs can provide a buffer during drought through discharges from the cold pool volume, however this becomes more difficult when drought persists for multiple years. Lower reservoir levels at the start of a drought year during which tributary inflows and precipitation are low may result in more rapid reduction of cold water volume during the summer when reservoir drawdown occurs. The duration of summer stratification may also be reduced. Such effects may be amplified if a drought year directly follows a year that the reservoir experienced large summer/fall drawdown (Nowlin et al. 2004).

The recent California drought highlights the urgency to provide adequate cold water habitat in the Sacramento River downstream of Shasta Dam, and provides insight into potential reservoir conditions of the future, considering that climate change predictions suggest more frequent and intense droughts. If the low tributary inflows and

reservoir levels at Shasta Lake during 2015 will be normal in the future, the 2015 conditions provide a valuable dataset for assessing the impact of projected air temperature increases associated with climate change on the water temperatures in Shasta Lake. This paper presents results from reservoir conditions modeled at Shasta Lake during 2015 with projected 2100 air and stream temperature increases for both high and low carbon emissions scenarios from California Climate Change Center (2012).

The extreme precipitation lows and temperature highs experienced between 2012 and 2015 led us to consider if alternate reservoir operations could have improved cold pool volumes in the reservoir and discharge temperatures during the fall of 2015. For the purposes of this study, cold pool is defined as the volume of water in the reservoir with water temperatures less than or equal to 9°C (Sapin et al. 2017). One strategy, which is currently used by managers at Shasta Dam, is to use TCD operations to release from the uppermost gates in the reservoir during the spring, thus releasing only warm water to preserve the cold pool. Reservoir managers then switch to lower and side gate releases from the hypolimnion during the late summer and fall to provide cold water for endangered winter-run Chinook salmon juvenile rearing habitat (Bartholow et al. 2001; Bartholow 2004). However, in extreme drought conditions such as those in 2015, this strategy alone was not enough to meet discharge temperature targets during the fall. Alternatively, limiting reservoir release quantities in the spring during drought years may preserve more cold pool storage for reservoir releases during the fall when it is most critical to discharge temperatures for winter-run Chinook salmon juvenile rearing (Bartholow 2004). It is hypothesized that minimizing or even withholding spring

discharges completely may not conserve enough cold pool to meet downstream temperature thresholds during the fall under 2015 drought conditions.

Operations during the previous year can affect cold pool accumulation during the following year. Nickel et al. (2004) found that less cold pool (~890 million cubic meters) accumulated in the spring following years when hypolimnetic discharges occurred in the late summer and fall, which suggests that there is a tradeoff between providing cold summer/fall discharge temperatures and cold pool accumulation in the following year. It is possible that operations during the fall of the previous year focused on conserving water could result in a higher reservoir elevation at the start of the next calendar year (January 1). If this could be done while continuing to use hypolimnetic withdrawals to provide cold discharge temperatures during the fall of the previous year, the tradeoff between the previous year's cold discharge temperatures and the following year's cold pool storage could be reduced. To test this concept, we simulated January 1 reservoir elevations higher than the January 1 reservoir elevation in 2015. If summer drawdown in the previous year (in this case, 2014) were minimized to conserve water for the following year, the larger volume of water in the reservoir on January 1, 2015 may provide a buffering effect against the warm air temperatures and low inflows that occurred during 2015.

Higher reservoir elevation at the start of a drought year may provide more cold pool volume and lower discharge temperatures during summer and fall drawdown of that year, which may improve conditions for downstream Chinook salmon populations. The simulations of different January 1 reservoir elevations were also used to investigate the

impact of January 1 reservoir volume on the fall discharge temperatures and cold pool storage of 2015. If cold pool conditions can be improved without a large tradeoff with warm summer and fall release temperatures, managers' ability to meet Chinook salmon thermal habitat needs downstream of Shasta Dam throughout the year may be enhanced.

Materials and Methods

Shasta Reservoir CE-QUAL-W2 model

Simulations were completed using a CE-QUAL-W2 (W2) model of Shasta Reservoir that was developed in the late 1990s to investigate the impact of the TCD on the temperature patterns, water quality, and fisheries within the reservoir (Hanna et al. 1999; Bartholow et al. 2001; Saito et al. 2001). W2 is a two-dimensional model developed by the U.S. Army Corps of Engineers (Cole and Wells 2011). The W2 model of Shasta Reservoir was updated to version 3.7 and calibrated to 1995 conditions, the only year with temperature profiles that are available throughout the reservoir. The calibration parameters used by Hanna et al. (1999) (Table 12 in Appendix A) were determined to be appropriate, and resulted in an average R^2 of 0.966 and an average root mean squared error (RMSE) of 0.947°C. The recalibrated model has been used to study the impacts of reservoir operations in extreme hydrologic and climatic conditions (Sapin et al. 2017) and to model head-of-reservoir conditions for downstream juvenile fish passage (Clancey et al. in press).

Simulated 2015 conditions

The calibrated Shasta Lake W2 model was set up and verified for 2015. Input data for 2015 were obtained from January 1 to December 31, 2015. The required input data

include bathymetry, inflow quantities for four tributaries (Pit River, Squaw Creek, McCloud River, and Sacramento River), inflow temperatures, outflow quantities, reservoir operations, and meteorological data (Hanna et al. 1999). A regression relationship from Saito (1999) was used to calculate the inflow for Squaw Creek from McCloud River flows because Squaw Creek flows are unavailable after 1963. The inflow temperatures used for Squaw Creek were the same as McCloud River temperatures, a method used for previous modeling of Lake Shasta with W2 (Bartholow et al. 2001; Clancey et al. in press; Sapin et al. 2017). National Oceanic and Atmospheric Administration (NOAA) Fisheries provided the necessary input data for 2015, which they obtained from the sources noted in Table 1.

Table 1. Input data necessary for the W2 model of Shasta Lake.

Data Type	**Data Source:**	**Temporal Resolution:**
Hydrologic Data, Shasta Lake, CA (Reservoir Storage, Reservoir Outflow)	CDEC[a]	Daily
Tributary Inflows (Sacramento, McCloud, and Pit River)	CDEC[a]	Hourly
Tributary Water Temperatures (Sacramento, McCloud, and Pit River)	CDEC[a]	Hourly
Gate Operations (Upper, Middle, Lower, and Side Gates)	USBR[b]	Daily
Meteorological Data (Air Temperature, Dewpoint Temperature, Wind Speed, Wind Direction, Cloud Cover	NARR[c]	Hourly

[a]CDEC = California Data Exchange Center - http://cdec.water.ca.gov/
[b]USBR = United States Bureau of Reclamation
[c]NARR = North American Regional Reanalysis - https://www.ncdc.noaa.gov/data-access/model-data/model-datasets/north-american-regional-reanalysis-narr

The W2 model of Shasta Lake with 2015 input data was validated against measured 2015 reservoir elevations obtained from the California Data Exchange Center

(CDEC) and water temperature data obtained from the United States Bureau of Reclamation (USBR) at model segment 21, the segment directly adjacent to Shasta Dam. W2-modeled reservoir elevation had a RMSE of 0.1312 meters and R^2 value of 0.99 (Figure 26 in Appendix A). Modeled temperature profiles for segment 21 were compared to twelve measured sonde data profiles throughout fall 2015, and had R^2 values ranging between 0.92 and 0.99, % bias values ranging between -5.45 and 0.028, and RMSE values ranging between 0.537 °C and 1.632 °C (Figure 27 and Table 13 in Appendix A). Based on these results, it was concluded that the W2 model provided a good representation of Shasta Reservoir volumes and water temperatures during 2015.

2100 carbon emissions

Air temperature increases

California Climate Change Center (2012) provided projections for monthly air temperature increases associated with anthropogenic carbon emissions. Air temperatures in 2100 for (1) B1 low carbon emissions estimate (1.6℃ - 3.3℃), and (2) A2 high carbon emissions (2.6℃ - 4.8℃) estimate were simulated (Table 14 in Appendix B). This was completed using the method from Sapin (2014) in which projected monthly air temperature increases were applied to air temperatures from 2015 on the 15th of each month and linearly interpolated for the days in between (Figure 28 in Appendix B).

Stream temperature increases

Regression relationships between air and stream temperatures were used to adjust stream temperatures for Lake Shasta's tributaries for 2100 estimated high and low emissions scenarios. Air temperatures for 2015 were plotted against stream temperatures to develop a linear regression relationship for the Pit River (R^2 = 0.83, n=364), the

McCloud River (R^2 = 0.91, n=364), and the Sacramento River (R^2 = 0.86, n = 364) during 2015 (Figure 29 in Appendix B). The regression equations were used to calculate new stream inflow temperatures for 2100 high and low emissions scenarios (Figure 30 in Appendix B). Values for adjusted Squaw Creek inflow temperatures were the same as adjusted McCloud River temperatures to be consistent with the Lake Shasta model for 2015 without stream or air temperature adjustments.

Climate Change Model Scenarios

The W2 model was used to complete five full-year simulations using projected air temperature and stream temperatures for both the low and high emissions projections for 2100 (Table 15 in Appendix C). A control run for 2015 had no changes applied from actual 2015 air and stream temperatures. All input data for the four additional emissions scenarios were unchanged from the 2015 model with the exception of air and/or stream temperature changes.

Reduced outflow volume operations

To examine the ability of reservoir operations to improve fall cold pool storage after previous drought years, operations were run in W2 for 2015 that focused on increasing cold pool storage during the spring by incrementally reducing reservoir releases between May 1 and June 30, 2015 by 10% (Table 16 in Appendix C). Modeled outflow reductions began with the onset of increased dam releases on May 1, and ended with the first use of the lower gate on the TCD on June 30, as occurred in 2015 (Figures 31 and 32 in Appendix C). No changes were made in the model to the position and timing of open gates. A small amount of water (only 3.2% of the total 2015 Shasta Dam outflow) was discharged through dam bypass outlets (i.e., not discharged through the

TCD) between April 16 and May 26, 2015. These releases were included in the control scenario, but were excluded from all reduction scenarios.

Different January 1 reservoir elevation

The W2 model was also used to examine the impact of a higher reservoir elevation at the start of the year on the discharge temperatures and cold pool storage during the fall. Reservoir elevation was incrementally increased from the January 1, 2015 elevation of 289.5 meters by approximately 10 meters up to 330 meters, because the highest model elevation is 336.81 meters (Figure 33 in Appendix C). Incremental increases in the starting reservoir elevation resulted in non-linear increases in reservoir storage because more volume occupies each incremental meter increase near the surface. The purpose of these model scenarios was to identify the impact of the previous calendar year's conditions and operations on the following year's cold pool and discharge temperatures. This information may be particularly important when multiple years of severe drought occur back-to-back. The control run used the 2015 gate operations schedule with no changes applied and the actual January 1 elevation at 289.5 meters in 2015. All model runs used unchanged 2015 gate operations (i.e., the position of open gates was not changed).

Model scenario evaluation

Cold pool volume in the reservoir was estimated for each model scenario from simulated water temperatures from segment 21 adjacent to Shasta Dam. Daily simulated discharge temperatures from the dam at 12PM for each model scenario were noted, along with the day on which the maximum simulated 12PM discharge temperature for 2015

occurred. Additionally, daily 12PM discharge temperatures throughout the year were plotted against the appropriate tier of target outflow temperatures from Future No Action CALSIM II simulations based on end of May storage levels for the reduced outflow scenarios and the different January 1 reservoir elevation scenarios (Tables 18 and 19 in Appendix C; USBR 2008). The start and end dates of stratification were quantified for all model scenarios. Stratification was defined as the time period when a temperature difference of >2°C from surface temperature became <25 meters deep (Robertson and Ragotzkie, 1990).

Results

Simulated 2015 conditions

According to USBR (2008) tier classifications for CALSIM II simulations for measured end of May Shasta Reservoir storage (Tables 18 and 19 in Appendix D), the drought year of 2015 was a Tier I extreme dry year. W2 simulated isothermal conditions in the reservoir until mid-March, when warm water temperatures occurred near the surface, eventually leading to stratified conditions during the summer, and a return to isothermal conditions in late December 2015. The upper gate (304.80 meters) was never submerged during 2015, and thus near surface discharges occurred from the middle gate (273.32 meters) in the spring. During summer and fall, discharges occurred from colder depths via the lower gate (243.84 meters) beginning in July, and finally the side gate (228.60 meters) in September. The W2 model simulated warm temperatures extending deeper into the reservoir during the fall as withdrawals were made from the lower and

side gates. Reservoir turnover was simulated to occur around the time that withdrawals stopped from the side gate on December 15, 2015 (Figure 2).

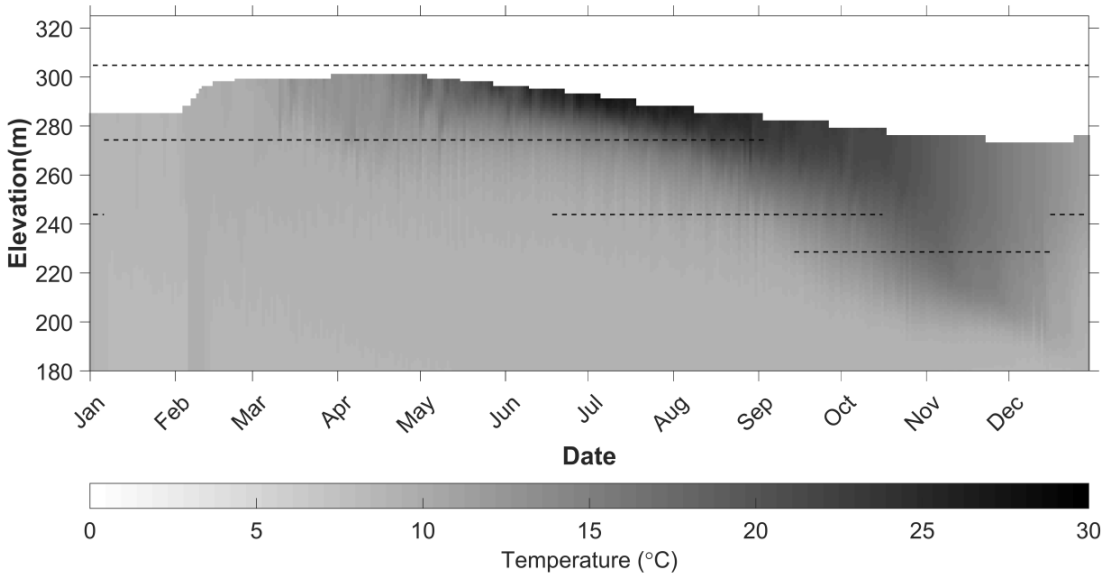

Figure. 2. Modeled temperature profiles for segment 21 just upstream of Shasta Dam throughout 2015. TCD intake elevations are shown as black horizontal dashed lines only during periods of operation.

2100 carbon emissions

All four of the climate change emissions scenarios resulted in higher simulated maximum and minimum reservoir discharge temperatures throughout the year (Table 2). Adjusting both the air and stream temperatures resulted in higher minimum and maximum discharge temperatures as compared to scenarios where only the air temperature was adjusted. The high emissions scenarios also produced larger increases in maximum and minimum discharge temperatures compared to the low emissions scenarios. Overall, the high emissions scenario with both air and stream temperatures adjusted had the most extreme results.

The modeled minimum cold pool decreased from around 8 to 4 million cubic meters for both the low and high emissions scenarios with both air and stream temperatures adjusted (Table 2). The number of days at minimum cold pool volume were much greater when both air and stream temperatures were adjusted. Additionally, the modeled maximum cold pool volume decreased only for the high emissions scenario with both air and stream temperature adjustments. The June 1 and November 1 cold pool volumes also decreased most for this scenario. Overall, the largest decreases in cold pool storage occurred for the scenarios with both air and stream temperature adjustments.

Simulated results indicated stratification began earlier and extended later into the year for the emissions scenarios, causing longer stratification as compared to 2015 (Table 2). This effect was more pronounced for high emissions simulations.

In general, the simulations with both stream and air temperatures adjusted showed a greater deviation from 2015 conditions than simulations adjusted only for air temperatures (Figure 3). The modeled amount of warm water in the epilimnion was greater for all of the emissions scenarios as compared to conditions in 2015 (Figure 3). The emissions scenarios resulted in warmer temperatures extending deeper into the reservoir during the stratified period. For the two scenarios with both air and stream tributary temperatures adjusted, the epilimnion extended deeper into the profile at the end of stratification during November (Figure 3).

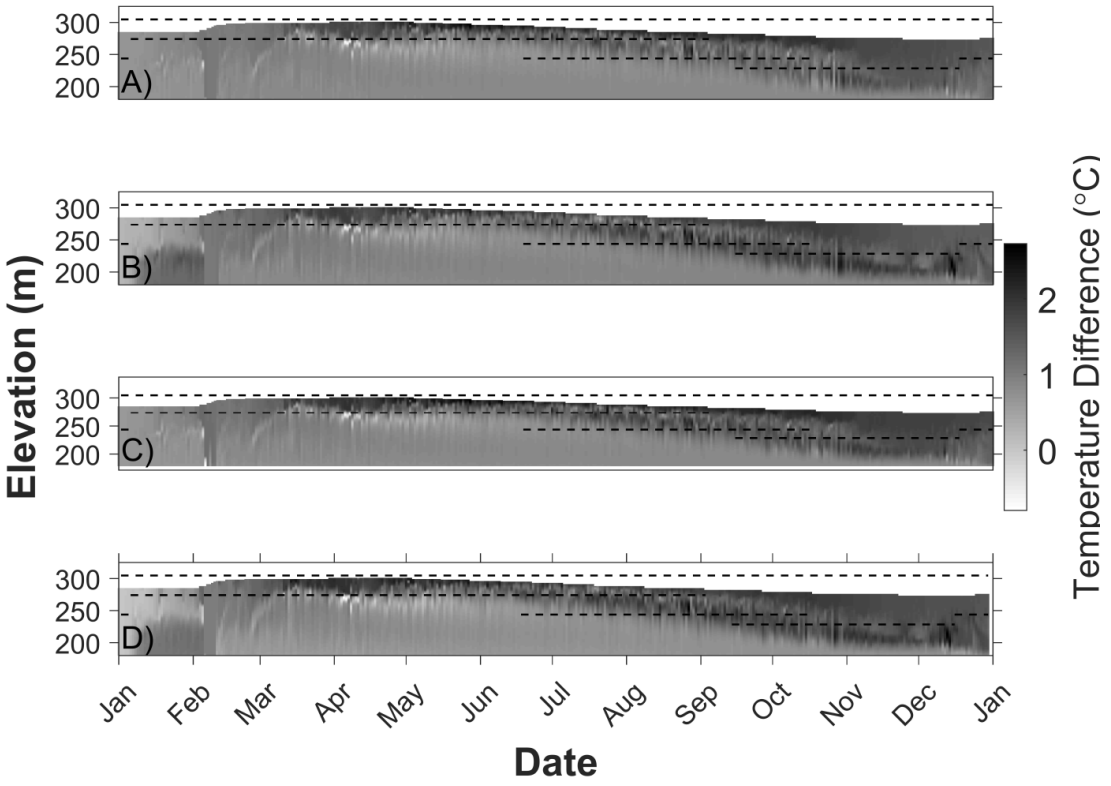

Figure 3. Temperature differences between 2015 modeled temperature and modeled: (A) low emissions with only air temperature adjusted (B) low emissions with both air and stream tributary temperatures adjusted, (C) high emissions with only air temperatures adjusted, and (D) high emissions with both air and stream tributary temperatures adjusted. Dam intake elevations are shown as black dashed lines only during periods of operation. Note that the highest intake was never submerged in 2015.

Table 2. Summary of maximum and minimum discharge temperatures, cold pool storages, and stratification patterns for 2015 each low emissions (LE) and high emissions (HE) climate change scenario.

Scenario	2015	2100 LE Air	2100 LE Air + Stream	2100 HE Air	2100 HE Air + Stream
Discharge Temperature (°C)					
Maximum	17.52	18.35	18.65	18.66	19.14
Minimum	8.37	8.57	8.69	8.66	8.75
Cold Pool Volume (m^3 x 10^6)					
Maximum	3026	3026	3026	3026	2908
Minimum	8	8	4	8	4
1-Jun	791	698	537	698	466
1-Nov	23	14	14	14	8
Number of Days at Minimum	1	1	17	2	23
Stratification Patterns					
Start Stratification	21-Apr	12-Mar	12-Mar	15-Mar	16-Mar
End Stratification	18-Oct	26-Oct	19-Oct	20-Oct	20-Oct
Stratification Duration (Days)	180	218	219	221	228

Reduced outflow volume operations

Substantial deviation from simulated 2015 water temperature conditions did not occur until model scenarios with outflow reductions of 80% or more. For this reason, only the 30% reduction and 80% reduction scenarios are shown in figures to display both the minimal effect of smaller reductions, and to highlight the extreme amount of reduction necessary to create more noticeable change in water temperatures from 2015 conditions. Results from all scenarios are discussed in the text.

Simulation results indicated that conserving reservoir discharge volumes in the spring of 2015 decreased the discharge temperatures through the year (Figure 4). A relatively linear decrease in discharge temperatures and reservoir storage occurred at the end of the simulated reduction period on June 30 as outflows were incrementally reduced. This linear trend resulted in a decrease in reservoir discharge temperature of approximately 0.02°C for each 1.0 m^3s^{-1} decrease in reservoir discharge in 2015. Based on this relationship, a maximum decrease in discharge temperature of 3.29°C was achieved by reservoir discharge reductions of 100% between May 1 and June 30.

Until flows were reduced by 80% or more, the maximum daily temperature discharged during 2015 occurred on August 6. The maximum daily water temperature discharged on November 17 for reductions between 80% - 100%. This shift occurred because there were discharge temperature peaks in early August and early November 2015 (Figure 4). For the 80% reduction scenario, simulated discharge temperatures in August were reduced enough for the simulated discharge temperature peak in November to be higher, which caused the date of maximum discharge temperature to shift (Figure 4). Scenarios with reductions between 10% - 30% fell under USBR (2008) CALSIM II Tier I target temperatures, while scenarios with 40% outflow reduction or greater fell under Tier II targets (Table 18 in Appendix D). Simulated discharge temperatures for all of the outflow reduction scenarios were above their corresponding CALSIM II tier targets between the months of May and December 2015 (Figure 4).

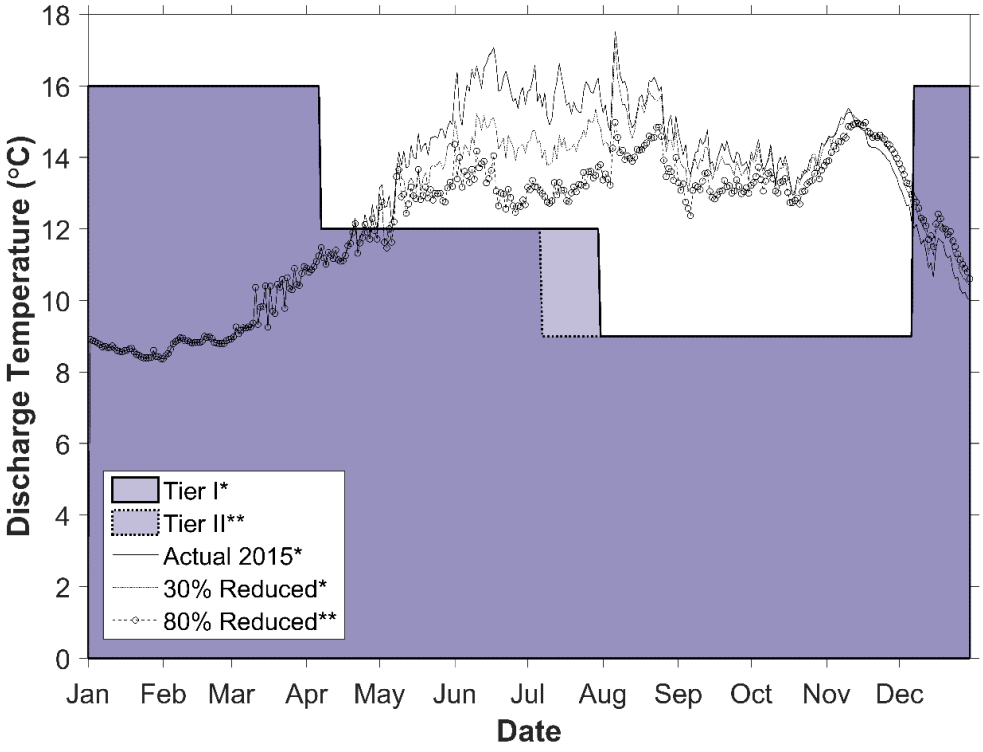

Figure 4. Simulated outflow temperatures for 2015 and reduction scenarios, as well as CALSIM II tiered target discharge temperatures for Shasta Reservoir (USBR 2008). Asterisks indicate which CALSIM II Tier corresponds to each scenario.

Minimum and maximum cold pool volumes estimated from simulated reservoir temperatures were relatively constant as outflows were reduced (Table 3). In all modeled scenarios, the minimum cold pool volume occurred in early December. For all scenarios (apart from the 90% reduction scenario) the cold pool volume on November 1 (the date used to represent the end of the critical season for winter-run Chinook salmon juvenile rearing) decreased from its level in the control scenario. The reservoir elevation on November 1 increased as releases were conserved in the spring, however the elevation and volume of the cold pool dropped several meters (Figure 5). The onset of stratification for all reduction scenarios shifted two days later than 2015. However, the end date of

stratification shifted slightly earlier as outflows were reduced, resulting in a shorter duration of stratification (Table 3).

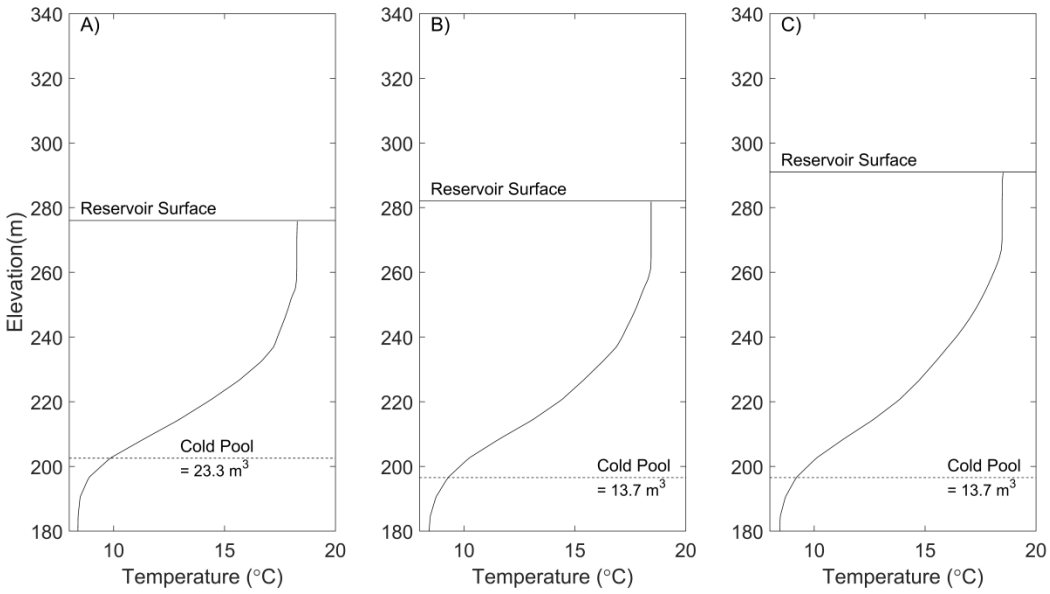

Figure 5. Simulated temperature profiles adjacent to the dam on November 1 for (A) actual 2015 conditions, (B) the 30% reduction scenario, and (C) the 80% reduction scenario. The estimated cold pool volume is noted and shown with a dashed line, and the reservoir surface is noted.

Table 3. Summary of maximum and minimum discharge temperatures, cold pool storages, and stratification patterns for 2015 and reduced outflow volume scenarios.

Scenario	2015	30% Reduction	80% Reduction
Discharge Temperature (°C)			
Maximum	17.52	17.19	14.98
Minimum	8.37	8.37	8.37
Cold Pool Volume (m^3 x 10^6)			
Maximum	3030	3030	3030
Minimum	8.27	8.27	8.27
1-Jun	791	791	791
1-Nov	23.4	13.8	13.8
Number of Days at Minimum	1	8	11
Stratification Patterns			
Start Stratification	21-Apr	23-Apr	23-Apr
End Stratification	18-Oct	3-Oct	2-Oct
Stratification Duration (Days)	186	168	170

Different January 1 reservoir elevation

The maximum simulated temperature discharged from the dam throughout the year decreased for higher January 1 reservoir elevations (Figure 6). The date on which the maximum discharge temperature occurred shifted from August 6, 2015 to November 27 to December 17, 2015 as the starting reservoir elevation increased. For January 1 elevations of 289.5 meters and 300 meters, the discharge temperatures fell above target temperatures from the corresponding CALSIM II tier after May 1 through December (Table 19 in Appendix D). However, starting reservoir elevations of 310 meters, 320 meters and 330 meters resulted in temperatures below their corresponding tier target temperature thresholds during the months of May, June, and July, but exceeded targets from August through December (Figure 6).

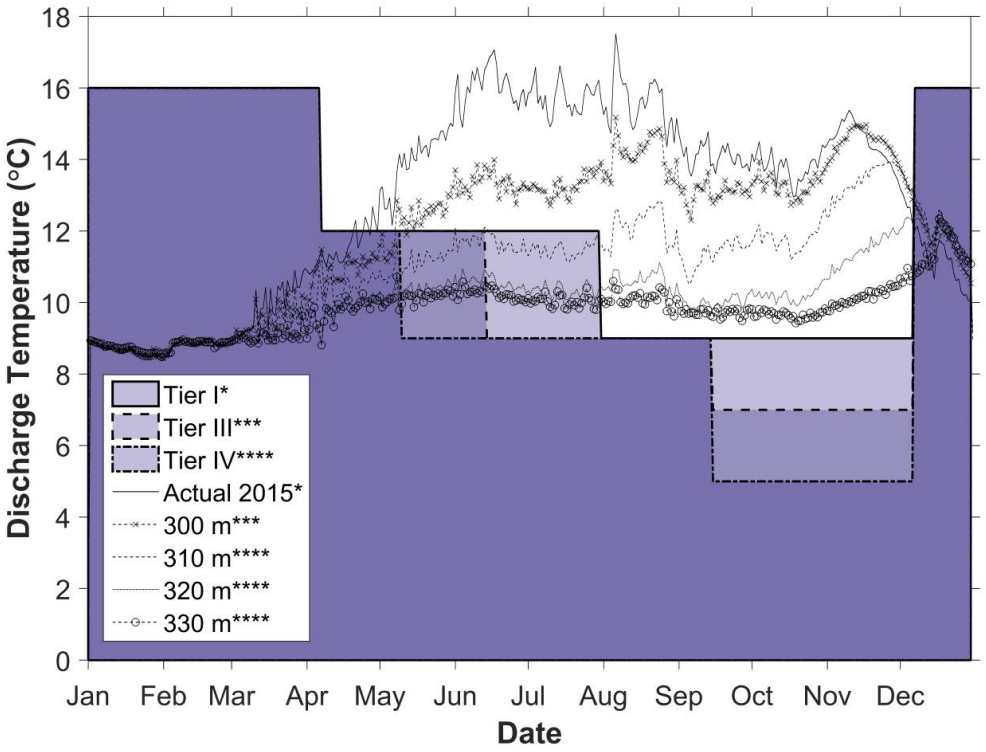

Figure 6. Simulated outflow temperatures for each January 1 reservoir elevation scenario, and CALSIM II Tier I, III, and IV temperature targets (USBR 2008). The tier used to assess discharge temperatures from each January 1 reservoir elevation simulation is noted with asterisks in the legend.

The minimum cold pool volume estimated from simulated reservoir temperatures in the reservoir increased as the January 1 reservoir elevation increased except for the January 1 elevation of 300 meters (Table 4). In all modeled scenarios, the minimum cold pool volume occurred in early December. Both the total reservoir volume and the cold pool volume on November 1 did increase as the January 1 reservoir elevation increased (Figure 7). However, no change in cold pool volume occurred between the 300 meter and 310 meter January 1 elevation model runs. Simulations indicated that the onset of stratification shifted later as the January 1 elevation increased (Table 4). The end date of stratification was earlier for all four increased January 1 elevation scenarios as compared

to 2015, and thus had shorter durations of stratification. However, as the January 1 elevation increased from 300 meters to 330 meters, the end date of stratification shifted later in the year, resulting in an increasing duration of stratification for the four operations scenarios (Table 4).

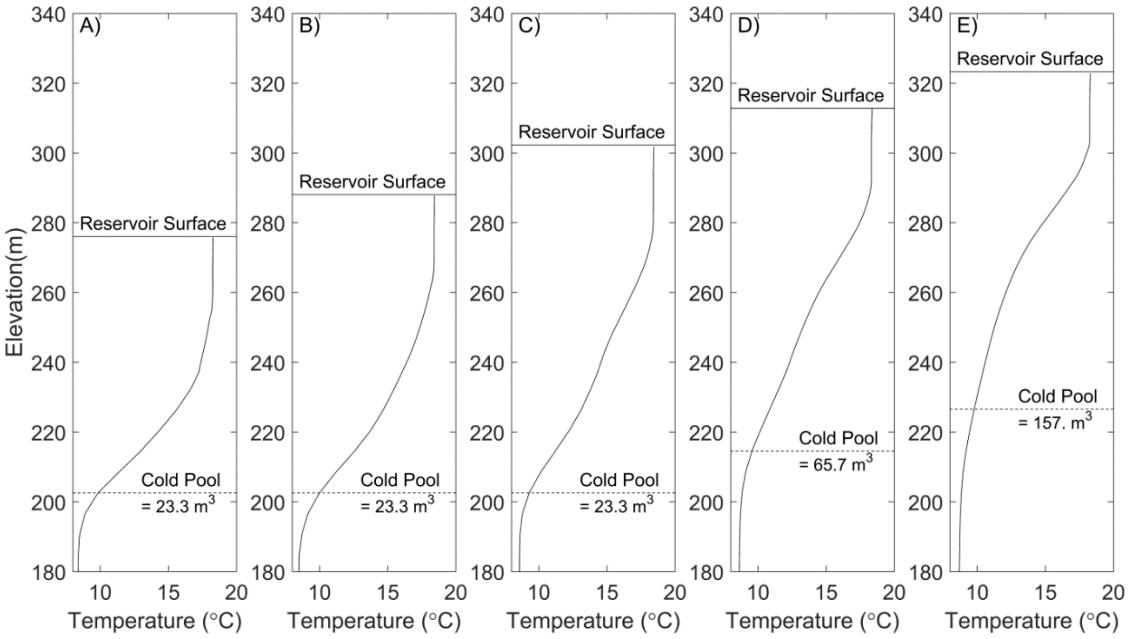

Figure 7. Modeled November 1 temperature profiles adjacent to the dam for (A) actual 2015 conditions (i.e., January 1 elevation 289.5 meters) (B) January 1 elevation 300 meters, (C) January 1 elevation 310 meters, (D) January 1 elevation 320 meters, and (E) January 1 elevation 330 meters. The reservoir surface elevation on November 1 is shown with a dashed line and the cold pool elevation threshold is shown with a solid line.

Table 4. Summary of maximum and minimum discharge temperatures, cold pool storages, and stratification patterns for 2015 and each different January 1 starting elevation scenario.

Scenario	289.5 meters	300 meters	310 meters	320 meters	330 meters
Discharge Temperature (°C)					
Maximum	12.38	12.58	13.96	15.17	14.98
Minimum	8.57	8.54	8.49	8.44	8.37
Cold Pool Volume (m^3 x 10^6)					
Maximum	3026	3805	4550	5567	5613
Minimum	8	4	8	14	23
1-Jun	791	891	1117	1526	1526
1-Nov	23	23	23	66	157
Number of Days at Minimum	1	1	10	5	8
Stratification Patterns					
Start Stratification	21-Apr	13-Apr	23-Apr	26-Apr	25-Apr
End Stratification	18-Oct	2-Oct	3-Oct	18-Oct	17-Oct
Stratification Duration (Days)	180	172	163	177	177

Discussion

The modeled 2100 emissions scenario results confirm what one would expect: discharge temperatures in the future will increase and the volume of cold water available to managers at Shasta Reservoir will likely decrease with climate change. The differences observed between model runs with only air temperatures adjusted, and those with both air and stream temperatures adjusted suggest that stream temperatures will have a large impact on reservoir temperatures and cold pool volume at Shasta Lake. This supports previous findings that meteorology and hydrology have greater impacts on reservoir conditions at Shasta Lake than operations, most likely due to the large surface area of the

reservoir (Bartholow et al. 2001). In particular, the large increase in the modeled number of days that the reservoir was at minimum cold pool storage when both stream and air temperatures were adjusted suggests that reservoir conditions will be worse in the future if stream temperatures increase to the levels projected here.

Literature suggests that stream temperatures will increase in the western U.S. with climate change (Chang and Lawler 2011). Rising summer temperatures will likely be due to lower late spring and summer streamflows as a result of declining snowpack and decreased summer precipitation (Chang and Jung 2010, Chang and Lawler 2011). Additionally, land use changes may result in the reduction of riparian buffers, which may reduce shade and increase solar radiation and thus stream temperatures (Chang and Lawler 2011).

Tributary inflows influence the timing of stratification in Shasta Reservoir. Model results suggest the onset of stratification will occur earlier in the year under climate change and thus result in increased duration of stratification, an effect that could be amplified further if spring runoff timing were to occur earlier in the year under climate change as suggested by Stewart et al. (2004) for western North America.

As expected, outflow temperatures were lower when reservoir discharge volumes in the spring were conserved because increasing the total reservoir volume increased the volume of cold water available for discharge, and provided more buffer to warm air temperatures. However, even reductions of 100% did not result in discharge temperatures below CALSIM II tiered temperature targets between May and December. The

magnitude of change of summer discharge temperatures was only several tenths of a degree Celsius for reduction scenarios less than 50%. Even extreme reductions of 80% and 100% simulated discharge temperature changes of approximately 2°C and 3°C respectively during the summer months, which still resulted in overall discharge temperatures above CALSIM II Tier temperature targets for Shasta Reservoir.

Model results showed that the date on which the minimum discharge temperature occurred shifted from August 6 to November 17 when reservoir releases were reduced by 80% or more. The model simulated two peaks in discharge temperatures for 2015, a peak of 17.5 ºC on August 6, and a lower peak of 15.4 ºC on November 17. Simulated discharge reductions of 80% or greater in May and June of 2015 reduced the temperature peak in August enough for it to fall below the November peak, however the magnitude of the two peaks was still close (Figure 4). It should be noted that this water temperature pattern may not occur every year. The simulated shift to November 17 falls after the end of the critical period for winter-run Chinook salmon rearing (Bartholow, 2004), but as noted previously, discharge temperatures were still above target temperature thresholds between May and November in these model scenarios (Figure 4).

Although modeled reservoir elevation increased in the fall as spring discharges were conserved, the volume of cold pool was less on November 1 for spring discharge reductions between 10% and 80% as compared to actual 2015 conditions (Figure 5 and Table 3), suggesting that total reservoir volume may not directly correlate with cold pool volume at Shasta. Nickel et al. (2004) also found a low correlation between increasing reservoir volume at Shasta Lake and cold pool volume between 1948 and 1999. The

lower cold pool on November 1 for these reduction scenarios may be due to the timing of reservoir mixing shifting slightly earlier into the year, and thus resulting in a more mixed profile on November 1. This is supported by the estimated end dates of stratification, which shifted earlier into the year for the reduction scenarios (Table 3). The earlier onset and end of stratification for all of the reduction and different January 1 starting reservoir scenarios may be related to hypolimnetic withdrawals affecting the thermal structure differently when the reservoir has a higher volume. The duration of stratification can also be shorter when large amounts of reservoir drawdown occur (Gelda et al. 1998). Hypolimnetic withdrawals result in a larger, differently shaped withdrawal zone when the reservoir is higher because withdrawal zone size and geometry is influenced by both the magnitude of outflows and the vertical density profile. A larger simulated withdrawal zone associated with a higher reservoir elevation may cause more mixing in the reservoir and thus result in earlier simulated fall turnover.

The lower summer Shasta Reservoir discharge temperatures from reducing reservoir outflows and thus increasing the volume of water conserved during the spring in our study is similar to the effect of increased duration of springtime reservoir volume conservation found by Mateus and Tullos (2017) in the Santiam River Basin in Oregon. Their study examined reservoir operations under climate change and found that variable rule curves may be effective in mitigating the impact of climate change on the ability of reservoirs to meet summer environmental flow temperature targets for protected Chinook salmon populations. Beginning storage conservation earlier in the year for dry years and later in the year for wet years increased the reliability of multiple reservoirs in the

Santiam River Basin to meet summer environmental flow thresholds (Mateus and Tullos 2017).

Similar to the spring discharge reduction scenarios, the maximum discharge temperature shifted later into the year as the January 1 reservoir elevation was increased (Figure 6). This appears to also be related to a larger volume of warm water, shorter duration of stratification and longer mixing period. Warm temperatures discharged after November 1 may have less impact on the downstream winter-run Chinook salmon population because November 1 marks the end of the critical period for rearing of endangered juvenile winter-run Chinook salmon (Bartholow 2004). While the maximum temperature discharged was reduced as the January 1 reservoir elevation increased, the amount of change was <1°C for the 300-meter scenario. Hence, for a substantial reduction in maximum discharge temperature to have occurred, the reservoir would have to have been increased from its January 1 elevation in 2015 of 289.5 meters to an elevation of 310 meters, which accounts for over 1700 million cubic meters of storage. This large increase in reservoir volume may not be feasible for reservoir operators, particularly since 2015 was preceded by several drought years and the reservoir volume was already low. Simulations with January 1 elevations of 320 and 330 meters resulted in discharge temperatures below temperature targets until May, and reduced outflow temperatures from August through November (Figure 6). Additionally, simulations indicate that increasing the starting reservoir volume increased the November 1 cold pool volume (Figure 6), as was expected. Such results support findings of Nickel et al. (2004), who found that raising the reservoir level to the maximum allowable elevation in January

can optimize cold pool storage because that is the coldest time of the year and has the coldest air temperatures. Both the reductions in discharge temperature and the increases in November 1 cold pool would provide better conditions for downstream Chinook salmon spawning and rearing than the conditions observed in 2015.

The issue of uncertainty must be considered when interpreting model results presented in this paper. Each instrument used to inform modeling efforts, such as temperature loggers, meteorological stations, and stream gauges have their own measurement uncertainty that is propagated into model simulations. In terms of simulating impacts of climate change, climate change models have varying projections on changes in evaporation and precipitation (Brekke et al. 2004) that were not simulated in this study. Climate change projections are also often done on a large scale of several hundred kilometers (Harvey and Hassol 1997), whereas the Shasta W2 model functions on a scale of several meters. Thus, there is uncertainty associated with downscaling and applying projections from climate models to the scale of Lake Shasta.

Error also exists in the estimates of stream temperature increases for the climate change scenarios, which were based on a linear relationship between air and stream temperatures. However, the relationship between increasing air temperature and water temperature is likely not linear (Chang and Lawler 2011). Better estimates of tributary temperature changes for Lake Shasta under climate change would likely improve the model results described above. Thus, future work using a hydrologic model of the watershed above Shasta Lake would be beneficial to predict inflows and stream temperature increases. The recently developed Watershed Environmental Hydrology

Hydro-Climate Model (WEHY-HCM) for the upper Sacramento basin could be used for this purpose (Trinh et al. 2016).

The model resolution is also relatively coarse at depth. From the top layer of the model to the reservoir floor, there are 30 layers of 1.5 meter depths, followed by 19 layers of 3 meter depths, followed by 11 layers of 6 meter depths. The coarse resolution of this model introduces uncertainty in estimating the amount of cold pool storage on a given date. For example, the decrease in cold pool storage simulated between 2015 and the 80% reduction scenario on November 1 was 9.60 million cubic meters. This volume is the storage difference for Shasta Lake between elevations of 202.56 meters and 196.56 meters, which is equivalent to one 6 meter model layer. Thus, the decrease in cold pool storage simulated in the 80% reduction scenario compared to 2015 may be exaggerated by the coarse resolution of the model at the elevation of the cold pool threshold. Another uncertainty is that there may be sources of leakage within the TCD device itself that are not captured by the model (Higgs and Vermeyen 1999). The Shasta Lake W2 simulations distribute withdrawals with flow weighted averages across open gates. However, failure to include significant leakage could lead to errors in modeled outflow temperatures.

An additional uncertainty exists because of mandated flood control releases in extreme wet years. Shasta Dam operations are influenced by the State Water Project and Central Valley Projects of California, and follow the Operations Criteria and Plan (OCAP) for these projects (USBR 1998). OCAP places management restrictions to ensure flood control during wet years that require storage to stay below a flood control curve and thus mandates that large amounts of water be discharged during wet years.

Sapin et al. (2017) used Shasta Lake W2 simulations to show that such releases affected the TCD's ability to improve cold pool storage in extreme wet years. Simulated January 1 reservoir elevations of 310 meters, 320 meters, and 330 meters would be classified as extreme wet years under the definition the CALSIM II tiers based on end of May reservoir storage (USBR 2008). However, simulated operations for the different January 1 reservoir elevation scenarios were from 2015 and did not account for OCAP flood control restrictions because 2015 was a dry year. Additionally, January 1 reservoir elevations increases of over 10 meters (such as those simulated here) may be unrealistic to achieve through management alone after multiple drought years when reservoir levels are already lower than average.

The 330 meter simulation falls above the current maximum storage capacity of Shasta Lake. The spillway elevation of the dam is 324.6 meters, and thus the reservoir cannot accommodate storage levels above this elevation (USBR 2015). However there is interest in raising the dam to accommodate more water storage and increase cold pool volume (USBR 2015). Thus, this simulation is representative of what reservoir conditions may look like if the dam were raised and storage capacity increased.

It is important to consider the feasibility of operations that reduce spring discharges to the extent of the scenarios modeled. For example, reducing flows by 80% would reduce hydropower generation for the months of May and June, and reduce flows to users along the Sacramento River such as farmers and urban centers. Regulations mandate dam releases to manage salinity in the San Francisco Delta (Sapin et al. 2017) and thus reduced flows may harm estuary ecosystems. For these reasons, the modeled

discharge reductions and increased January 1 storage presented in this paper are not recommended as actual management strategies at Lake Shasta. Instead, they are presented as an example of the extent to which reservoir operations may be used to preserve cold pool and reduce reservoir discharge temperatures in the fall.

Conclusions

This study evaluated both the potential impacts of climate change on Shasta Reservoir conditions, and a suite of reservoir operations that may be needed to combat drought year conditions to meet water temperature thresholds for developing Chinook salmon eggs in the Sacramento River. Key findings from model simulations include (1) simulated reservoir discharge temperatures increase with projected air and stream temperatures under climate change, and will likely have negative impacts on Chinook salmon populations downstream of Shasta Dam; (2) the duration of stratification in Shasta Reservoir will likely increase under climate change, and result in warmer near surface temperatures extending later into the year; (3) outflow reductions during the spring had minimal effects on reservoir discharge temperatures and cold pool storage during the late summer and fall; (4) only January 1 reservoir elevations above 310 meters improved both discharge temperatures and cold pool volumes during the fall, which accounts for a substantial increase in reservoir volume and thus may not be feasible to obtain through fall storage conservation during the previous year; and (5) the modeled duration of stratification decreases when reservoir discharges are withheld and when January 1 reservoir elevation is increased, suggesting that larger volumes of water in Shasta Lake reduce the time during which the reservoir is stratified. These findings

suggest that managing Shasta Lake for water temperatures will be more difficult under projected climate change conditions, and that efforts to increase the reservoir volume in the spring of a drought year or during the fall of the previous year may not be realistic management options.

Acknowledgements

This project was funded by the U.S. Bureau of Reclamation and National Oceanic and Atmospheric Administration. David Busby was funded on National Science Foundation Research Experiences for Undergraduates Program at the University of Nevada Reno (Award Number 1263352). We thank Tracy Vermeyen, June Borgwat, Paul Zedonis, and Janet Martin of the U.S. Bureau of Reclamation, Katherine Clancey and Nicole Goehring from the University of Nevada Reno, Jason Caldwell from MetStat, Inc., as well as Cherisa Friedlander, Skip Bertolino, and Andrew Pike from National Oceanic and Atmospheric Administration for providing field support and insights into the project.

References

AghaKouchak, A., L. Cheng, O. Mazdiyasni, and A. Farahmand. 2014. Global warming and changes in risk of concurrent climate extremes: Insights from the 2014 California drought. Geophysical Research Letters 41:8847–8852.

Bartholow, J. M. 2004. Modeling Chinook Salmon with SALMOD on the Sacramento River, California. Hydroecologie Appliquee 1:193–219.

Bartholow, J. M., R. B. Hanna, L. Saito, D. Lieberman, and M. Horn. 2001. Simulated limnological effects of the Shasta Lake temperature control device. Environmental Management 27:609–626.

Brekke, L. D., E. P. Maurer, J. D. Anderson, M. D. Dettinger, E. S. Townsley, A. Harrison, and T. Pruitt. 2009. Assessing reservoir operations risk under climate change. Water Resources Research 45:1–16.

Brekke, L.D., N.L. Miller, K.E. Bashford, N.W.T. Quinn, J. A. Dracup, 2004. Climate

Change Impacts Uncertainty for Water Resources in the San Joaquin River Basin, California. J. Am. Water Resour. Assoc. 40, 149–164. doi:10.1111/j.1752-1688.2004.tb01016.x

California Climate Change Center. 2012. Our Changing Climate 2012: Vulnerability & Adaptation to the Increasing Risks from Climate Change in California. A Summary Report on the Third Assessment from the California Climate Change Center. CEC-500-2012-007. Date Accessed: June 10 2016. http://www.energy.ca.gov/2012publications/

Chang, H., and I. W. Jung. 2010. Spatial and temporal changes in runoff caused by climate change in a complex large river basin in Oregon. Journal of Hydrology 388:186–207.

Chang, H., and K. Lawler. 2011. Impacts of Climate Variability and Change on Water Temperature in an Urbanizing Oregon Basin, USA. International Union of Geodesy and Geophysics 348:123–128.

Clancey, K., L. Saito, K. Hellmann, C. Svoboda, J. Hannon, and R. Beckwith. (in press). Evaluating head-of-reservoir water temperature for juvenile Chinook Salmon and Steelhead at Shasta Lake with modeled temperature curtains. Accepted to North American Journal of Fisheries Management.

Cole, T., and S. Wells. 2011. CE-QUAL-W2: A two-dimensional, laterally averaged, hydrodynamic and water quality model, version 3.7. User Manual. Instruction Report EL-11-1. US Army Corps of Engineers, Washington (DC).

Gelda, R. K., E. M. Owens, and S. W. Effler. 1998. Calibration, verification, and an application of a two-dimensional hydrothermal model [CE-QUAL-W2 (t)] for Cannonsville Reservoir. Lake and Reservoir Management 14:186–196.

Griffin, D., K.J. Anchukaitis, 2014. How unusual is the 2012 – 2014 California drought ? Geophys. Res. Lett. 41, 9017–9023. doi:10.1002/2014GL062433.1.

Hanna, R. B., L. Saito, and J. M. Bartholow. 1999. Results of Simulated Temperature Control Device Operations on In-Reservoir and Discharge Water Temperatures Using CE-QUAL-W2. Lake and Reservoir Management 15:87–102.

Harvey, D., S. Hassol, 1997. Scaling From Site-Specific Observations to Global Model Grids, Aspen Global Change Institute.

Higgs, J. A., and T. B. Vermeyen. 1999. Shasta Temperature Control Device CFD Modeling Study. U.S. Bureau of Reclamation Technical Services Center, Water Resources Research Laboratory.

Joyce, E. 2016, January 21. California Drought Improves; 2015 Warmest Year On Record. Capital Public Radio. Date Accessed: May 14 2017.

http://www.capradio.org/articles/

Mateus, M. C., and D. Tullos. 2017. Reliability, Sensitivity, and Vulnerability of Reservoir Operations under Climate Change. Journal of Water Resources Planning and Management 143(4):4016085.

McCullough, D., 1999. A review and synthesis of effects of alterations to the water temperature regime on freshwater life stages of salmonids, with special reference to Chinook salmon. Region 10 Water Resources Assessment Report No. 910-R-99-010, United States EPA, Seattle.

Mills, T., D. R. McEwan, and M. R. Jennings. 1997. California Salmon and Steelhead: Beyond the Crossroads. In: Stouder, D. J., P. A. Bisson, and R. J. Naiman. 1997. Pacific Salmon and their ecosystems: status and future options. Chapman and Hall, New York, N.Y. Pages 375–387.

NMFS, National Marine Fisheries Service. 2011. 5-Year Review: Summary and Evaluation of Sacramento River Winter-run Chinook Salmon ESU. Long Beach.

Nickel, D. K., M. T. Brett, and A. D. Jassby. 2004. Factors regulating Shasta Lake (California) cold water accumulation, a resource for endangered salmon conservation. Water Resources Research 40:W05204.

Nowlin, W. H., J.-M. Davies, R. N. Nordin, and A. Mazumder. 2004. Effects of Water Level Fluctuation and Short-Term Climate Variation on Thermal and Stratification Regimes of a British Columbia Reservoir and Lake. Lake and Reservoir Management 20:91–109.

Robertson, D.M., R.A. Ragotzkie, 1990. Changes in the thermal structure of moderate to large sized lakes in response to changes in air temperature. Aquatc Science 52, 360–380. doi:10.1007/BF00879763

Saito, L. 1999. Interdisciplinary Modeling at Shasta Lake. Colorado State University (Ph.D. dissertation).

Saito, L., B. M. Johnson, J. M. Bartholow, and R. B. Hanna. 2001. Assessing ecosystem effects of reservoir operations using food web-energy transfer and water quality models. Ecosystems 4:105–125.

Sapin, J. 2014. Impacts of Reservoir Operations with Extreme Hydrologic and Climatic Conditions on Fish Sustainability below Shasta Lake. University of Nevada, Reno (M.S. thesis).

Sapin, J. R., L. Saito, A. Dai, B. Rajagopalan, and R. B. Hanna. (2017). Demonstration of Integrated Reservoir Operations and Extreme Hydroclimate Modeling of Water Temperatures for Fish Sustainability below Shasta Lake. Journal of Water Resources Planning and Management. 143(10), 04017062.

DOI:10.1061/(ASCE)WR.1943-5452.0000834

Stene, E. A. 1996. Shasta Division: Central Valley Project. Bureau of Reclamation.

Stewart, I. T., D. R. Cayan, and M. D. Dettinger. 2004. Changes in snowmelt runoff timing in western North America under a “business as usual” climate change scenario. Climatic Change 62:217–232.

Swain, D., M. Tsiang, M. Haugen, D. Singh, A. Charland, B. Rajaratnam, and N. Diffenbaugh. 2014. The Extraordinary California Drought of 2013/2014: Character, Context, and the Role of Climate Change. American Meteorological Society 95:S2–S7.

Trenberth, K. E., A. Dai, G. Van Der Schrier, P. D. Jones, J. Barichivich, K. R. Briffa, and J. Sheffield. 2014. Global warming and changes in drought. Nature Climate Change 4:17–22.

Trinh, T., S. Jang, K. Ishida, N. Ohara, Z. Q. Chen, M. L. Anderson, Y. Darama, J. Chen, and M. L. Kavvas. 2016. Reconstruction of historical inflows into and water supply from Shasta Dam by coupling physically based hydroclimate model with reservoir operation model. Journal of Hydrologic Engineering 21:1–12.

USBR, US Bureau of Reclamation, 2015. Shasta Lake Water Resources Investigation: Feasibility Report, Department of the Interior. Mid-Pacific Region. doi:10.1017/CBO9781107415324.004

USBR, US Bureau of Reclamation, 2008. Biological Assessment on the Continued Long-term Operations of the Central Valley Project and the State Water Project. Mid-Pacific Region.

USBR, US Bureau of Reclamation, 1998. Shasta Dam and Reservoir Enlargement. Mid-Pacific Region.

Chapter 3: Improved model representation of the 2015 drought at Lake Shasta, California

[1]Rachel Hallnan, [2]Laurel Saito, [3]Scott Tyler, [4]Eric Danner, [5]Miles Daniels, and [6]Mark Hausner

[1]Graduate Research Assistant
Graduate Program of Hydrologic Sciences,
University of Nevada – Reno
Reno, NV, USA 89557

[2]Nevada Water Program Director
The Nature Conservancy
1 East First Street Suite 1007, Reno, NV, USA 89501

[3]Professor
Department of Geological Sciences and Engineering
University of Nevada – Reno, Mail Stop 172
Reno, NV, USA 89557

[4]Research Ecologist
NOAA Fisheries
110 Shaffer Rd, Santa Cruz, CA, USA 95060

[5]Associate Specialist
University of California, Santa Cruz
Institute of Marine Sciences
1156 High Street, Santa Cruz, CA 95064

[6]Assistant Research Professor
Desert Research Institute
775 E. Flamingo Rd, Las Vegas, Nevada 89119

Abstract

Reservoir managers at Shasta Dam in northern California face increased difficulty in managing discharge and reservoir temperatures for downstream habitat of endangered Chinook salmon, particularly during years of drought. California experienced its driest and warmest consecutive years ever recorded between 2012 and 2015. A pilot deployment of distributed temperature sensing (DTS) technology at Shasta Dam during 2015-16 captured high-resolution temperature data of the reservoir conditions during this drought, and showed a large reduction of cold water in the reservoir during fall 2015. The high-resolution DTS data provided a valuable dataset for improving the resolution of hydrodynamic modeling of temperatures at Shasta Lake. The DTS data were compared to modeled temperature profiles from a CE-QUAL-W2 model of Shasta Lake with three different model layer resolutions of reservoir bathymetry, and were used to assess the ability to each model configuration to capture reservoir temperature conditions. The comparison suggests that the model with the highest spatial resolution along the depth profile is the best at simulating measured DTS temperatures in the fall of 2015 and spring of 2016. DTS technology is shown here to be useful in aiding hydrodynamic modeling efforts of reservoir temperatures, a new application of the technology.

Keywords

Distributed temperature sensing, hydrodynamic modeling, CE-QUAL-W2, model resolution, reservoir temperatures, Chinook salmon

Introduction

Increased population and development of the western United States, coupled with droughts and rising annual air temperatures associated with climate change, place increasing stress on existing water resources (Stene 1996, Luo et al. 2017). The driest and warmest four consecutive years in California occurred between 2012 and 2015, creating the worst drought in over a century (Griffin and Anchukaitis 2014, He et al. 2017). More frequent and extreme droughts are expected with climate change, and will likely result in warmer water temperatures in rivers and reservoirs in California (Brekke et al. 2009). Similarly, earlier spring snowmelt runoff as a result of warmer air temperatures may cause increased winter and spring flooding, while extending the duration of summer droughts throughout the western U.S. (Stewart et al. 2004). In light of these predictions, reservoir managers face increased pressure to implement management policies that will continue to meet the needs of both downstream users and ecosystems.

Following the construction of Shasta Dam in 1945 in northern California, winter-run Chinook salmon in the downstream Sacramento River faced population declines that caused them to be listed as endangered under the Endangered Species Act (ESA) in 1993 (NMFS 2011). In order to mitigate these declines, a selective withdrawal structure called a temperature control device (TCD) began operating at Shasta Dam in 1997 (Bartholow et al. 2001). This device allows managers to control downstream water temperatures while still generating hydropower through the penstocks. Selective withdrawals from the near-surface occur during the winter and spring, while colder water at depth is conserved for release during the summer-fall period (Bartholow et al. 2001). This strategy aims to provide appropriate downstream temperatures for spawning and rearing of Chinook

salmon by taking advantage of density-driven temperature stratification within the reservoir. Such operations assist managers with meeting mandated temperature thresholds set downstream of the dam (Nickel et al. 2004). Temperature profile measurements just upstream of Shasta Dam in the reservoir allow managers to better understand the thermal resources available to them for selective withdrawal throughout the year in order to maintain downstream temperature thresholds.

The physical structure of Lake Shasta can be classified as monomictic, meaning that the reservoir typically mixes once per year (Bartholow et al. 2001). Warm air temperatures during the summer result in strong thermal stratification and a defined thermocline. As the fall progresses, cooler air temperatures lessen the temperature gradient between the epilimnion and hypolimnion. Once this gradient is low enough to allow mixing, the lake turns over and experiences isothermal conditions throughout the winter. Rains and snowmelt recharge the reservoir between December and March (Bartholow et al. 2001).

Understanding stratification patterns is important for modeling lake hydrodynamics (Ellis et al. 1991). This is especially true for reservoirs because temperature dynamics can be influenced by reservoir operations. At reservoirs such as Shasta where large withdrawals occur, a withdrawal zone develops near the outlets. Reservoir stratification has an impact on both the size and geometry of the withdrawal zone (Deas and Lowney 2000) because stratification inhibits vertical mixing within the reservoir profile (Ellis et al. 1991). The duration of stratification can also be shorter when large amounts of reservoir drawdown occur (Gelda et al. 1998). Thus, understanding

reservoir temperature dynamics is important for informing reservoir operations for downstream temperature control and to aid decision making throughout the year.

Hydrologic processes occur at a variety of spatial and temporal scales ranging from the micro-scale to the macro-scale. Traditionally, water temperature dynamics such as stream mixing or reservoir stratification have been measured with point sensors, such as HOBO temperature loggers or sondes (Ellis et al. 1991, Sinokrot and Stefan 1993, Brown et al. 2005). To capture processes occurring at multiple spatial scales, scientists may deploy many point sensors in close proximity to each other. This is neither cost effective nor efficient (Selker et al. 2006a). Over the past decade or so, distributed temperature sensing (DTS) technology has been applied in hydrologic systems as an alternative to point sensor measurements of temperature. DTS allows for temperature data of high spatial and temporal resolution to be collected along the length of a standard fiber optic communications cable (Selker et al. 2006b).

The general concept of DTS technology is to observe the time it takes a laser pulse to travel along a known distance of fiber optic cable at a known speed (i.e., the speed of light). In a fiber optic cable, light is backscattered at each point due to the crystalline structure of glass. The location of backscatter can be determined by measuring the time it takes light to travel out from the DTS instrument to a given molecule and return. The temperature of the glass at the location of backscatter can then be determined from a relationship between backscattered Raman spectra frequencies, called Stokes and Anti-Stokes (Selker et al. 2006b, Hausner et al. 2011). More explanation of this process is described in Appendix E.

DTS technology has been applied in a variety of hydrologic settings to measure temperature dynamics. Selker et al. (2006a) used DTS fiber optic technology to quantify stream temperature dynamics and groundwater inflows for the Maisbich stream in Luxembourg. This study was the first to use DTS technology in the context of stream flow. Kobs et al. (2014) successfully quantified basal melting of the ice shelf to the ocean by generating thermal profiles of Antarctic ice sheets. Additionally, Hausner et al. (2013) used DTS technology in conjunction with computational fluid dynamics modeling to classify the thermal regime of Devils Hole, California. Model output temperatures were compared to temperatures recorded by a DTS instrument installed at Devils Hole (Hausner et al. 2013).

The high resolution obtainable by DTS systems has also been used to observe stratification, mixing, interface erosion, and freshwater re-supply in a solar pond at scales that may not have been achievable with traditional temperature sensors (Suarez et al. 2011). Tyler et al. (2009) further discuss the use of DTS technology in a stratified limnologic setting. A DTS cable deployed in Lake Tahoe, California successfully captured the thermal stratification of the lake. Internal gravity waves created by several days of high wind were identified through observed small-scale oscillations of the thermocline (Tyler et al. 2009). Both studies demonstrate the ability of DTS technology to capture high-resolution temperature dynamics within stratified hydrologic systems.

A pilot deployment of a DTS instrument and fiber optic cable was completed at Shasta Lake, California, and has been collecting data since August 19, 2015. Temperatures upstream of the dam are currently monitored by the United States Bureau of Reclamation (USBR) using sonde data profiles taken approximately every 2 weeks,

and a HOBO temperature monitoring string that collects data every 15 minutes that is attached to an exclusion zone buoy line around the TCD. Sonde data profiles provide spatial resolution between 0.001 meters near the surface and 3 meters at depth. The HOBO temperature loggers provide a spatial resolution between approximately 3 and 8 meters. Thus, the sonde profiles provide relatively high spatial resolution with low temporal resolution, while the HOBO data loggers have relatively high temporal resolution with lower spatial resolution. An additional constraint is that the HOBO data are downloaded only every three to five months.

The DTS data provide an alternative method of monitoring the temperature profile upstream of Shasta Dam that is characterized by both high spatial and temporal resolution, and thus provide a better understanding of the thermal stratification patterns in Shasta Reservoir. The high-resolution data obtained by the DTS offer an opportunity to examine changes in the thermal structure of the reservoir at a finer resolution, and to inform existing modeling efforts at Lake Shasta. Access to more frequent, higher resolution water temperature profiles behind the dam in the form of both measured DTS data and higher resolution simulated temperature data within the reservoir may improve the ability to meet downstream temperature requirements through use of the TCD. This paper describes the DTS pilot deployment at Lake Shasta, methods of calibration, and the data collected between August 19, 2015 and June 1, 2016, and their use to inform hydrodynamic modeling at Lake Shasta.

Several modeling efforts have been completed at Shasta Reservoir using CE-QUAL-W2, a two-dimensional hydrodynamic model developed by the U.S. Army Corps of Engineers (Cole and Wells 2011). These include investigating the impact of the TCD

on changes in reservoir ecology and downstream water temperature patterns (Hanna et al. 1999, Bartholow et al. 2001, Saito et al. 2001a, 2001b); simulating impacts of extreme climatic conditions and reservoir operations on downstream temperature management in the Sacramento River (Sapin et al. 2017); and the evaluation of reservoir temperature conditions for downstream juvenile fish passage (Clancey et al. in press). Sapin et al. (2017) found that the low resolution provided by CE-QUAL-W2 at depth in the reservoir created large amounts of uncertainty in calculating cold pool storage, a key metric in assessing the cold water resources available to managers to meet downstream temperature thresholds. Cold pool storage was calculated as the volume of water in the reservoir less than or equal to 9°C (Sapin et al. 2017). Clancey et al. (in press) also recommended higher model resolution along the tributary segments to assess tributary temperatures for fish passage.

The current CE-QUAL-W2 model of Lake Shasta consists of 63 segments along the length of the reservoir, and up to 60 layers, depending on water surface elevation. The depth of each layer depends on its location within the depth profile: the top 30 layers have 1.5 meter depths and are followed by 19 layers with 3 meter depths, and then 11 layers having 6 meter depths at the reservoir bottom. The thick bottom layers of this model result in coarse resolution for estimation of the amount of cold pool storage on a given date. This may make downstream temperature management more difficult. The high spatial resolution DTS data collected in 2015-16 provide an opportunity to examine the performance of the W2 model of Lake Shasta with higher bathymetric resolution. This paper describes an assessment of the Lake Shasta CE-QUAL-W2 model's ability to

represent the 2015 drought with the original model bathymetry and two alternative finer vertical bathymetric resolutions.

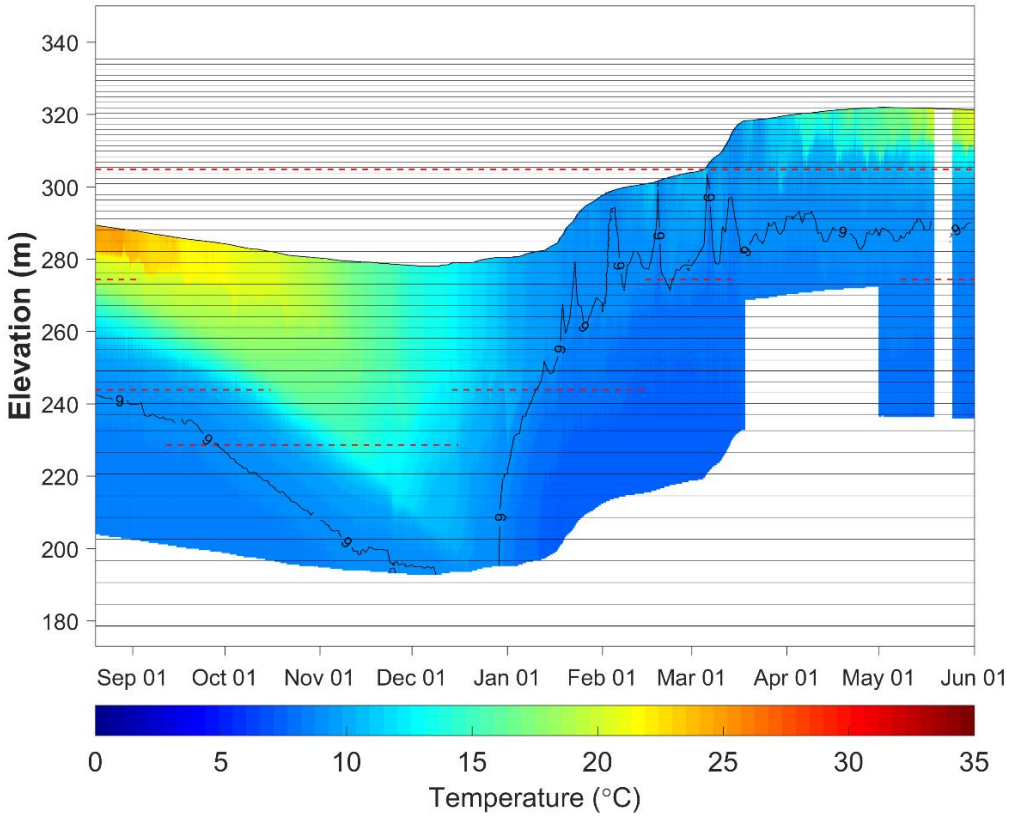

Figure 8. Temperature profile captured just upstream of Shasta Dam by DTS technology from August 19, 2015 through June 1, 2016. Cold pool threshold temperature of 9.0°C is shown with a black contour. W2 model layers are shown with black horizontal lines. Dashed red lines represent the elevation of TCD gates (upper, middle, lower, and side) when they were open during actual Shasta Dam operations in 2015 and 2016. Measurements from a fixed length of cable are plotted, so the water surface and the bottom of the plot move up and down as the reservoir water surface rises and falls. White space during the spring represents missing data due to power outage or cable malfunction.

Methods

DTS deployment at Lake Shasta

A Silixa Ultima DTS provided by the Center for Transformative Environmental Monitoring Programs (CTEMPs) was used to monitor temperatures along a vertical

profile of the reservoir behind Shasta Dam from August 19, 2015, to August 25, 2016 (only data through June 30 2016 is presented in this study to overlap with the 18-month W2 model timeframe). CTEMPs is a joint program between Oregon State University and the University of Nevada, Reno that provides environmental monitoring systems such as DTS for short and intermediate-term projects (CTEMPS 2015). The DTS instrument was placed inside the dam just behind the fifth coaster gate room door (Figure 9). The device was placed inside the dam to minimize ambient temperature fluctuations (Suarez et al. 2011). A wireless modem was installed just outside the coaster gate room door, which connects directly to the Silixa Ultima.

A 0.9525 centimeter (3/8 inch) diameter fiber optic cable with a braided stainless steel outer shield was deployed in the reservoir. The cable begins at the Silixa Ultima and proceeds directly into an ambient temperature calibration bath. Approximately 10 meters of cable is coiled within the ambient temperature water bath. Four independent temperature sensors are also located within the bath: two PT100 temperature probes that connect directly to the Silixa Ultima, and two RBRSolo temperature probes that contain an internal USB that stores data. The cable then extends out the coaster gate room door, down the side of the TCD into the reservoir, and along an exclusion zone buoy line to its farthest point. At this location, the cable drops vertically into the reservoir, and then returns to the surface where it terminates (Figure 9 and 10).

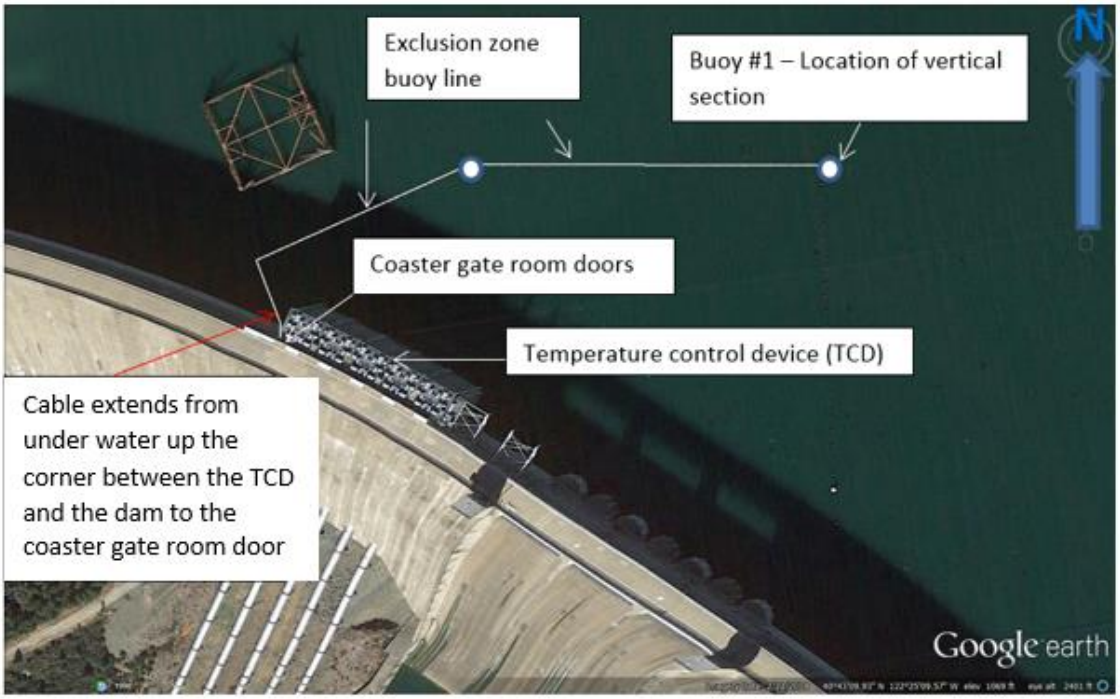

Figure 9. Plan view of cable deployment at Shasta Lake. White line indicates path of cable, and the red arrow indicates the location of the DTS instrument.

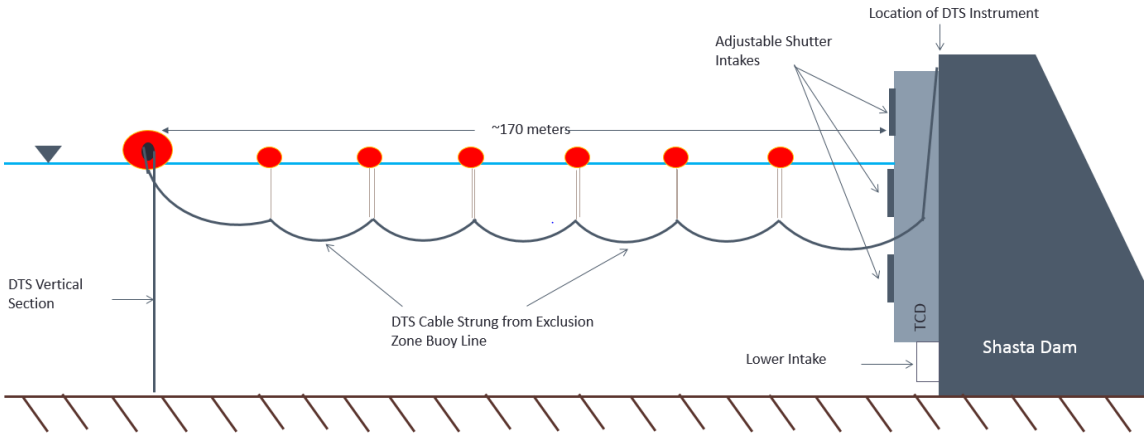

Figure 10. Schematic of DTS deployment from a side view of Shasta Dam (not to scale). The DTS instrument is located just inside the dam at the top of the TCD. The cable extends from the device, outside and down the west side of the TCD to the water. It then follows along the exclusion zone buoy line (orange circles) and down from the water surface to the vertical water profile.

Data acquisition and calibration

DTS data collected at Shasta Dam were transmitted to a server run by CTEMPS every four hours via the wireless modem installed at the dam. From here, the data were downloaded weekly and processed via a processing routine with the following output parameters: distance along cable, internally calibrated temperature, date and time of measurement, Stokes frequency, and anti-Stokes frequency. These data were internally calibrated by the DTS Silixa Ultima instrument. Internal calibration used the two PT100 temperature probes located in the temperature bath and directly connected to the instrument. The data were re-calibrated using a single-ended Raman distributed temperature sensing method (Hausner et al. 2011). The governing equation is as follows:

$$T(z) = \frac{\gamma}{\ln\frac{P_S(z)}{P_{as}(z)} + C - \Delta\alpha z} \quad (1)$$

where T(z) refers to temperature at a specific z location along the cable, γ, α, and C are calibration parameters, and $P_S(z)$ and $P_{aS}(z)$ are the frequency of the Stokes and anti-Stokes backscatter, respectively. Three external temperature points were used in the calibration to obtain the calibration parameters. These included one of the independent temperature measurements from the ambient temperature bath, and two additional temperature measurements provided by the USBR. The USBR takes temperature profile measurements using sonde data probes every 2 – 4 weeks throughout the year at the location of the exclusion zone buoy from which the DTS vertical profile was deployed. The sonde temperatures at the location corresponding to the deepest extent of the DTS cable in the vertical profile were used as second and third calibration points (one at the bottom for the descending cable, and one at the bottom for the ascending cable). This location was chosen because temperatures at depth remain relatively constant throughout

the measurement timeframe, varying between approximately 10°C in August 2015 and 7°C in July 2016. Since the sonde profiles were available only every several weeks, calibration parameters were held constant between measurements. Calibrated DTS temperature data had an average R^2 of 0.996, % bias of 3.880, and root-mean-squared-error (RMSE) of 0.587°C compared to measured sonde temperature profiles (Table 20 and Figures 34, 35, 36, and 37 in Appendix F). All measured water temperatures in the remainder of this paper are from calibrated DTS temperature profiles.

Updated CE-QUAL-W2 bathymetry

Two alternative bathymetric resolutions for the original 60-layer W2 model of Lake Shasta (Figure 11a; Table 21 in Appendix G) were developed: (1) a 90-layer W2 version (Figure 11b), and (2) a 109-layer W2 version (Figure 11c). From this point forward, the three versions will be referred to as the "60-layer W2 model," the "90-layer W2 model," and the "109-layer W2 model." The 90-layer W2 model has 1.5-meter layer thicknesses between 336.81 meters (top model elevation) and 292.56 meters, 3-meter layer thicknesses between 292.56 meters and 235.56 meters, and 1.5-meter layer thicknesses from 235.56 meters to 175.56 meters (the bottom reservoir elevation; Figure 11b). The 109-layer W2 model has 1.5-meter layer thicknesses throughout the depth profile from 335.81 meters to 175.56 meters (Figure 11c). The lengths and widths of model segments were not changed from the original 60-layer W2 model. Thus, the total reservoir volume for each model version stayed essentially the same (Appendix H).

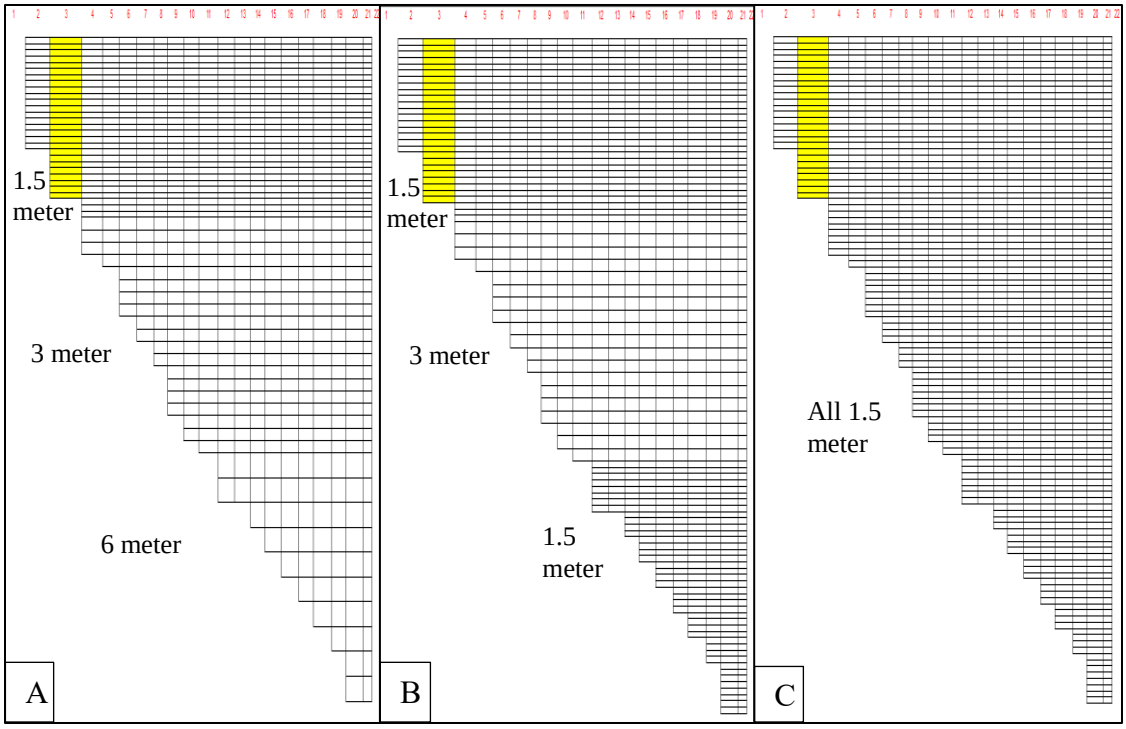

Figure 11. Lake Shasta W2 model resolution for the main body of the reservoir (segments 1 – 22) for (A) the 60-layer W2 model, (B) the-90 layer W2 model, and (C) the 109-layer W2 model. The longitudinal length of model segments is not to scale.

Model setup

The required input data for the Shasta W2 model includes bathymetry, inflow quantities for four tributaries (Pit River, Squaw Creek, McCloud River, and Sacramento River), inflow temperatures, outflow quantities, reservoir operations, and meteorological data (Hanna et al. 1999). A regression relationship from Saito (1999) was used to calculate the inflows for Squaw Creek from McCloud River flows because Squaw Creek flows are unavailable after 1963. An 18-month model for 2015-16 (i.e., January 1, 2015 to June 30, 2016) was chosen to overlap with the DTS data collection time period, and to capture stratification in fall of 2015, isothermal conditions in winter of 2016, and the onset of stratification in spring of 2016. Personnel at NOAA Fisheries provided all model input data for the 18-month model timeframe in 2015-16, which they obtained from the

sources noted in Table 5.

Table 5. Input data collected for the CE-QUAL-W2 model.

W2 Model Input Data	**Data Source:**	**Temporal Resolution**
Hydrologic Data, Shasta Lake, CA (Reservoir Storage, Reservoir Outflow)	CDEC[1]	Daily
Tributary Inflows (Sacramento, McCloud, and Pit River)	CDEC[1]	Hourly
Tributary Water Temperatures (Sacramento, McCloud, and Pit River)	CDEC[1]	Hourly
Gate Operations (Upper, Middle, Lower, and Side Gates)	USBR[2]	Daily
Meteorological Data (Air Temperature, Dewpoint Temperature, Wind Speed, Wind Direction, Cloud Cover	NARR[3]	Hourly

1. CDEC = California Data Exchange Center - http://cdec.water.ca.gov/
2. USBR = United States Bureau of Reclamation
3. NARR = North American Regional Reanalysis - https://www.ncdc.noaa.gov/data-access/model-data/model-datasets/north-american-regional-reanalysis-narr

Model recalibration

The original 60-layer W2 model of Shasta was calibrated for 1995, the only year when temperature profiles were taken throughout the reservoir. The calibrated 60-layer W2 model had an average R^2 of 0.966 and an average RMSE of 0.947°C for 1995. The 90-layer W2 model and 109-layer W2 model were re-calibrated using 1995 input data. The original 60-layer W2 model of Lake Shasta was sensitive to adjustments made to five specific calibration coefficients: wind sheltering coefficient (WSC), coefficient of bottom heat exchange (CBHE), temperature of the sediments (TSED), and light extinction coefficients (EXH2O and BETA) (Hanna et al. 1999). These five values were adjusted within the ranges specified in the CE-QUAL-W2 manual (Cole and Wells 2011) for both the 90-layer W2 model and the 109-layer model. The model output was checked by 1)

comparing the modeled and measured reservoir elevation throughout 1995, and 2) comparing modeled reservoir temperature profiles from segments 13, 16, 19, 41, and 53/54 to measured temperature profiles in those locations within the reservoir and tributaries on Julian days 131, 171, 207, 242, 265, 292, and 318 in 1995 (Figure 12). Comparisons were assessed using RMSE, percent bias, and R^2.

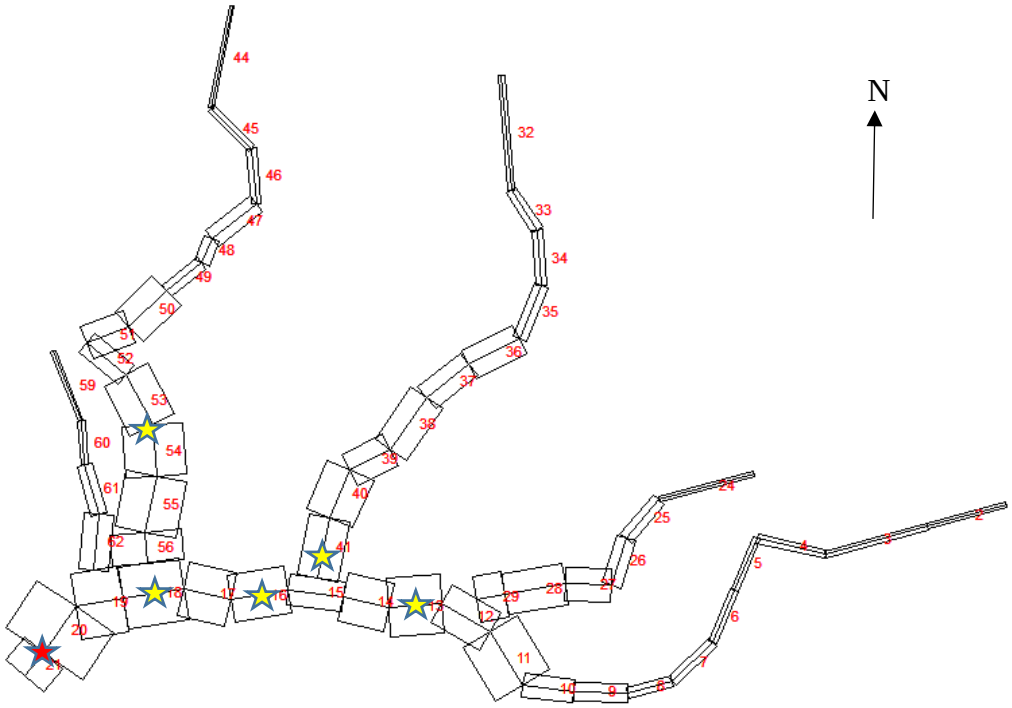

Figure 12. Spatial location of CE-QUAL-W2 model segments for Shasta Reservoir. Model segments corresponding to temperature profiles taken in 1995 and used for calibration are noted with yellow stars. The general location of the DTS vertical profile and sonde data profiles is indicated with a red star.

Shasta W2 model comparisons to DTS data

The following sections describe the three methods used to compare each W2 model with different bathymetric resolutions to the DTS data: (a) temperature profile differences, (b) stratification patterns, and (c) cold pool storage.

(a) Temperature profile differences

Modeled temperatures from all three W2 models of Shasta Lake were compared to measured DTS data between August 19, 2015 and June 30, 2016. The absolute temperature difference was calculated between segment 21 modeled temperatures at 12:00 PM and DTS temperatures measured closest to 12:00 PM on each day during this time period. This was completed by developing a MATLAB code that subtracted the measured DTS temperature at each depth corresponding to the middle of each W2 model layer from the W2-simulated temperature at that depth. In addition, RMSE, percent bias, and R^2 were used to evaluate comparisons between measured DTS temperature profiles and modeled temperature profiles on 22 dates corresponding to sonde data collection by the USBR between August 20, 2015 and June 30, 2016.

(b) Stratification patterns

The onset date of stratification and the end date of stratification (Table 6) were evaluated to see how well each different bathymetric resolution model represented the changes in reservoir temperature structure that were captured by the DTS data. These metrics were evaluated because the model's ability to capture thermal stratification influences the cold pool estimates made from model results. For example, if a model predicts a shorter duration of stratification than the true lake conditions, the estimates of cold pool volume in the reservoir will likely deviate from actual cold pool volumes around the time of the year when stratification begins and ends (Deas and Lowney 2000).

The onset and end dates of stratification were calculated from simulated water temperatures for each W2 model version between August 19, 2015 and June 30, 2016, and compared to onset and end dates of stratification calculated with the DTS

temperature data. Stratification was defined as the time period when the temperature difference between the surface and 25 meter depth was >2°C (Robertson and Ragotzkie 1990). Since the DTS installment at Shasta occurred mid-way through the stratified period in 2015, and did not operate until the end of the stratified period in 2016, DTS temperature data for a complete season of stratification were not available. Therefore, the onset of stratification was calculated for the 2016 stratification period, and the end of stratification was calculated for the 2015 stratification period. Note that chronologically, this caused the calculated end date of stratification in fall of 2015 to occur before the calculated onset of stratification in spring of 2016.

Table 6. Metrics used to evaluate reservoir thermal structure.

Metric	**Parameter**
Onset of stratification	Date when temperature difference of >2°C from surface temperature becomes <25 m deep
End of Stratification	Date when temperature difference of >2°C from surface temperature becomes >25 m deep

(c) Cold pool storage

The cold pool volume in the reservoir was estimated from simulated temperatures from each of the W2 model bathymetric resolutions throughout the year. Simulated cold pool volumes estimated from each W2 model were compared to the cold pool volume calculated from the DTS temperatures on each day to evaluate each model's ability to predict cold pool storage. Cold pool was defined as the volume of water less than or equal to 9 °C (Sapin et al. 2017). The cold pool volume on November 1 was reported for each W2 model and the DTS data because it is used by reservoir managers to assess the end of the critical rearing period for juvenile endangered winter-run Chinook salmon

downstream of Shasta Dam (Bartholow 2004). The cold pool volumes on June 1 were also recorded, because it is also of interest to reservoir managers (Sapin et al. 2017)

Results

Model recalibration

The values for the five sensitive calibration parameters used in Hanna et al. (1999) were unchanged for the 60-layer W2 model (Table 7). The CBHE value was changed from 7.0 E-8 $m^{0.5}$ sec^{-1} to 0.3 $m^{0.5}$ sec^{-1} for the 90-layer W2 model and 109-layer W2 model, which is the value recommended in the CE-QUAL-W2 manual. The finer layer discretization near the bottom of the reservoir may allow more heat exchange to occur between the reservoir bottom and the hypolimnion, resulting in higher sensitivity to such heat exchange with the 1.5-meter bottom layer depths, whereas the 60-layer W2 model was less sensitive to bed heat exchange. Other calibration parameters were unaltered for the 90-layer and 109-layer W2 models. The 90-layer W2 model had the best % bias and R^2 values, and the 60-layer W2 model had the best RMSE (Table 8). For a complete summary of calibration statistics across all five segments and all seven days in 1995, see Tables 23, 24, and 25 in Appendix I.

Table 7. Calibration coefficients used for the three different bathymetric resolutions of the Shasta Lake W2 model: wind sheltering coefficient (WSC), coefficient of bottom heat exchange (CBHE), temperature of the sediments (TSED), and light extinction coefficients (EXH2O and BETA).

W2 Model	WSC	CBHE ($m^{0.5}$ sec^{-1})	TSED (°C)	EXH2O (m^{-1})	BETA
60-Layer	1.0	7.0 E-8	15.9	0.40	0.45
90-Layer	1.0	0.3	15.9	0.40	0.45
109-Layer	1.0	0.3	15.9	0.40	0.45

Table 8. Calibration statistics for 1995 for the three bathymetric resolutions of W2 and measured temperature profiles in Shasta Reservoir.

W2 Model	R-Squared	% Bias	RMSE
60-Layer	0.967	3.527	0.930
90-Layer	0.968	2.987	1.028
109-Layer	0.956	5.684	1.566

Shasta W2 model comparisons to DTS data

The following sections describe results of: (a) temperature profile differences, (b) stratification patterns, and (c) cold pool storage from simulations from each W2 model with a different bathymetric resolution and the DTS data.

(a) Temperature profile differences

A full summary of statistics from simulated temperatures profiles from each W2 model versus 22 measured DTS temperature profiles for 2015-16 are in Tables 26, 27, and 28 in Appendix J. Average statistics across all dates were better for the 90-layer W2 model and the 109-layer W2 model than the 60-layer W2 model (Table 9). The 109-layer W2 model had the best R^2, % bias, and RMSE of all three W2 models.

Table 9. Average statistics for 2015/2016 for the three bathymetric resolutions of W2 and the DTS data. Positive % bias indicates warmer modeled temperatures than measured DTS temperatures.

W2 Model	R-Squared	% Bias	RMSE (°C)
60-Layer	0.928	3.262	1.256
90-Layer	0.945	2.851	0.896
109-Layer	0.946	2.377	0.816

The 60-layer model simulated a shallower temperature gradient during stratification, particularly in September and October of 2015, than did the 90-layer and 109-layer W2 models (Figures 13, 14, 17, 18, 21, and 22). In September and early October, the 90-layer W2 model simulated temperatures closer to the measured DTS temperature profiles than the 109-layer W2 model (Figures 13, 17 and 21). However, the

109-layer W2 model simulated temperatures closer to the measure DTS data beginning in mid-October through the end of 2015 than 90-layer W2 model (Figures 14, 18, and 22). Statistics for all three models were similar for January, February, and March 2016. Beginning in April 2016, the 109-layer W2 model simulated water temperatures closer to measured DTS data than the 90-layer W2 model until the end of June 2016 (Figures 20 and 24).

March 15, 2016 stood out from other dates with R^2 values of 0.39, 0.41, and 0.42 for the 60-layer W2 model, 90-layer W2 model, and 109-layer W2 model, respectively. For the same date, the % bias values were -0.78, 0.54, and 2.11, and the RMSE values were 0.63, 0.65, and 0.64 °C for the 60-layer W2 model, 90-layer W2 model, and 109-layer W2 model, respectively (Figures 15, 19, and 23; Tables 26, 27, and 28 and in Appendix J). Simulated temperature profiles on March 15 were relatively uniform throughout the profile, except for the top few meters where warmer water temperatures were simulated. In contrast, the DTS measured profile on March 15 showed slightly warmer temperatures that penetrated 25 meters down into the reservoir, although measured temperatures only varied by a magnitude of 1.896 °C through the whole profile. Thus, all three models under-represent temperatures in the upper 25 meters of the reservoir and over-represent temperatures below 25 meters depth in the reservoir during mid-March (and Figures 15, 19, and 23).

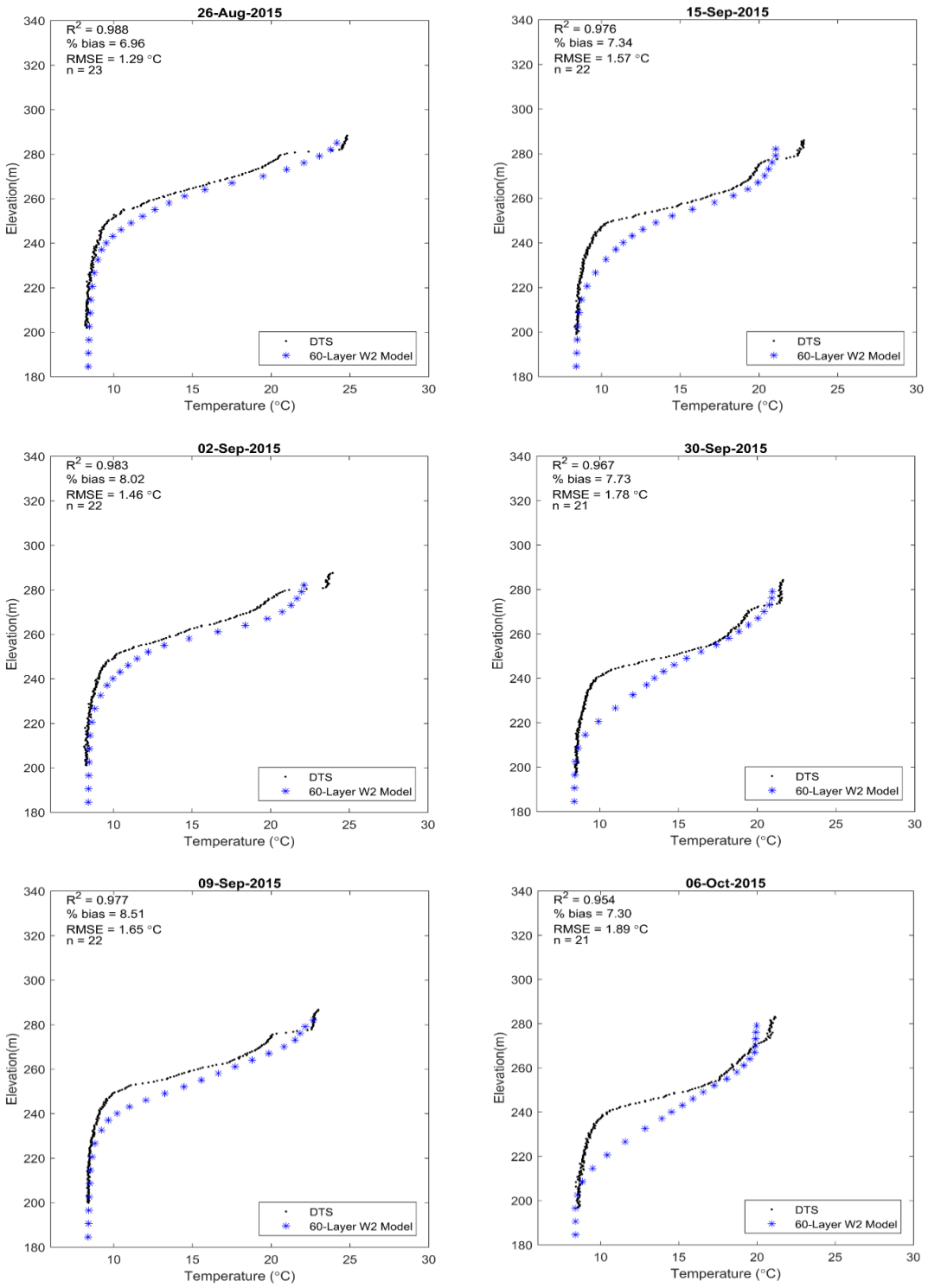

Figure 13. DTS temperature profile data just upstream of Shasta Dam compared to modeled temperature profiles for the 60-layer W2 model adjacent to the dam between August and October 2015. Positive % bias indicates warmer modeled temperatures than DTS temperatures.

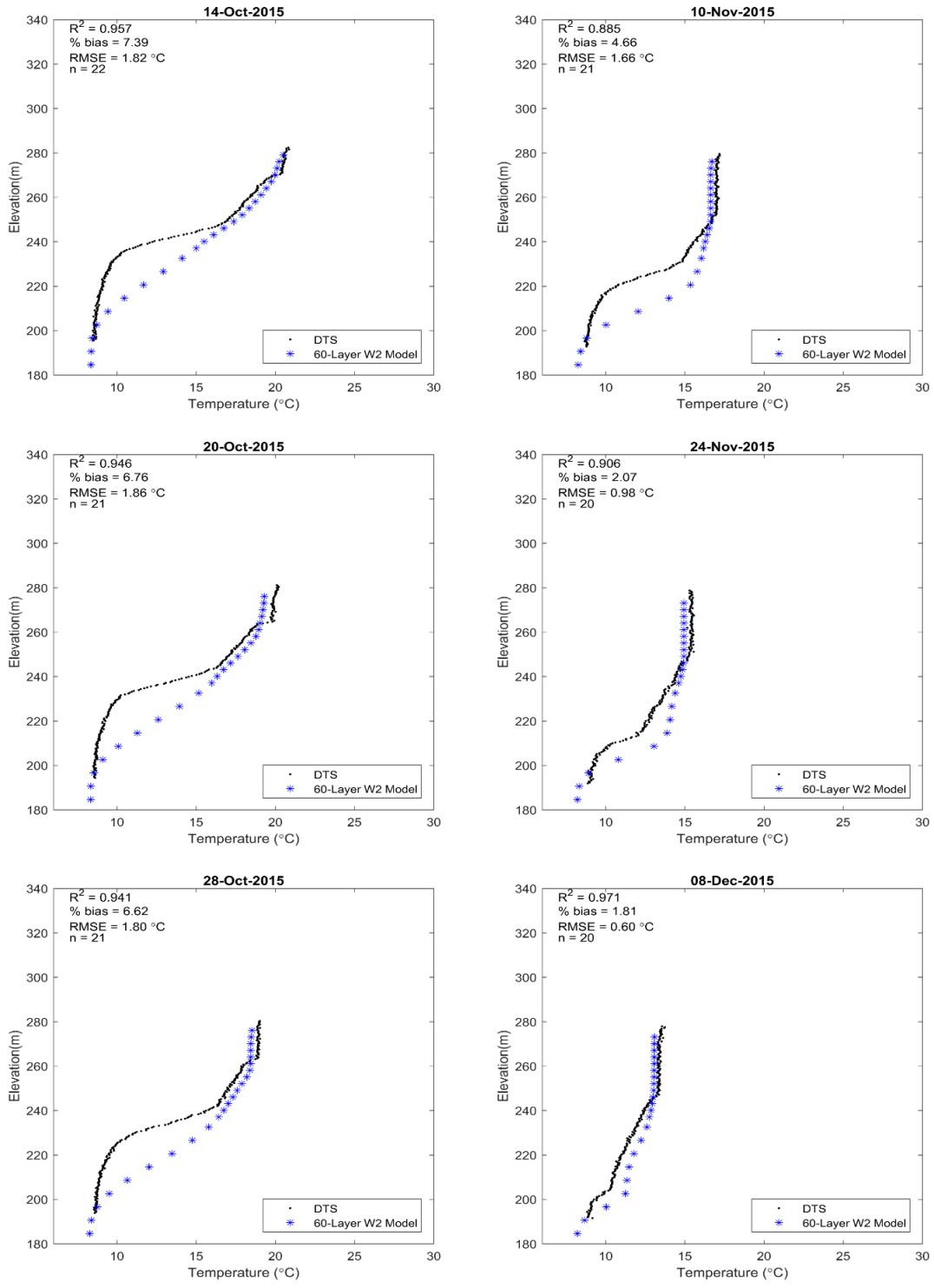

Figure 14. DTS temperature profile data just upstream of Shasta Dam compared to modeled temperature profiles for the 60-layer W2 model adjacent to the dam between October and December 2015. Positive % bias indicates warmer modeled temperatures than DTS temperatures.

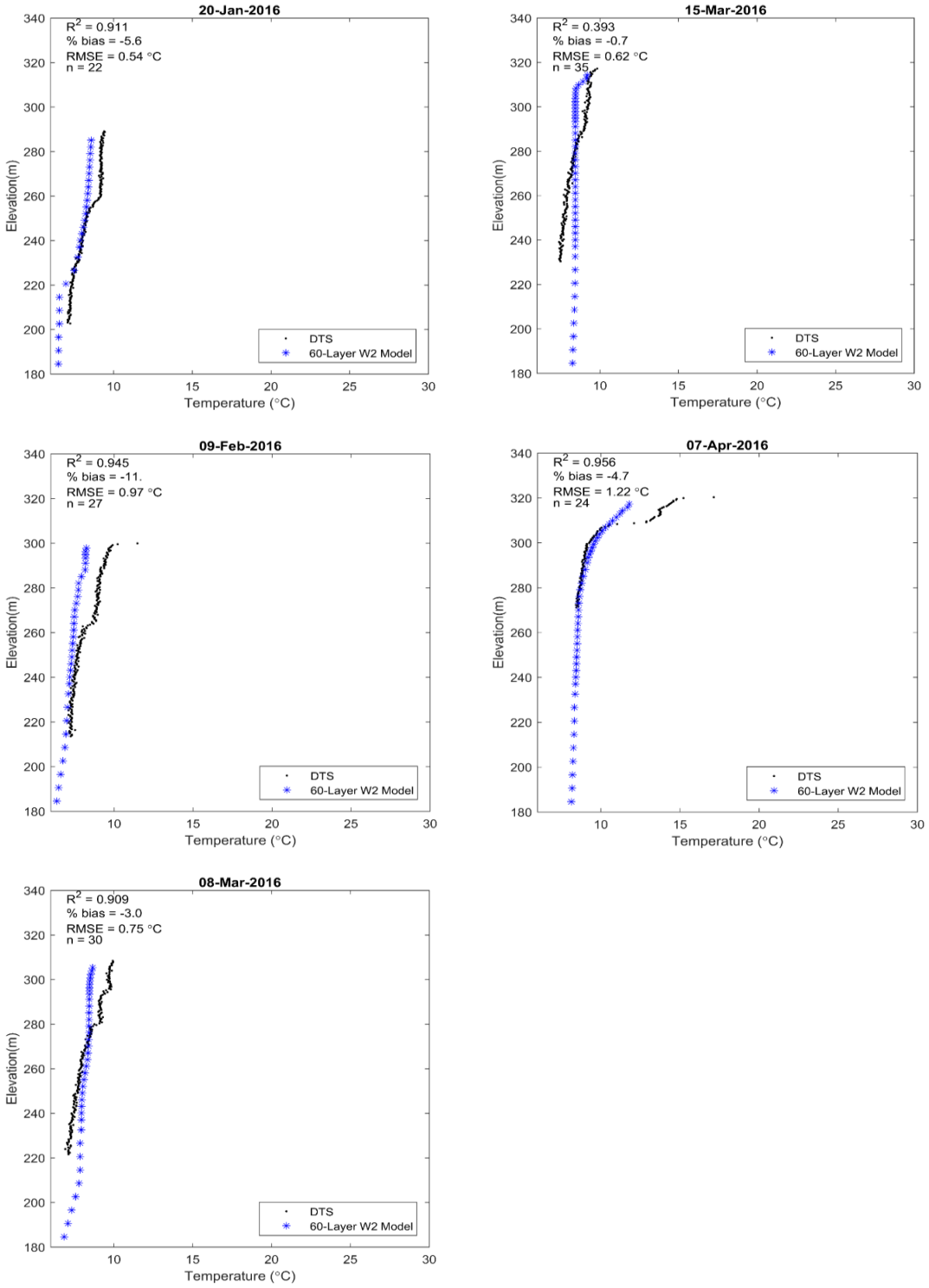

Figure 15. DTS temperature profile data just upstream of Shasta Dam compared to modeled temperature profiles for the 60-layer W2 model adjacent to the dam between January and April 2016. Positive % bias indicates warmer modeled temperatures than DTS temperatures.

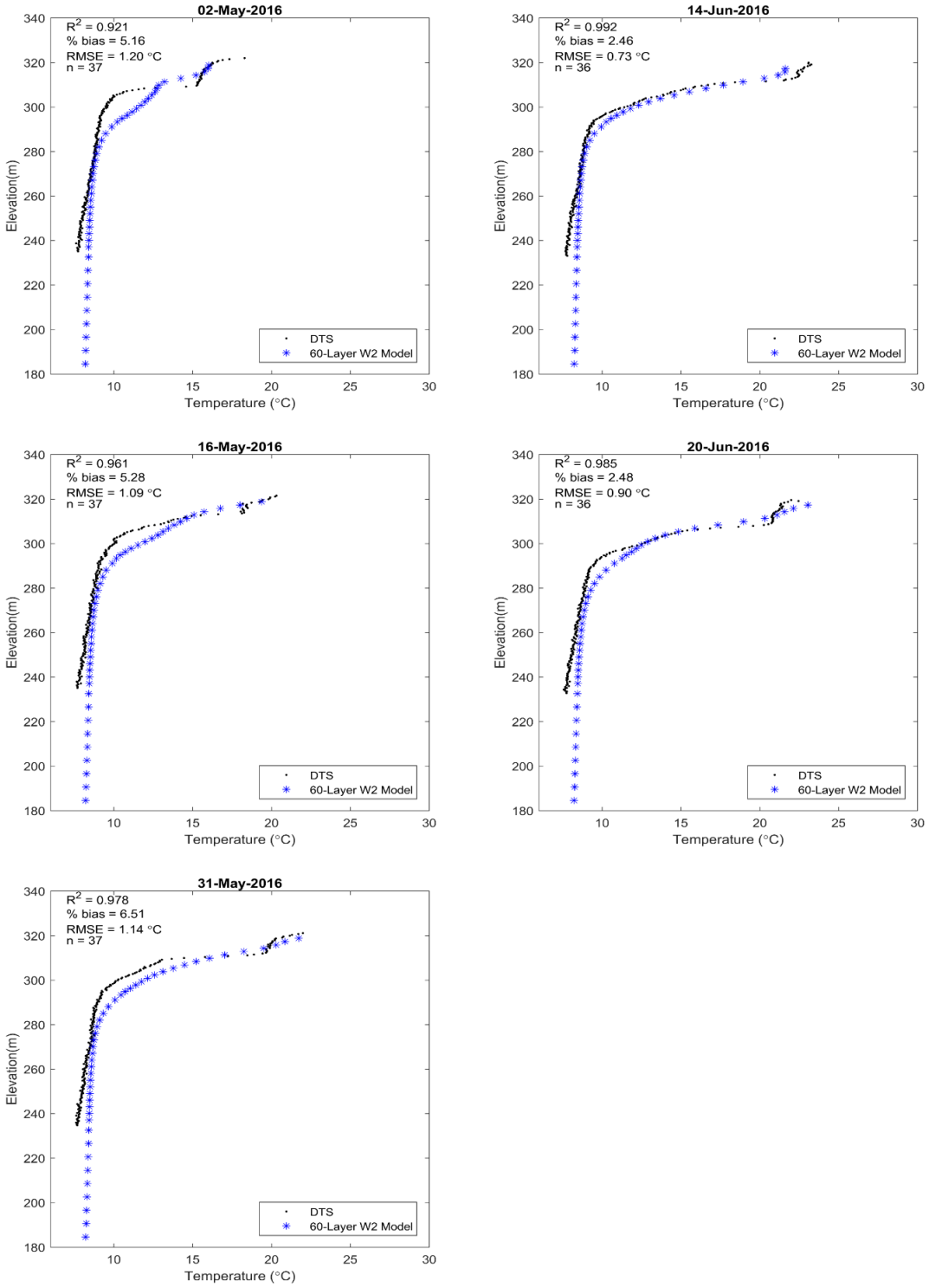

Figure 16. DTS temperature profile data just upstream of Shasta Dam compared to modeled temperature profiles for the 60-layer W2 model adjacent to the dam between May and June 2016. Positive % bias indicates warmer modeled temperatures than DTS temperatures.

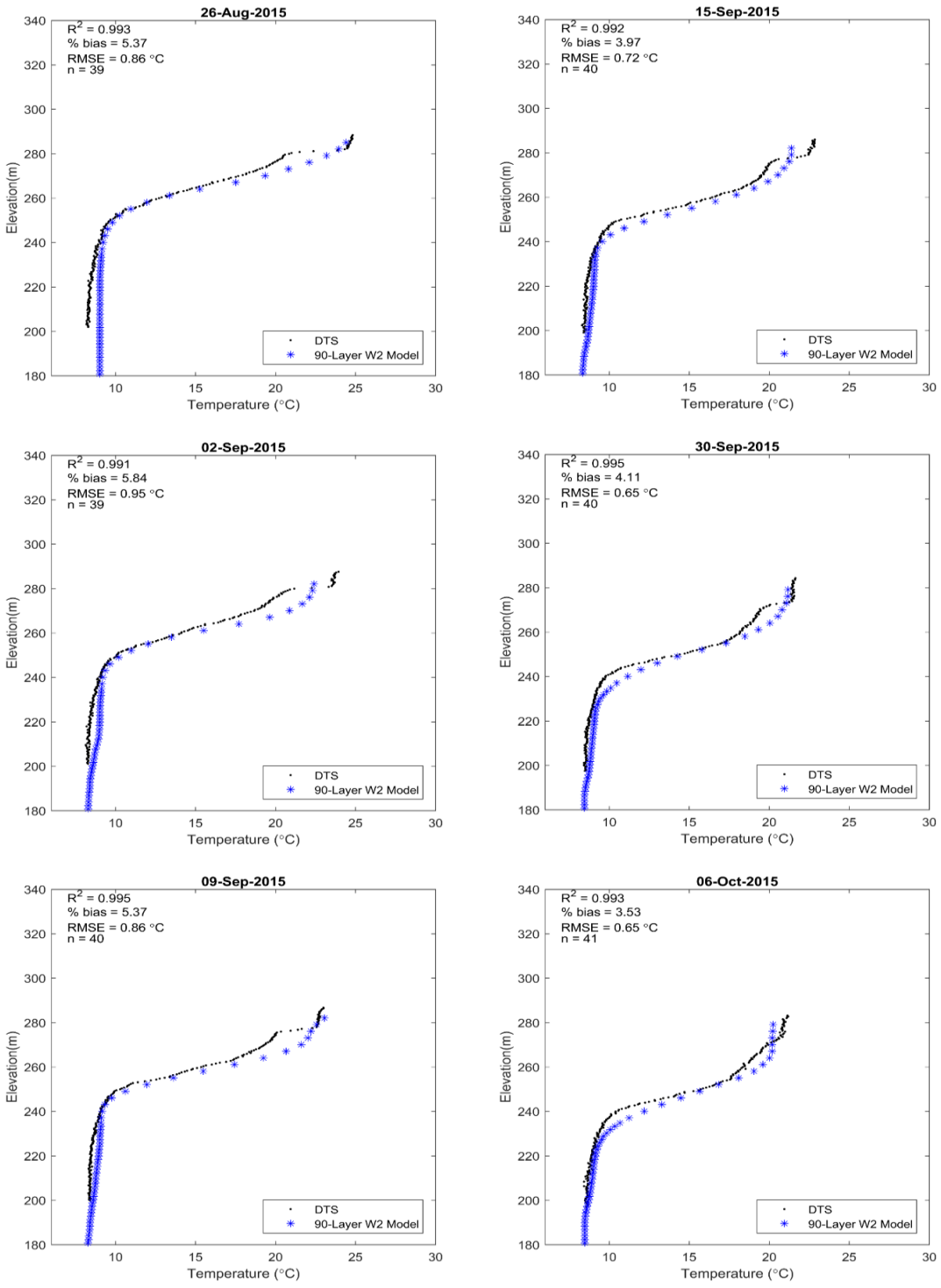

Figure 17. DTS temperature profile data just upstream of Shasta Dam compared to modeled temperature profiles for the 90-layer W2 model adjacent to the dam between August and October 2015. Positive % bias indicates warmer modeled temperatures than DTS temperatures.

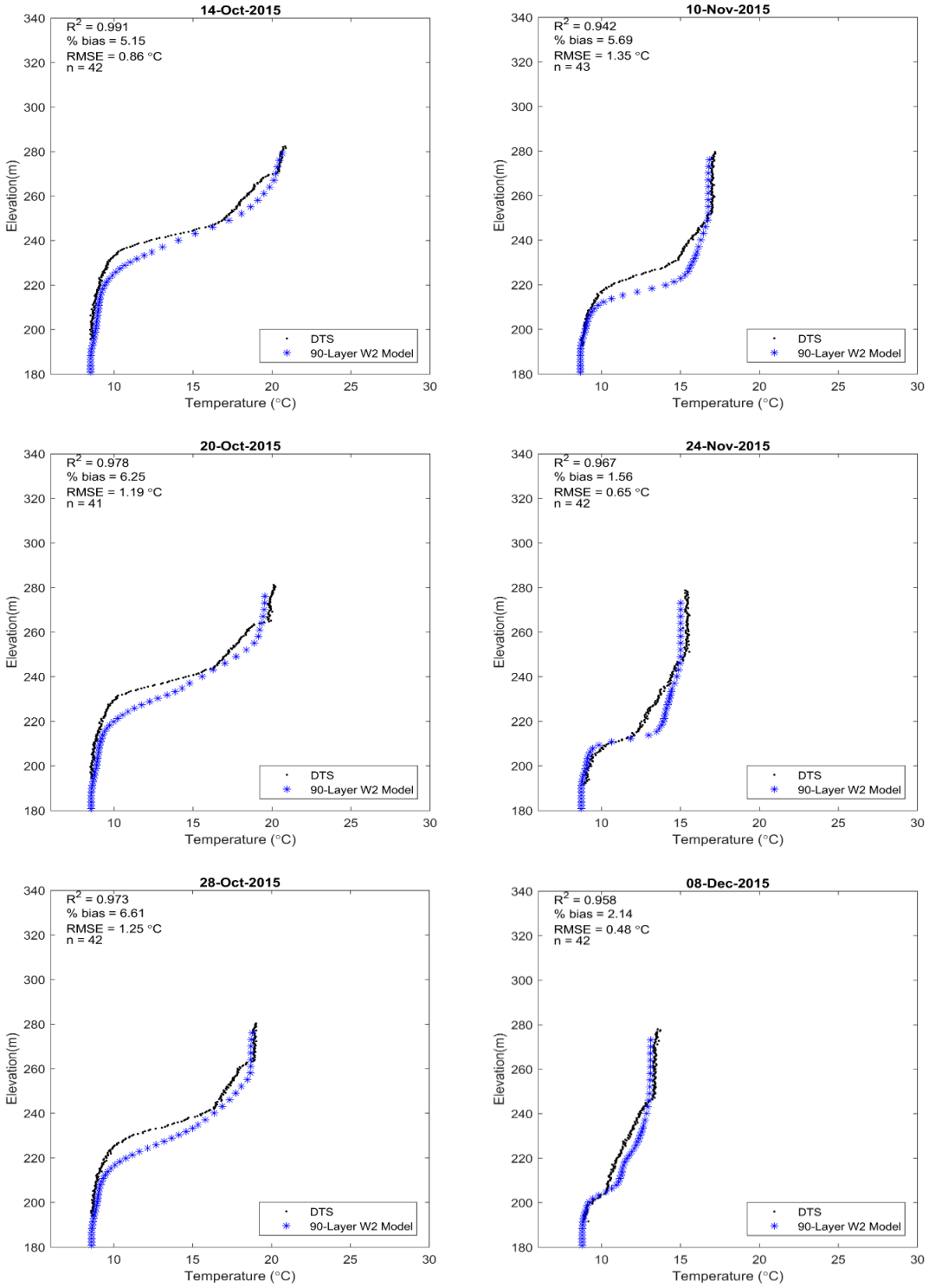

Figure 18. DTS temperature profile data just upstream of Shasta Dam compared to modeled temperature profiles for the 90-layer W2 model adjacent to the dam between October and December 2015. Positive % bias indicates warmer modeled temperatures than DTS temperatures.

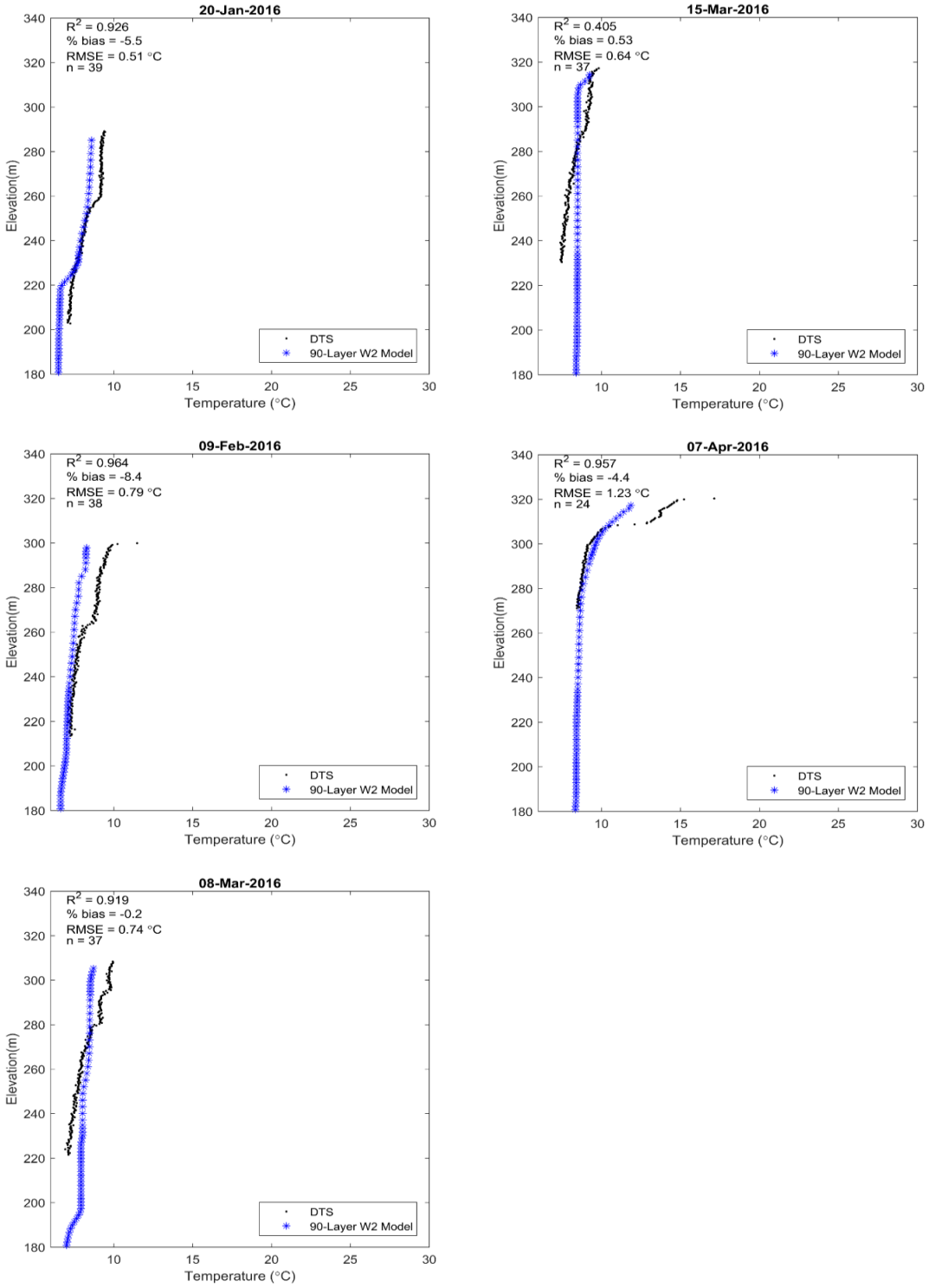

Figure 19. DTS temperature profile data just upstream of Shasta Dam compared to modeled temperature profiles for the 90-layer W2 model adjacent to the dam between January and April 2016. Positive % bias indicates warmer modeled temperatures than DTS temperatures.

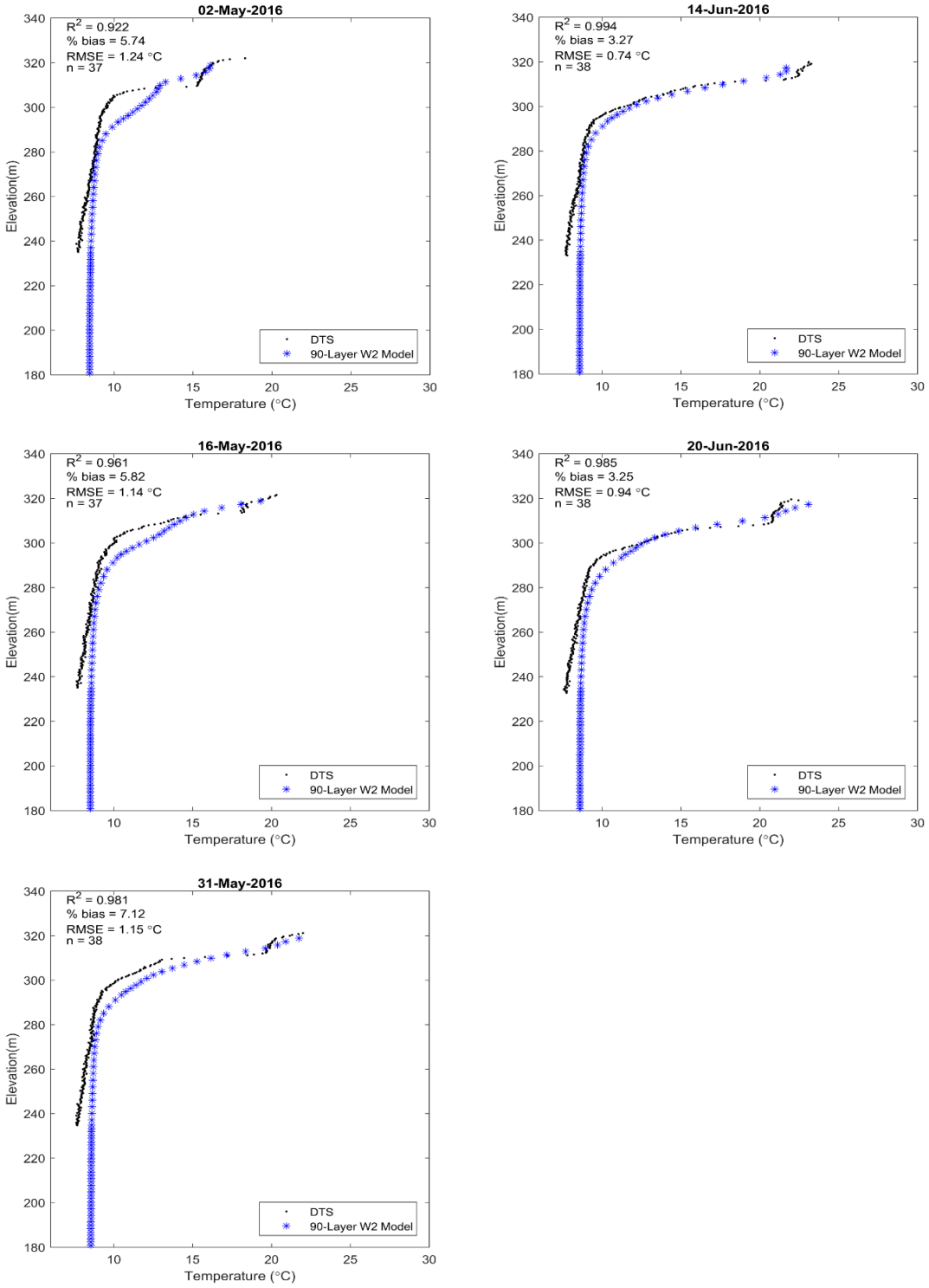

Figure 20. DTS temperature profile data just upstream of Shasta Dam compared to modeled temperature profiles for the 90-layer W2 model adjacent to the dam between May and June 2016. Positive % bias indicates warmer modeled temperatures than DTS temperatures.

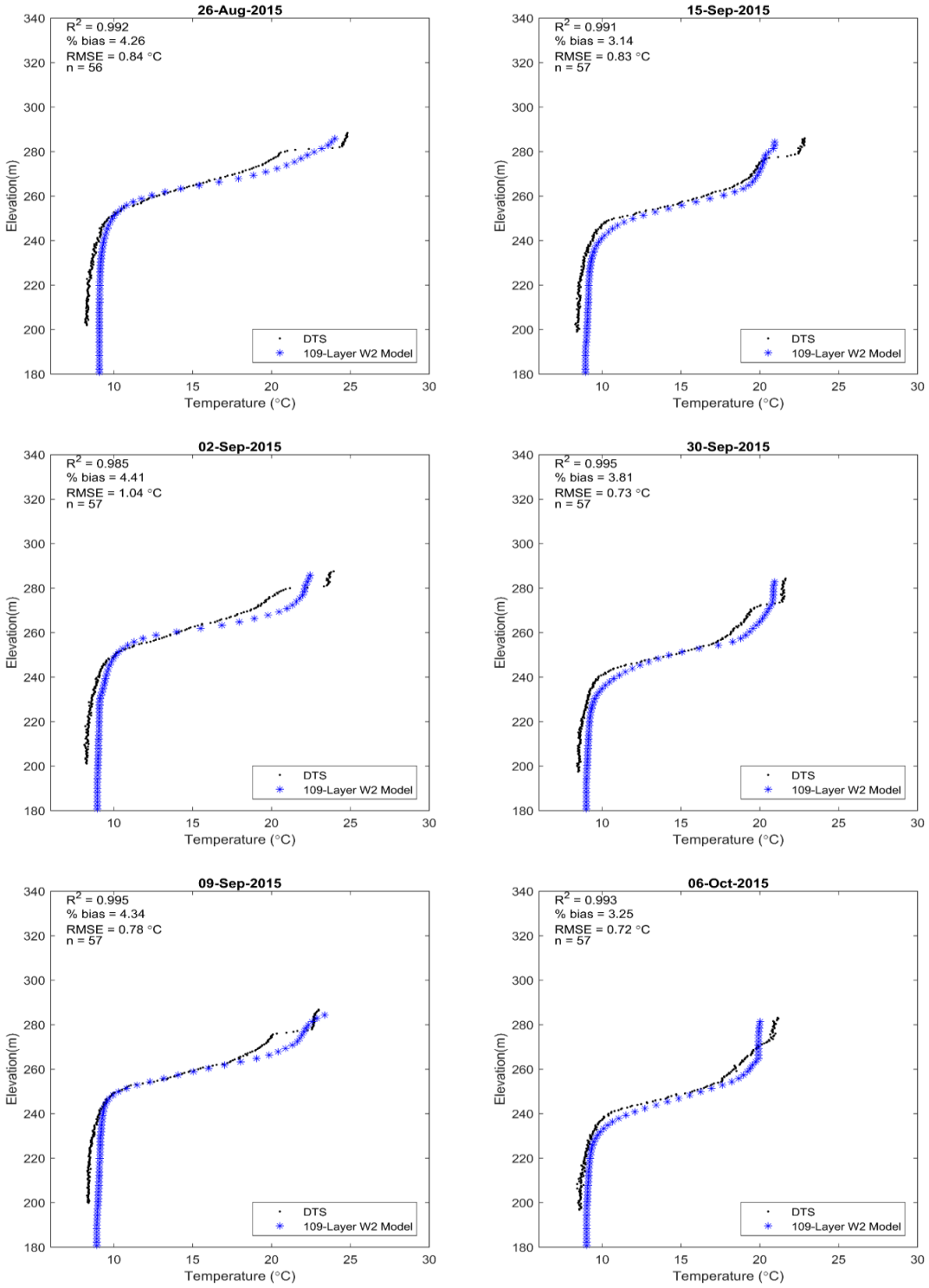

Figure 21. DTS temperature profile data just upstream of Shasta Dam compared to modeled temperature profiles for the 109-layer W2 model adjacent to the dam between August and October 2015. Positive % bias indicates warmer modeled temperatures than DTS temperatures.

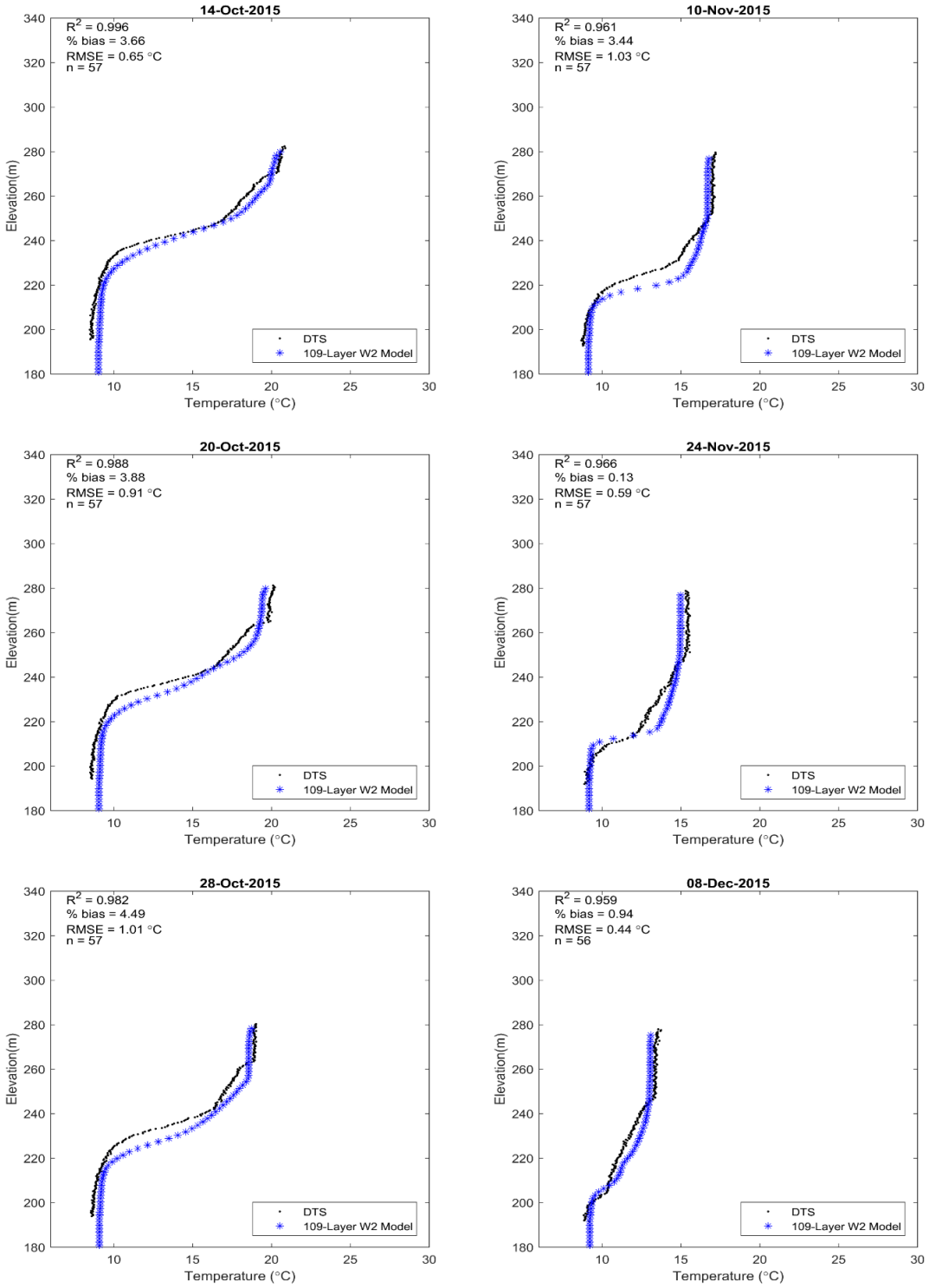

Figure 22. DTS temperature profile data just upstream of Shasta Dam compared to modeled temperature profiles for the 109-layer W2 model adjacent to the dam between October and December 2015. Positive % bias indicates warmer modeled temperatures than DTS temperatures.

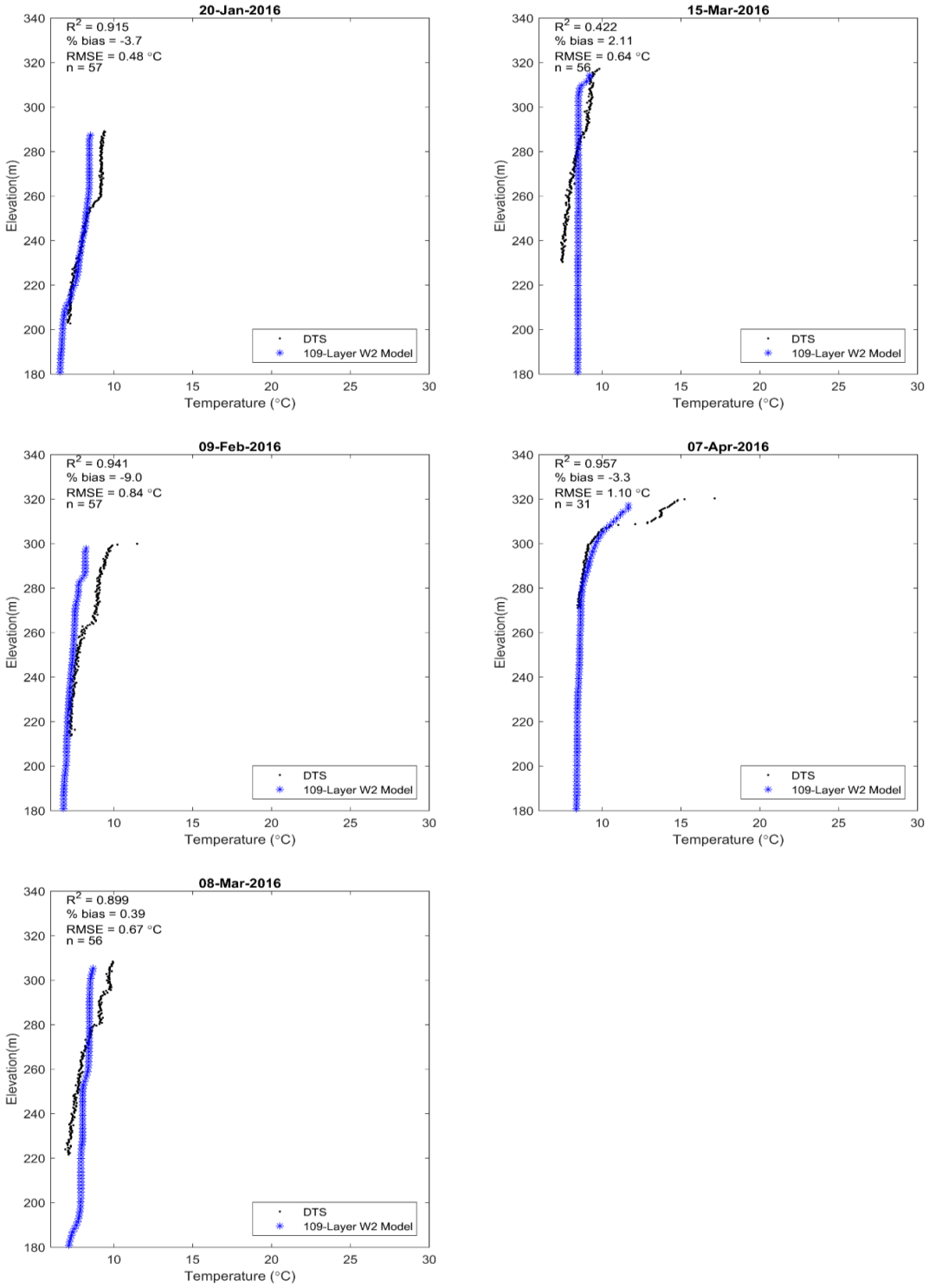

Figure 23. DTS temperature profile data just upstream of Shasta Dam compared to modeled temperature profiles for the 109-layer W2 model adjacent to the dam between January and April 2016. Positive % bias indicates warmer modeled temperatures than DTS temperatures.

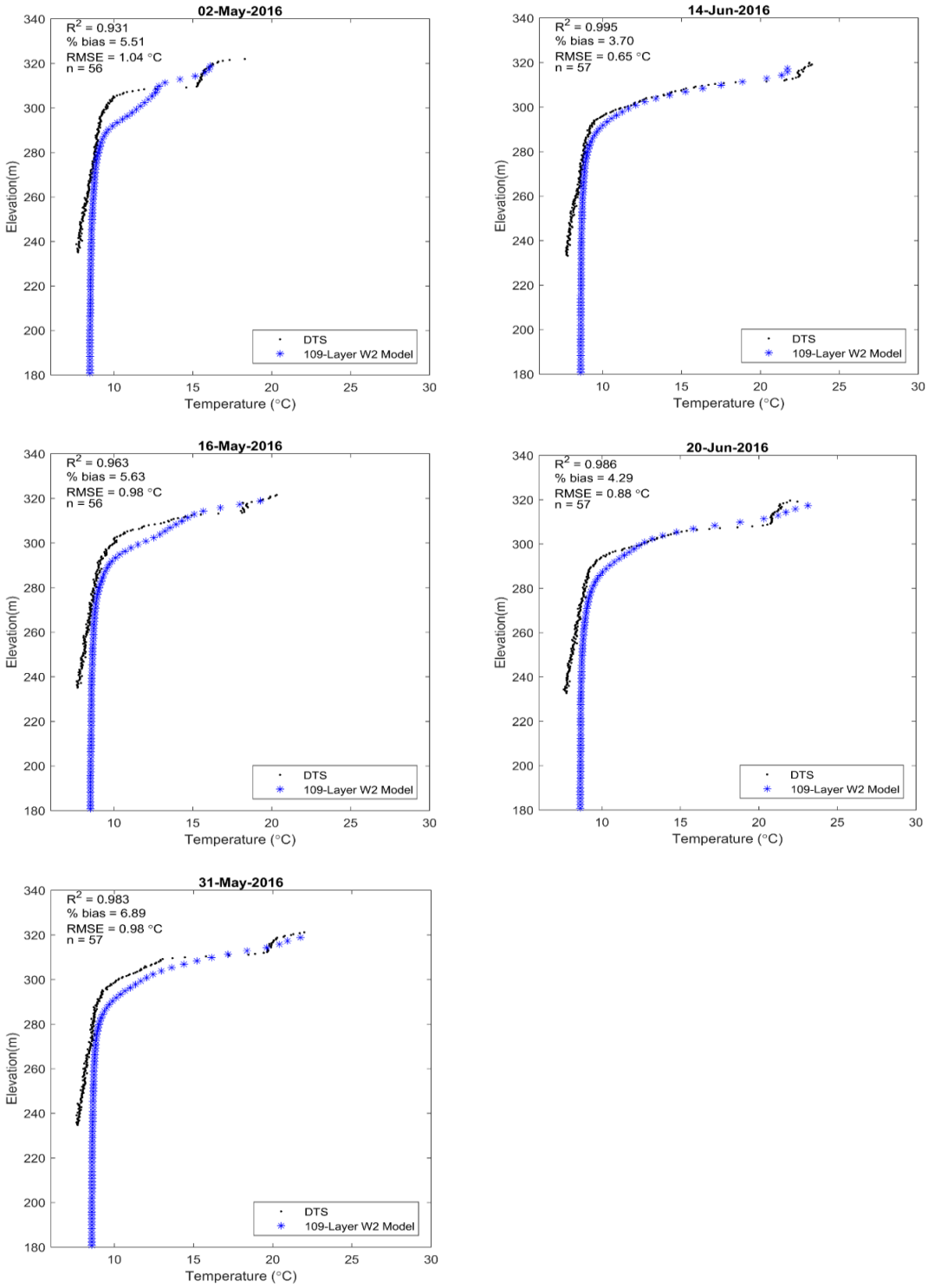

Figure 24. DTS temperature profile data just upstream of Shasta Dam compared to modeled temperature profiles for the 109-layer W2 model adjacent to the dam between May and June 2016. Positive % bias indicates warmer modeled temperatures than DTS temperatures.

The temperature difference plots generated by the MATLAB code showed relatively close temperatures between the DTS and each of the W2 models for most of the fall of 2015 and winter of 2016 (Figure 38 in Appendix J). In the fall, there appeared to be a somewhat linear threshold with elevation over time with the 60-layer W2 model and the 90-layer W2 model, where modeled temperatures were warmer than DTS temperatures in the upper part of the hypolimnion. This trend began in September and extended deeper into the reservoir through November (Figure 38a and 38b in Appendix J). The 109-layer W2 model had a similar threshold, but simulated temperatures were slightly cooler than measured DTS data (Figure 38c in Appendix J). The location of this threshold generally corresponded with plunging warm waters from the epilimnion into the hypolimnion as the reservoir thermal structure progressed towards fall turnover. During the spring of 2016, the temperature difference plot generated by the MATLAB code showed modeled hypolimnetic temperatures to be close to measured DTS temperatures, however simulated epilimnetic temperatures were up to 10°C warmer during this time (Figure 38 in Appendix J). This large difference in epilimnetic temperatures was not apparent in the raw temperature data or in individual profile plots between each of the W2 models and the DTS data (Figures 16, 20, and 24). Thus, there is likely an error in the MATLAB code itself that will be corrected in future work.

(b) Stratification patterns

The same date for the onset of stratification was estimated from the results for all three W2 models (Table 10). This date (February 12, 2016) was only two days later than the date that was estimated from the DTS data (February 10, 2016). The 60-layer W2 model, 90-layer W2 model, and 109-layer W2 model estimated the end of stratification

six, four, and eight days earlier, respectively, than estimated with the DTS data (Table 10).

Table 10. Summary of stratification patterns for the DTS data and the three W2 models for Lake Shasta.

	Start Stratification (2016)	**End Stratification (2015)**
DTS	2/10/2016	11/2/2015
60-Layer	2/12/2016	10/27/2015
90-Layer	2/12/2016	10/29/2015
109-Layer	2/12/2016	10/25/2015

(c) Cold pool storage

The cold pool volume in the reservoir calculated with the DTS data was higher than the cold pool volume estimated with the three W2 Shasta models during most of the year, particularly in the spring of 2016 (Figure 25). Exceptions to this occurred between December 2015 and mid-April 2016 when the reservoir was mostly isothermal. During that time period, the calculated cold pool with DTS temperatures fluctuated above and below modeled cold pool estimates. The 60-layer W2 model estimated lower cold pool storage than estimated cold pool from the other two W2 models and the calculated cold pool with the DTS temperatures during the fall of 2015. A sharp increase of approximately 1000 million cubic meters in cold pool storage from simulated and measured temperatures occurred in mid-December. During late March and early April 2016, the calculated cold pool with DTS temperatures dropped at the same time that simulated cold pool from all three W2 models peaked. Following this, there was a large difference in cold pool calculated from the DTS temperatures and simulated cold pool volumes by all three W2 models which continued through the months of April, May, and

June. In general, cold pool estimates from the 109-layer W2 model were closest to cold pool volume calculated from DTS temperatures (Figure 25). Estimates of both November 1, 2015 and June 1, 2016 cold pool storage with the 109-layer model were closest to DTS estimates (Table 11). The cold-pool volume estimated on November 1 with the 60-layer W2 model was the farthest from cold pool volume calculated from DTS temperatures. The estimated cold pool storage values on June 1, 2016 were the same for both the 60-layer W2 model and the 90-layer W2 model, and both values were less than the cold pool calculated with DTS data and estimated from the 109-layer W2 model.

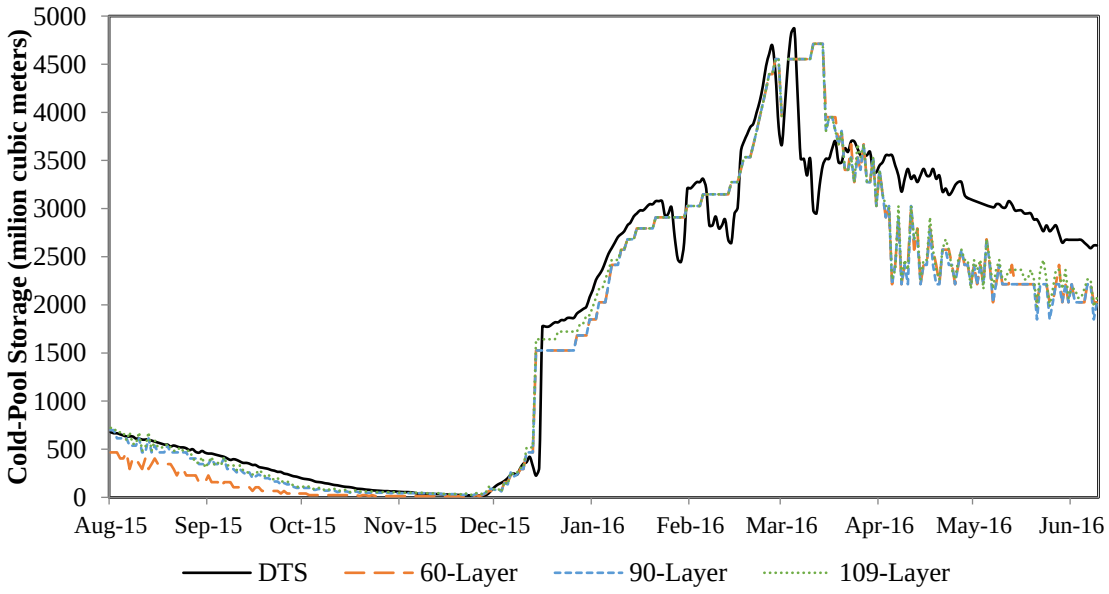

Figure 25. Cold pool storage between August 19, 2015 and June 30, 2016 calculated from measured DTS temperature profiles and simulated temperature profiles from all 3 W2 model bathymetric resolutions.

Table 11. Cold pool storage for the measured DTS data and the three W2 models of Lake Shasta. Cold pool represents the amount of water at or below 9°C.

	November 1, 2015	June 1, 2016
DTS	111.45	2981.12
60 layer	23.37	2214.51
90 layer	61.88	2214.51
109 layer	78.48	2363.48

Discussion

The 109-layer W2 model had the worst calibration statistics for 1995 of the three W2 model resolutions included in this study (Table 8), even though it simulated water temperature profiles closest to measured DTS temperature profiles for 2015-16 (Table 9). This difference in model performance could reflect different meteorology in 1995 as compared to 2015-16. The weather conditions in 1995 started as a wet year with a high starting reservoir elevation, but had low summer and fall precipitation and inflows, resulting in lower reservoir volume during the fall (Saito et al. 2001b). In contrast, 2015 was meteorologically dry, with low precipitation and inflow throughout the year, and the spring of 2016 experienced higher precipitation and tributary inflow volumes, causing the reservoir to refill rapidly (CDEC 2017). Thus, differences in performance of the different resolution W2 models may be a function of the model year's hydrology. This supports the finding of Bartholow et al. (2001) that simulated reservoir thermodynamics for the 60-layer W2 model were more sensitive to hydrology and meteorology than reservoir operations.

In addition, measured temperatures in 1995 and in 2015-16 were collected at different locations within Shasta Reservoir. In 1995, temperature profiles were collected at five locations within the reservoir that corresponded to model segments 13, 16, 19, 41,

and 53/54 on several dates throughout the year. In 2015-16, measured temperature profiles were only available adjacent to the dam at a location corresponding to model segment 21. No measured temperature profiles were taken in the tributaries during 2015-16, so comparisons of water temperatures in model segments 13, 16, 41, and 53/54 could not be made. Model segment 19 is the closet segment to the dam with measured temperature profiles available in 1995, and is 12 meters shallower than segment 21 (Figure 12). Thus, the better statistics for 2015-16 compared to the statistics for 1995 for the 109-layer W2 model could be due to the model's ability to represent water temperatures in segment 21 versus segment 19 or the rest of the reservoir .

During the fall of 2015, the 60-layer W2 model simulated temperatures in the metalimnion and upper hypolimnion that were warmer than temperatures measured by the DTS, which supports results from model simulations completed by Boegman et al. (2001), in which hypolimnetic temperatures were over-predicted by a CE-QUAL-W2 model of Lake Erie. Boegman et al. (2001) also found that the model failed to reproduce a distinct thermocline during stratification in the central basin of the reservoir, which was attributed to the coarse model layer resolution. Similarly, the coarse 60-layer W2 model resolution could have contributed to the shallower temperature gradient simulated by this model as compared to the both DTS temperature profiles and temperature profiles simulated by the two finer W2 layer resolutions in our study. The 109-layer W2 model with finer vertical grid resolution had simulated gradients in the metalimnion closest to the DTS temperature data among the three W2 models, suggesting that finer layer resolution does improve W2's ability to simulate thermal stratification.

However, the 109-layer W2 model predicted the onset of stratification eight days earlier than the date calculated from DTS data, an estimate worse than estimates made by the other two W2 models. Stratification can be shortened by large volumes of hypolimnetic withdrawals (Gelda et al. 1998). The finer discretization of the 109-layer W2 model with depth may cause TCD withdrawals from a given gate elevation to occur across a different distribution of model layers than the 60-layer W2 model and 90-layer W2 models. This could change the simulated withdrawal zone for each model, causing models with more layers to simulate more cold water volume being withdrawn from the hypolimnion, and thus simulating earlier onset of stratification.

The temperature shallower temperature gradient gradient during stratification and thickening of the metalimnion simulated by the 60-layer W2 model could be because numeric diffusion may be greater than physical diffusion in some locations within the depth profile (Boegman et al. 2001; Figures 13, 14, 17, 18, 20, and 21). In model systems with strong temperature gradients, numerical diffusion in the W2 model can overwhelm physical diffusion (Cole and Wells 2011). This problem has been observed in models of water bodies with strong stratification and horizontal advection, such as estuaries (Kurup et al. 2000). At Shasta Lake, strong thermal stratification typically occurs during the summer and into the fall (Deas and Lowney, 2000). Horizontal advection may also be present near the dam because of TCD reservoir withdrawals from different reservoir depths. Since our study compared temperature profiles near the dam where there was both strong summer stratification and possible horizontal advection during the late summer and fall of 2015, one could argue that the Shasta system meets the criteria for when numerical diffusion might overwhelm physical diffusion.

In their study, Kurup et al. (2000) found that CE-QUAL-W2 performed better in modeling the strong stratification of the Swan River Estuary in Western Australia than a TISAT model (a laterally averaged model developed for estuaries). They attributed the better performance to W2's use of the QUICKEST transport scheme, an explicit third-order horizontal/vertical transport scheme that reduces numerical diffusion better than the upwind-differencing algorithm used in TISAT (Kurup et al. 2000). Griffies et al. (2000) examined effective vertical diffusivity corresponding to numerical transport processes in a generalized ocean model and found more diffusivity on average (and thus more spurious mixing) to occur in the model with coarser vertical grid resolution. Thus, even though the three W2 models all employ the QUICKEST transport scheme, the coarser grid resolution of the 60-layer W2 model may have led to simulation of more vertical diffusion and spurious mixing that resulted in lower simulated temperature gradients in the metalimnion of the three W2 models.

Another factor that may contribute to the difference in gradient in the metalimnion simulated by the 60-layer W2 model compared to the 90-layer and 109-layer W2 models (Figures 13, 14, 17, 18, 21, and 22) is that the W2 model calculates the mixing length for turbulent eddy viscosity based on layer thickness (Cole and Wells 2011). Longer mixing lengths allow fluid parcels to remain a constant temperature for longer distances across temperature gradients before mixing with the surrounding fluid. Thus, thicker model layers may result in shallower temperature gradients because of the longer mixing lengths for eddy viscosity. This could also explain why a weaker temperature gradient was simulated by the 60-layer W2 model and 90-layer W2 model as compared to the 109-layer W2 model during stratification. The shallower gradient during

summer/fall stratification in 2015 also could have led to the simulated warmer temperatures in the upper hypolimnion the 60-layer W2 model and 90-layer W2 model than the DTS data.

Small mixing lengths for turbulent eddy viscosity for the surface 1.5 meter layer thicknesses in all three models may also explain why all three models simulated shallower penetration of warm surface temperatures during March 2015, which caused simulated temperature profiles to be a different shape than measured profiles during this time. R^2 values for mid-March for all three models were lower than those calculated for the rest of the measurement timeframe between August 2015 and June 2016, although the % bias and RMSE values were within the range of calculated values for these statistics for other dates between August 2015 and June 2016 (Tables 26, 27, and 28 in Appendix J). Warmer model temperatures were likely simulated as a result of rising air temperatures in the spring, but they only penetrated several meters into the reservoir, possibly because the small model layer thicknesses of 1.5 meters near the surface caused warm surface fluid parcels to mix more quickly with surrounding fluid, thus not allowing warm temperatures to penetrate very deeply into the reservoir. However, it is important to note that the measured DTS temperatures only varied by 1.896 °C on March 15, and thus the measured temperature profile was almost isothermal.

The ability of the W2 model to simulate cold pool volume was improved with higher bathymetric resolution, as expected. For the layer breakdown in the 60-layer W2 model, the cold pool threshold temperature of 9°C fell into the 6-meter layer depth range beginning in early fall of 2015 and extended through January 2016. For example, the 9°C contour dropped down into the 6-meter model resolution range in the early fall of 2015,

and stayed there until January 2016 (Figure 8). Thus, during this time period, cold pool volume calculations made with the original 60-layer W2 model have coarse resolution. For example, the storage difference between the top (235.56 meters) and bottom (229.56 meters) of layer 50 (the shallowest 6 meter layer) is approximately 80 million cubic meters. However, a 1.5 meter thick layer in this location would result in a storage difference between the top (235.56 meters) and bottom (234.06 meters) of the layer of approximately 20 million cubic meters. Therefore, a model resolution of 1.5 meters at the cold-pool transition may reduce the uncertainty associated with cold pool volume, particularly during years when the reservoir is low, such as 2015.

Several physical explanations exist for the patterns observed in the measured and estimated cold pool storage throughout the year. First, the sudden increase in both calculated cold pool from DTS temperatures and simulated cold pool from modeled temperatures that occurred in late December coincided with a change in reservoir operations from discharges made through the side gate (elevation of 228.6 m) to discharges made through the lower gate (elevation of 243.84 m). Reservoir withdrawals from the side gate promote mixing by depleting cold water from the reservoir at depth and pulling warm epilimnetic temperatures downward. This can cause stratification to break down earlier in the year (Gelda et al. 1998), and cold pool volume to be reduced more rapidly than in systems without hypolimnetic withdrawal structures (Nickel et al. 2004). Once the side gate closed on December 15th, 2015 and withdrawals were shifted higher in the reservoir profile, warm temperatures were no longer pulled down in the reservoir's depth profile and the cold pool volume rebounded. Cooler air temperatures in December associated with the winter season also promoted isothermal conditions (Deas

and Lowney 2000) that correspond to the rebound in cold pool observed in late December.

Secondly, the smaller DTS-calculated cold pool that occurred in late March while the simulated cold pool from all three models was the greatest may be partially explained by a DTS cable malfunction. On March 17, 2016, a cable inspection was performed in which the portion of the cable suspended from the farthest exclusion zone buoy (i.e,. the vertical profile section) was pulled out of the water and examined for kinks. After this date, temperature profiles from the DTS vertical section exhibited a mirror pattern, suggesting that the cable was hung up on a foreign object in the reservoir and no longer hanging vertically. Temperatures decreased from the reservoir surface to approximately halfway down the vertical section, at which point temperatures began to increase back to water surface temperatures. It is likely that when the vertical section of cable was dropped into the reservoir after inspection, the end caught on something submerged in the reservoir (such as another buoy anchor chain, submerged debris, or on itself). The DTS data were processed to discard temperatures below the point at which temperatures began to increase abnormally. However, if the cable was caught in such a way that it descended at an angle into the reservoir, the temperatures recorded on the upper section of cable (which were kept and used in this study) may have been skewed slightly warmer than those that would be expected if the cable extended vertically into the reservoir as assumed. The cable was caught for approximately 1 month, and following this time it detached on its own and returned to hanging vertically in the reservoir as it had originally.

Changes to the DTS installation at Shasta Lake could improve the calibration of the DTS temperature dataset and the comparisons made between measured DTS temperatures and the W2 models of Shasta discussed in this study. Ideally, two independent calibration temperatures would exist along the vertical section of the fiber optic cable in the reservoir. In this study, we used sonde data taken every few weeks for these two calibration points. However, measurements that have the same temporal resolution as the DTS data would reduce any error associated with holding calibration parameters constant between sonde measurements. Fixing several independent temperature sensors along the cable in the vertical profile could address this issue. Calibrated temperature profiles from the DTS were consistently colder than temperatures measured by the sonde every few weeks between August 2015 and June 2016, resulting in positive average calibration % bias of 3.880. The implication for this study is that if comparisons were made using simulated temperatures from the three W2 models of Shasta against sonde temperature profiles instead of DTS temperature profiles, positive % bias would have been reduced and negative % bias would have increased. However, average calibration R^2 was 0.996 and average RMSE was 0.587°C for the DTS versus sonde temperature profiles, demonstrating that the shape and magnitude of DTS temperature measurements were very close to sonde temperature profiles. Any differences in results that may have occurred from comparing simulated temperatures to the sonde temperatures instead of the DTS temperatures would likely not change the findings of this study.

A consideration for all three bathymetric resolutions in this study is that the bathymetry of the Shasta Lake W2 was based on topographic maps of the area before

Shasta Dam was constructed in 1945 (Bartholow et al. 2001). Thus, over seventy years of erosive processes and sediment deposition may have changed the bathymetry from the topography prior to reservoir impoundment. A current bathymetric survey of Lake Shasta would reveal any changes in the topography of the reservoir bottom. Model error associated with unknown changes in reservoir bathymetry could then be addressed by modifying the Shasta Lake W2 model bathymetry file to reflect such changes.

Finally, the overall importance of model scale must be scrutinized for this study. It is important to consider whether or not higher discretization along the depth profile of the Shasta Reservoir W2 model provides better representation of the system. For example, some hydrology and ecology models have been shown to represent certain systems better with large spatial scales rather than with fine ones (Constanza and Sklar 1985; Warwick 1989). However, considering that the 109-layer model did simulate the thermal stratification of Shasta Reservoir and estimate cold pool volume closer to the DTS data, higher vertical discretization within the W2 model's depth profile does appear to provide better representation of thermal profile of Shasta Reservoir.

Conclusions

This study evaluated the performance of three different bathymetric model resolutions on the performance of the Lake Shasta W2 model with high resolution DTS temperature data with specific focus on cold pool volume estimates. Key findings from this study include: (1) the higher vertical layer resolution provided by the 109-layer W2 model improved W2's ability to simulate thermal stratification in 2015-16 and capture the temperature gradient in the metalimnion during stratification, (2) the higher vertical layer resolution provided by the 109-layer W2 model also improved W2's ability to estimate

cold pool volume for 2015-16, and (3) DTS technology provided a useful dataset for comparison between estimated cold pool volumes from the three W2 models of Shasta Lake with different bathymetric resolutions, and aided assessment of a higher vertical discretization of the Shasta Lake W2 model. The higher resolution 109-layer W2 model developed in this study may be helpful in developing late summer and fall TCD operations based on cold pool volume targets set to help ensure cold discharges are available for downstream salmon thermal habitat.

Acknowledgements

This project was funded by the U.S. Bureau of Reclamation and National Oceanic and Atmospheric Administration. We thank Tracy Vermeyen, June Borgwat, Paul Zedonis, and Janet Martin of the U.S. Bureau of Reclamation, Eileen Umana, Alexis Garrett, Weston Fettgather, Clement Delcourt, Theresa O'Halloran, Adrian Harpold, Katherine Clancey and Nicole Goehring from the University of Nevada Reno, Jason Caldwell from MetStat, Inc., Paula Adkins, as well as Miles Daniels, Cherisa Friedlander, Skip Bertolino, and Andrew Pike from National Oceanic and Atmospheric Administration for providing field support and insights into the project.

References

Bartholow, J. M. 2004. Modeling Chinook Salmon with SALMOD on the Sacramento River, California. Hydroecologie Appliquee 1:193–219.

Bartholow, J. M., R. B. Hanna, L. Saito, D. Lieberman, and M. Horn. 2001. Simulated limnological effects of the Shasta Lake temperature control device. Environmental Management 27:609–626.

Boegman, L., M. R. Loewen, P. F. Hamblin, and D. a Culver. 2001. Application of a two-dimensional hydrodynamic reservoir model to Lake Erie. Canadian Journal of Fisheries and Aquatic Sciences 58:858–869.

Brekke, L. D., E. P. Maurer, J. D. Anderson, M. D. Dettinger, E. S. Townsley, A.

Harrison, and T. Pruitt. 2009. Assessing reservoir operations risk under climate change. Water Resources Research 45:1–16.

Brown, L. E., D. M. Hannah, and A. M. Milner. 2005. Spatial and temporal water column and streambed temperature dynamics within an alpine catchment: Implications for benthic communities. Hydrological Processes 19:1585–1610.

CDEC, California Data Exchange Center, C. 2017. Shasta Dam (USBR) (SHA). Date Accessed: May 15 2017. https://cdec.water.ca.gov/.

Clancey, K., L. Saito, K. Hellmann, C. Svoboda, J. Hannon, and R. Bechwith. (in press. Evaluating head-of-reservoir water temperature for juvenile Chinook Salmon and Steelhead at Shasta Lake with modeled temperature curtains. Accepted to North American Journal of Fisheries Management.

Cole, T., and S. Wells. 2011. CE-QUAL-W2: A two-dimensional, laterally averaged, hydrodynamic and water quality model, version 3.7. User Manual. Instruction Report EL-11-1. US Army Corps of Engineers, Washington (DC).

Constanza, R. and F. H. Sklar. 1985. Articulation, accuracy, and effectiveness of mathematical-models – a review of fresh-water applications. Ecological Modelling 27 (1-2):45-68.

CTEMPS, Center for Transformative Environmental Monitoring Programs. 2015. ctemps.org. Date Accessed: June 15 2016.

Deas, M. L., and C. L. Lowney. 2000. Water Temperature Modeling Review. Bay Delta Modeling Forum.

Ellis, C. R., H. G. Stefan, and R. Gu. 1991. Water temperature dynamics and heat transfer beneath the ice cover of a lake. Limnology & Oceanography 36:324–334.

Gelda, R. K., E. M. Owens, and S. W. Effler. 1998. Calibration, verification, and an application of a two-dimensional hydrothermal model [CE-QUAL-W2] for Cannonsville Reservoir. Lake and Reservoir Management 14:186–196.

Griffies, S. M., R. C. Pacanowski, and R. W. Hallberg. 2000. Spurious Diapycnal Mixing Associated with Advection in a z-Coordinate Ocean Model. Monthly Weather Review 128:538–564.

Griffin, D., and K. J. Anchukaitis. 2014. How unusual is the 2012 – 2014 California drought ? Geophysical Research Letters 41:9017–9023.

Hanna, R. B., L. Saito, and J. M. Bartholow. 1999. Results of Simulated Temperature Control Device Operations on In-Reservoir and Discharge Water Temperatures Using CE-QUAL-W2. Lake and Reservoir Management 15:87–102.

Hausner, M. B., F. Suárez, K. E. Glander, N. van de Giesen, J. S. Selker, and S. W. Tyler.

2011. Calibrating single-ended fiber-optic Raman spectra distributed temperature sensing data. Sensors 11:10859–79.

Hausner, M. B., K. P. Wilson, D. B. Gaines, F. Suarez, and S. W. Tyler. 2013. The shallow thermal regime of Devils Hole, Death Valley National Park. Limnology & Oceanography: Fluids & Environments 3:119–138.

Hausner, M.B. 2017. Desert Reserch Institute, Las Vegas. Personal Communication on May 4, 2017.

He, M., M. Russo, and M. Anderson. 2017. Hydroclimatic Characteristics of the 2012–2015 California Drought from an Operational Perspective. Climate 5:5.

Kobs, S., D. M. Holland, V. Zagorodnov, A. Stern, and S. W. Tyler. 2014. Novel monitoring of Antarctic ice shelf basal melting using a fiber-optic distributed temperature sensing mooring Geophysical Research Letters 41:6779–6786.

Kurup, R. G., D. P. Hamilton, and R. L. Phillips. 2000. Comparison of two 2-dimensional, laterally averaged hydrodynamic model applications to the Swan River Estuary. Mathematics and Computers in Simulation 51:627–638.

Luo, L., D. Apps, S. Arcand, H. Xu, M. Pan, and M. Hoerling. 2017. Contribution of temperature and precipitation anomalies to the California drought during 2012-2015. Geophysical Research Letters 44:3184-3192

NMFS, National Marine Fisheries Service. 2011. 5-Year Review: Summary and Evaluation of Sacramento River Winter-run Chinook Salmon ESU. Long Beach.

Nickel, D. K., M. T. Brett, and A. D. Jassby. 2004. Factors regulating Shasta Lake (California) cold water accumulation, a resource for endangered salmon conservation. Water Resources Research 40:W05204.

Robertson, D. M., and R. A. Ragotzkie. 1990. Changes in the thermal structure of moderate to large sized lakes in response to changes in air temperature. Aquatic Sciences 52:360–380.

Saito, L. 1999. Interdisciplinary Modeling at Shasta Lake. Colorado State University (Ph.D. dissertation).

Saito, L., D. G. Fontane, B. M. Johnson, and J. M. Bartholow. 2001a. Interdisciplinary modelling to assess ecosystem effects of reservoir operations. IAHS: Integrated Water Resource Management:373–378.

Saito, L., B. M. Johnson, J. M. Bartholow, and R. B. Hanna. 2001b. Assessing ecosystem effects of reservoir operations using food web-energy transfer and water quality models. Ecosystems 4:105–125.

Sapin, J. R., L. Saito, A. Dai, B. Rajagopalan, and R. B. Hanna. (2017). Demonstration of Integrated Reservoir Operations and Extreme Hydroclimate Modeling of Water Temperatures for Fish Sustainability below Shasta Lake. Journal of Water Resources Planning and Management. 143(10), 04017062. DOI:10.1061/(ASCE)WR.1943-5452.0000834.

Selker, J., N. Van De Giesen, M. Westhoff, W. Luxemburg, and M. B. Parlange. 2006a. Fiber optics opens window on stream dynamics. Geophysical Research Letters 33:L24401.

Selker, J. S., L. The, H. Huwald, A. Mallet, W. Luxemburg, N. Van De Giesen, M. Stejskal, J. Zeman, M. Westhoff, and M. B. Parlange. 2006b. Distributed fiber-optic temperature sensing for hydrologic systems. Water Resources Research 42:W12202.

Sinokrot, B. A., and H. G. Stefan. 1993. Stream temperature dynamics: Measurements and modeling. Water Resources Research 29:2299–2312.

Stene, E. A. 1996. Shasta Division: Central Valley Project. Bureau of Reclamation.

Stewart, I. T., D. R. Cayan, and M. D. Dettinger. 2004. Changes in snowmelt runoff timing in western North America under a “business as usual” climate change scenario. Climatic Change 62:217–232.

Suarez, F., J. E. Aravena, M. B. Hausner, A. E. Childress, and S. W. Tyler. 2011. Assessment of a vertical high-resolution distributed-temperature-sensing system in a shallow thermohaline environment. Hydrology and Earth System Sciences 15:1081–1093.

Tyler, S. W., J. S. Selker, M. B. Hausner, C. E. Hatch, T. Torgersen, C. E. Thodal, and S. G. Schladow. 2009. Environmental temperature sensing using Raman spectra DTS fiber-optic methods. Water Resources Research 45:W00D23.

Warwick, John J. 1989. Interplay between parameter uncertainty and model aggregation error. Water Resources Bulletin 25(2):275-283.

Chapter 4: Conclusions and Summary

Conclusions to Thesis

Reservoir managers are faced with increasingly difficult decision making in the face of warming reservoir temperatures associated with climate change, and more intense and frequent droughts, as well as increased concern with the environmental impacts of reservoir operations downstream. The drought in California between 2012 and 2015 placed a large amount of stress on endangered Chinook salmon populations in the Sacramento River, and such drought conditions may be representative of future climatic conditions. Multiple years of high air temperatures and low tributary inflows make it difficult for managers to provide cold discharge temperatures for downstream Chinook salmon, while simultaneously trying to maintain a pool of cold water within the reservoir to last through fall. Accurate representation and prediction of reservoir temperature conditions with modeled and measured data can provide assistance to managers and inform their difficult decision-making process.

The research presented in this thesis demonstrates how hydrodynamic modeling can be used to provide a picture of different operations options under drought and potential future conditions under climate change. This information may be used by managers to inform management decisions in future droughts and warmer climatic conditions. The results suggest that 2100 projected air and stream temperature increases will have negative impacts on Chinook salmon in the Sacramento River under the TCD operations schedule used in 2015. Climate change will likely increase the duration and intensity of stratification in the reservoir, and result in warmer discharge temperatures and more rapid reduction of cold pool storage in the reservoir. Reservoir operations focused on volume conservation, such as extreme reductions in discharges during the

spring when the reservoir is recharging, were shown to improve summer and discharge temperatures and cold pool volumes. However, even with extreme operations that are not feasible, discharge water temperatures did not meet desired temperature targets. Thus, these methods may not be useful for droughts lasting multiple years, when conserving water in the reservoir to provide a higher reservoir elevation at the start of the next year will be difficult, as simulations did not indicate feasible improvements to discharge temperatures or cold pool storage.

This study also demonstrated how the bathymetric resolution of hydrodynamic modeling can be improved by using high-resolution temperature measurements to inform model performance. The high temporal and spatial resolution obtained with DTS technology can both deliver information about current reservoir conditions and provide high resolution cold pool calculations in the reservoir. In this study, a comparison of DTS data with three different bathymetric model resolutions of the CE-QUAL-W2 Shasta Lake model was used to evaluate the performance of each model in simulating temperature profiles adjacent to the dam and estimating cold pool storage for the 2015/2016 period of extreme drought. The comparison suggests that the finest resolution model (i.e., the 109-layer W2 model) simulated temperature profiles adjacent to the dam and estimated cold pool volumes that compared best to DTS data. The use of DTS technology to inform hydrodynamic modeling is a new application that was shown here to be beneficial in discriminating between model resolutions.

Recommendations for Future Work

Future work may include a full-scale watershed climate model to better predict stream temperature increases under climate change to constrain tributary inflow

temperatures used in the 2100 climate change scenarios. Investigation of possible leakages within the TCD device and applying these to the W2 model will likely improve the model's ability to predict discharge temperatures at Shasta Lake. The bathymetry for all versions of the Shasta Lake W2 model used in this thesis was based on topographic maps of the area before the dam was built. Shasta Reservoir was impounded in the late 1940's, and thus the bathymetry likely has changed from the original topography due to both erosive processes and sediment deposition. An updated survey of the reservoir bathymetry would improve modifications made to the model's bathymetry file resolution.

Further investigation into the large temperature differences shown in the plots between the DTS data and each different bathymetric resolution of the Shasta Lake W2 model is needed (Figure 38 in Appendix J). As discussed in Chapter 3, the large magnitude of difference observed in these plots is likely due to an error in the MATLAB code used to generate them. Thus, future work must focus on finding and addressing any errors in the code that may be causing a false representation of the temperature difference between DTS and W2 temperatures in the epilimnion at Shasta in the Spring of 2015.

Additionally, calibration of the Shasta Lake W2 model relied on temperature profiles from the reservoir in 1995 before the TCD was installed. New temperature profiles in other locations within the reservoir and tributaries would allow for model calibration to a dataset representative of post-TCD conditions throughout the reservoir, and better assessment of model performance in locations other than just immediately upstream of Shasta Dam. This could be accomplished with the use of DTS technology in other locations within the reservoir, particularly at the location of tributary inflows. Finally, the DTS temperature data could be calibrated with finer precision if a permanent

calibration temperature sensor was installed at the bottom of the fiber optic cable. Real-time representation of the thermal profile could be accomplished by having remote access to this third calibration point, and would provide reservoir managers with a high-resolution picture of the temperature dynamics within the reservoir throughout the day.

Appendix A. Calibration and Validation Lake Shasta W2 model

Table 12: Calibrated values of the wind sheltering coefficient (WSC), coefficient of bottom heat exchange (CBHE), temperature of the sediments (TSED), and light extinction coefficients (EXH2O and BETA) for the Shasta Lake W2 model (Hanna et al. 1999).

WSC	CBHE ($m^{0.5}$ sec^{-1})	TSED (°C)	EXH2O (m^{-1})	BETA
1.0	7.0 E-8	15.9	0.40	0.45

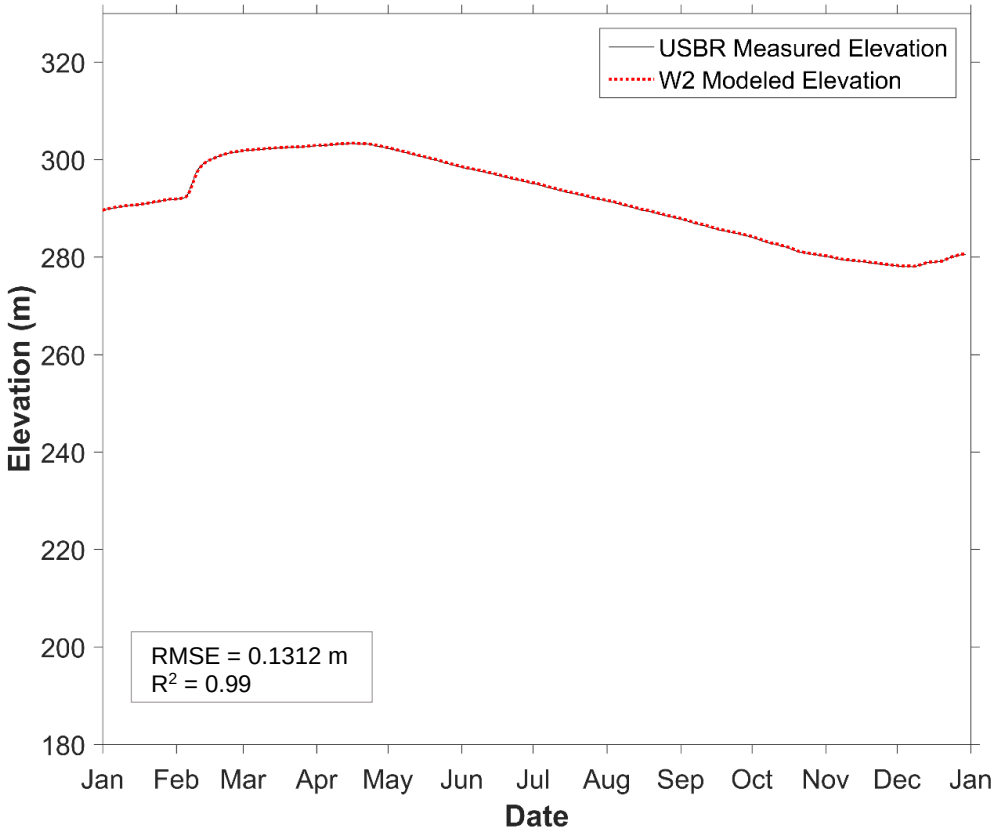

.

Figure 26. W2 modeled reservoir elevation and USBR measured elevation throughout 2015. Comparison had an RMSE of 0.1312 meters and R^2 value of 0.99.

Table 13: Statistics for temperature profile comparisons between USBR measured sonde profiles and W2 segment 21 output temperature profiles for 2015.

Date	R-Squared	% Bias	RMSE (°C)	Number of Observations
8/26/2015	0.995	0.028	0.537	13
9/2/2015	0.991	-0.812	0.717	13
9/9/2015	0.989	-1.482	0.847	13
9/15/2015	0.988	-0.703	1.047	13
9/30/2015	0.976	-3.324	1.203	12
10/6/2015	0.967	-4.494	1.406	12
10/14/2015	0.958	-5.420	1.632	12
10/20/2015	0.950	-5.174	1.711	12
10/28/2015	0.949	-5.042	1.617	12
11/10/2015	0.915	-4.109	1.541	12
11/24/2015	0.919	-3.378	1.051	10
12/8/2015	0.952	-0.801	0.534	11
Average	**0.962**	**-2.893**	**1.154**	

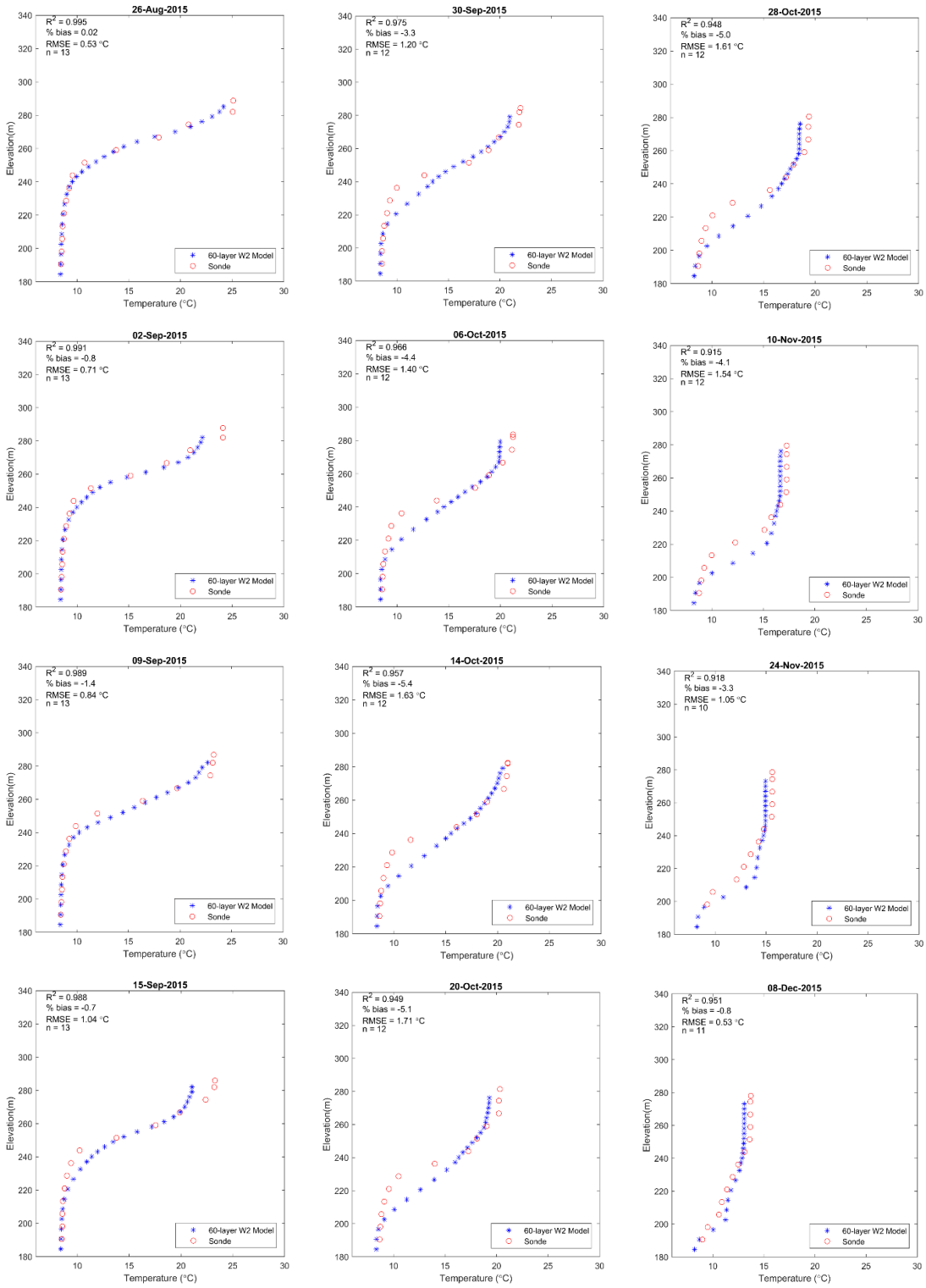

Figure 27. Reservoir temperature profile comparisons for twelve days during fall 2015.

Appendix B. Air and stream temperatures for 2100 emissions

Table 14: Projected monthly air temperature increases for 2100 for a low carbon emissions estimate and a high carbon emissions estimate (California Climate Change Center 2012).

Scenario	Jan	Feb	Mar	Apr	May	June	July	Aug	Sept	Oct	Nov	Dec
Low Emissions (℃)	1.6	1.7	1.9	2.5	3.1	3.3	3.3	3.3	3.1	2.5	1.9	1.7
High Emissions (℃)	2.6	2.8	3.1	3.6	4.2	4.4	4.8	4.4	4.2	3.6	3.1	2.8

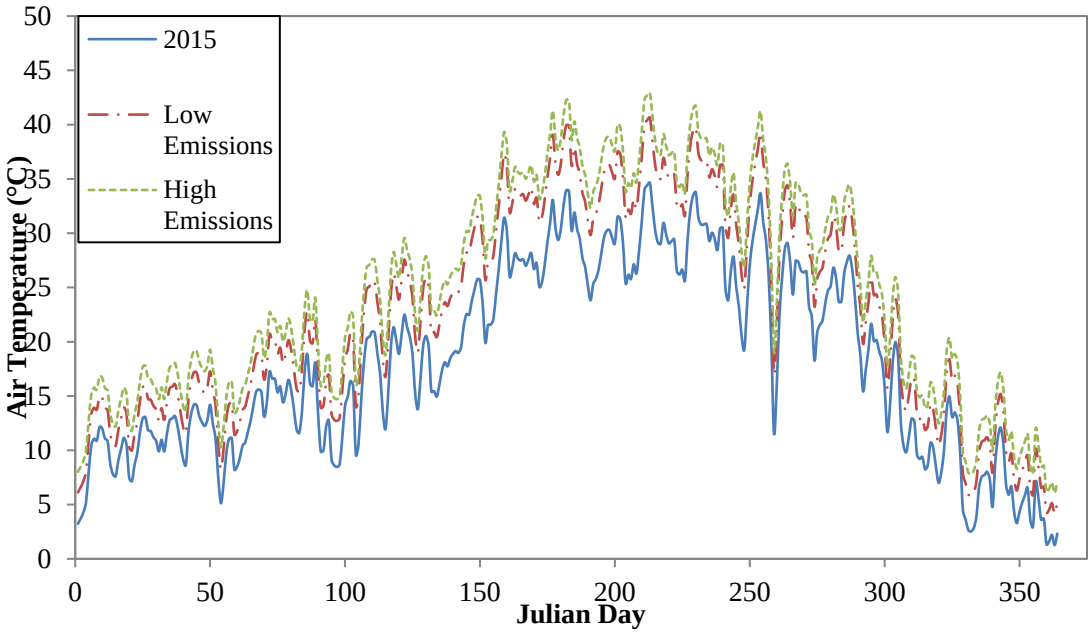

Figure 28. Air temperatures used for 2015 and climate change simulations.

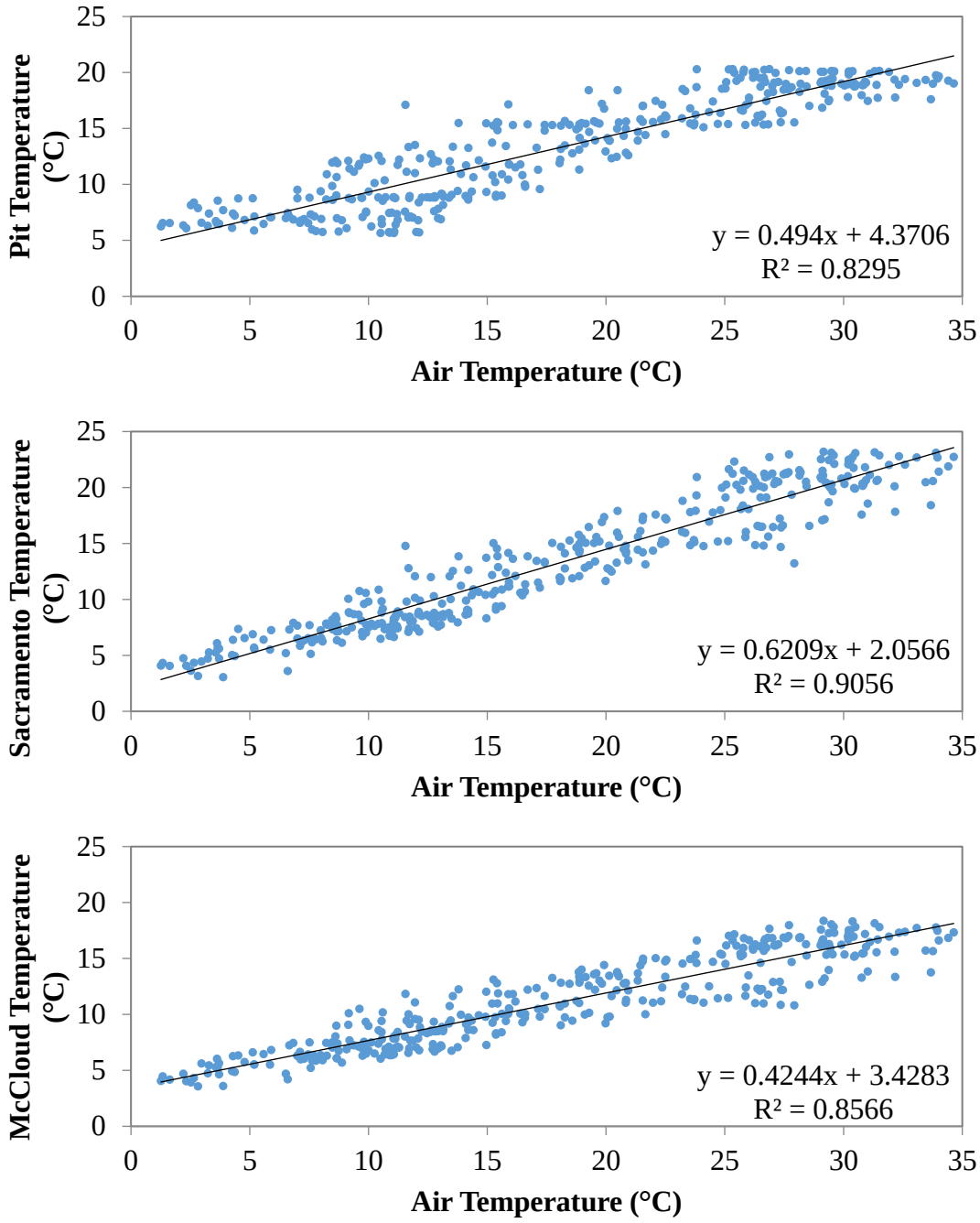

Figure 29. Linear regression relationships between 2015 air temperatures and stream temperatures for the Pit, Sacramento, and McCloud Rivers.

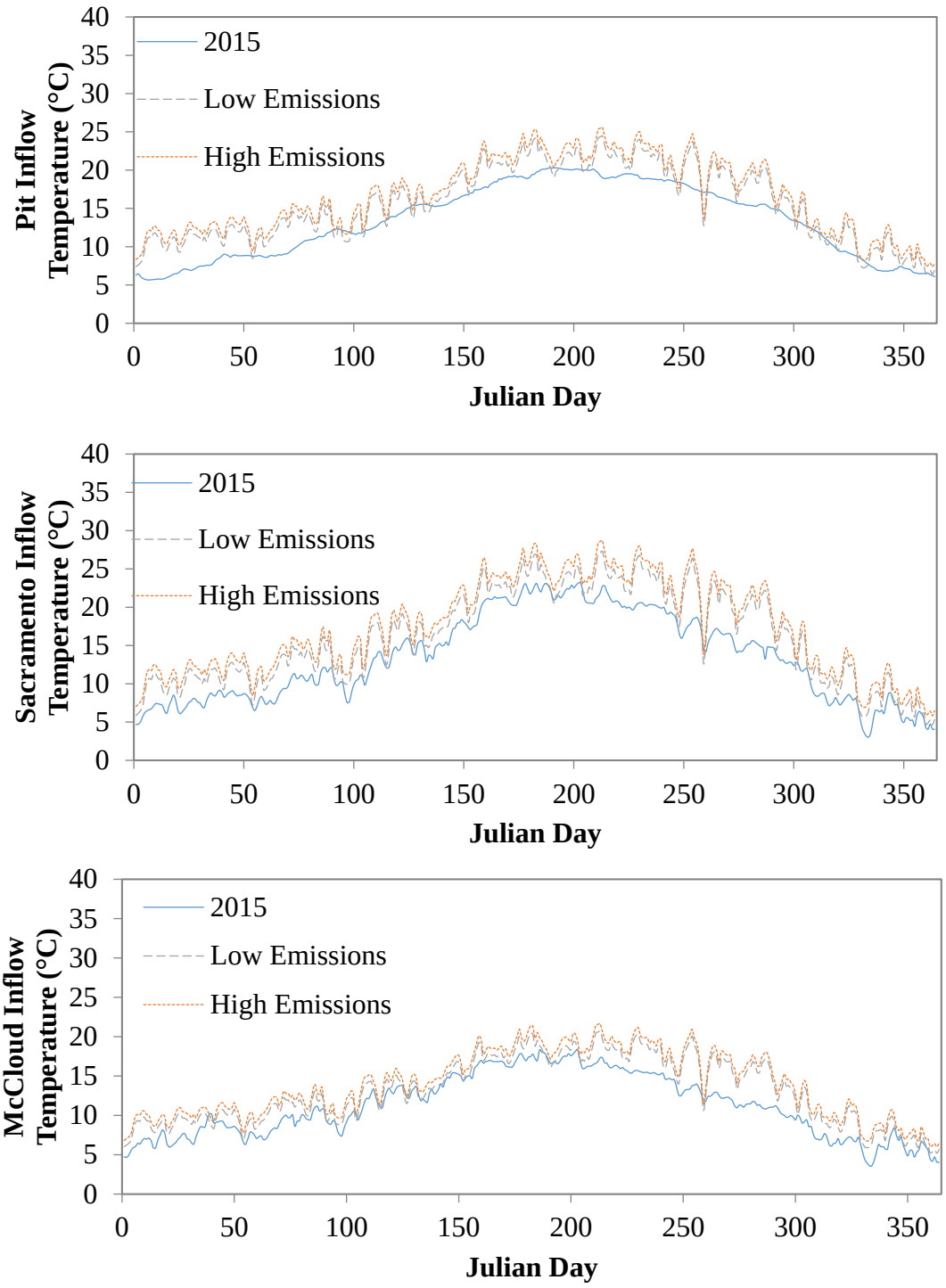

Figure 30. Calculated inflow temperatures for the Pit, Sacramento, and McCloud Rivers to Lake Shasta.

Appendix C. Additional model scenario information

Table 15: Five different climate change scenarios modeled in CE-QUAL-W2 for B1 low emissions (LE) and A2 high emissions (HE) air and stream temperatures.

Simulation	Air Temperature			Stream Temperature		
	2015	LE	HE	2015	LE	HE
2015	✓			✓		
2100 LE Air		✓		✓		
2100 LE Air + Stream		✓			✓	
2100 HE Air			✓	✓		
2100 HE Air + Stream			✓			✓

Table 16: Summary of operations scenarios that focus on reducing reservoir outflow volumes between May 1 and June 30, 2015

Operations Scenario	Percent Reduction of Reservoir Outflow
Control	None
1	10%
2	20%
3	30%
4	40%
5	50%
6	60%
7	70%
8	80%
9	90%
10	100% - No Releases

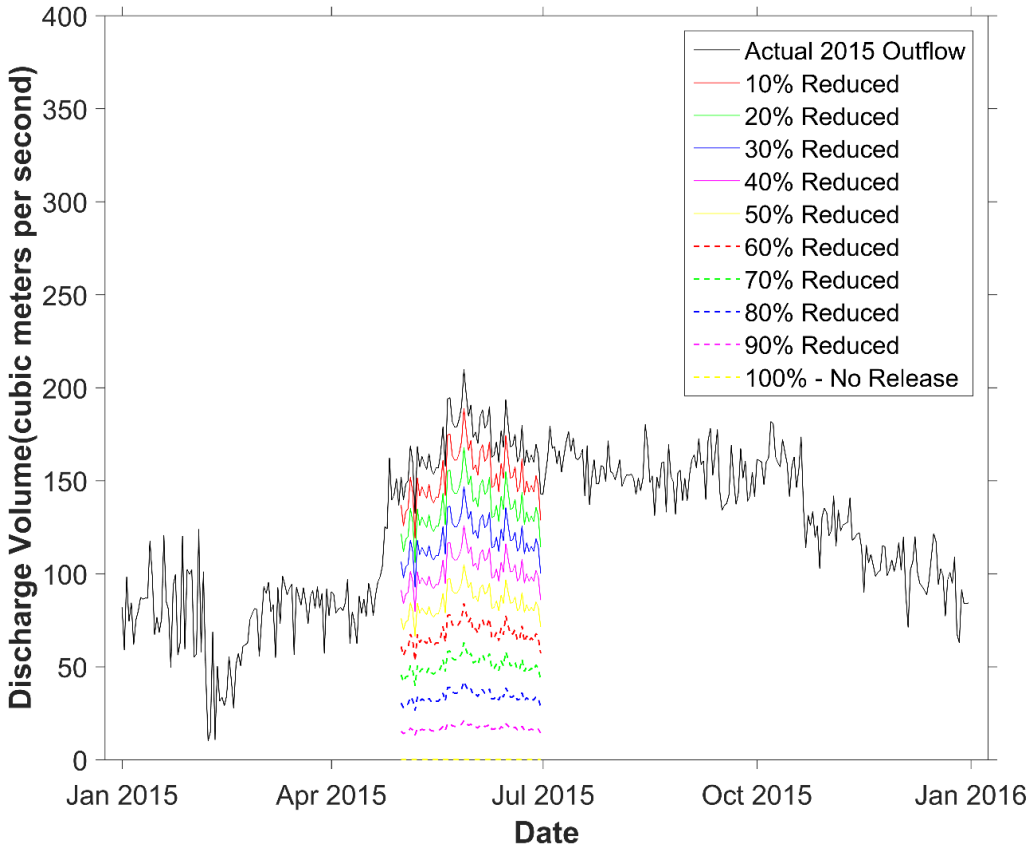

Figure 31. Shasta Reservoir releases for calendar year 2015 and the modeled volume reductions.

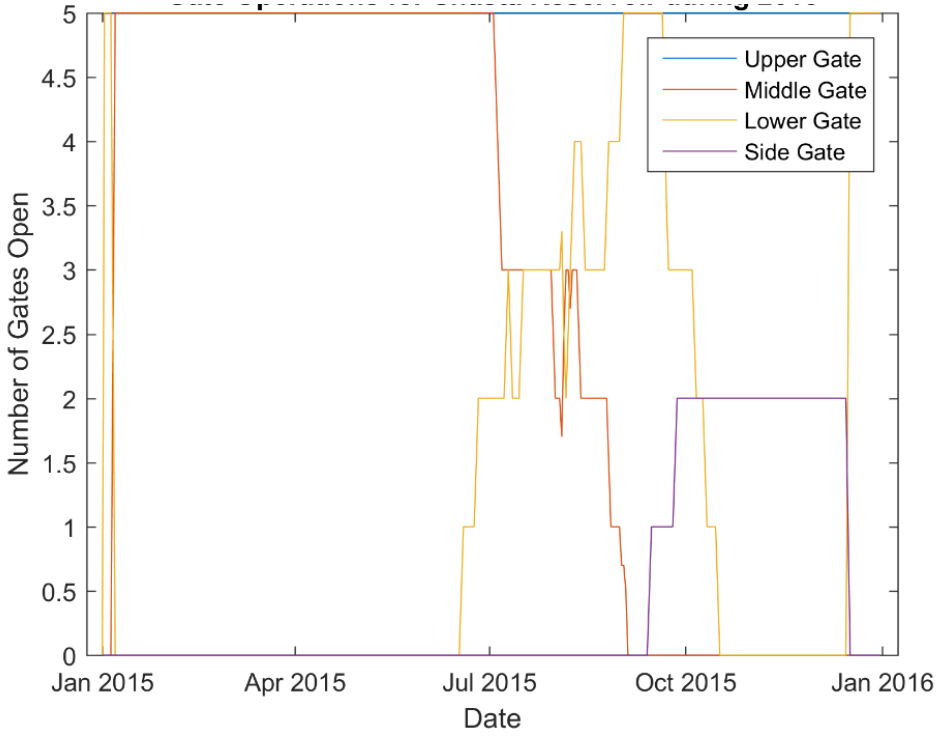

Figure 32. Actual gate operations performed during 2015.

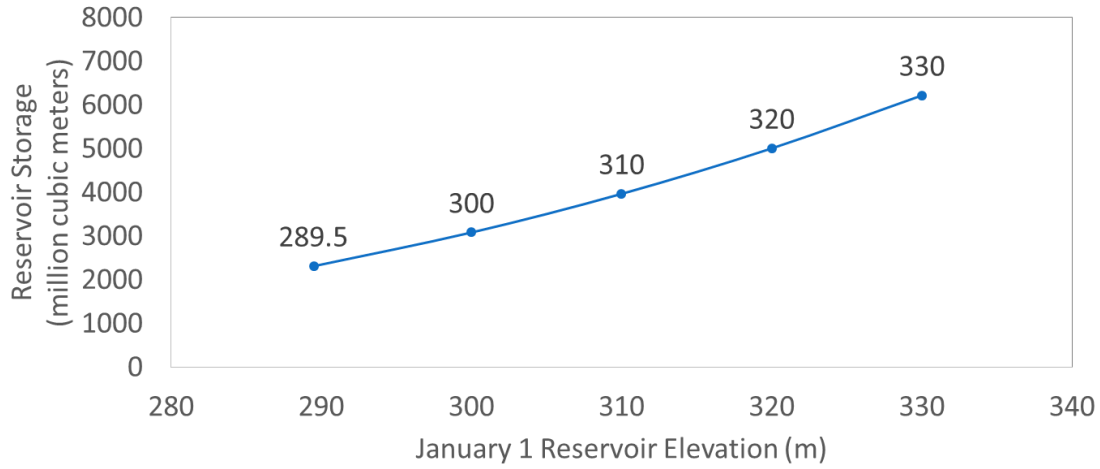

Figure 33. Summary of operations scenarios that increase the elevation of the reservoir on January 1, 2015. Note that 289.5 meters was the actual January 1 reservoir elevation for 2015.

Appendix D. Determining the appropriate No Future Action CALSIM II simulation Tier for simulated reservoir operations scenarios.

The Future No Action CALSIM II simulations have four tiers of outflow temperature targets based on 82 years of end-of-May Shasta Reservoir storage levels (Table 17; USBR 2008). The simulated end of May storage for each reduced outflow volume operations scenario was calculated to determine the appropriate Tier temperature targets to compare to simulated reservoir discharge temperatures (Table 18). The simulated end of May storage was also calculated for each different January 1 starting reservoir elevation scenario and used to determine the appropriate tier to compare to simulated reservoir discharge temperatures (Table 19).

Table 17: Temperature targets used to assess the reduced outflow volume operations and different January 1 starting reservoir operations from the No Future Action CALSIM II simulation.

Tier	End of May Storage (million cubic meters)	Target Temperature	
		Date	Temperature °C
Tier I	< 3100	1-Jan	16
		7-Apr	12
		31-Jul	9
		7-Dec	16
Tier II	< 3500	1-Jan	16
		7-Apr	12
		7-Jul	9
		7-Dec	16
Tier III	< 4100	1-Jan	16
		7-Apr	12
		14-Jun	9
		15-Sep	7
		7-Dec	16
Tier IV	> 4100	1-Jan	16
		7-Apr	12
		10-May	9
		15-Sep	5
		7-Dec	16

Table 18. Simulated end of May Shasta Reservoir storage and the appropriate CALSIM II Tier for the reduced outflow volume operations scenarios.

Scenario	End of May Storage (million cubic meters)	CALSIM II Tier
Control	2967	Tier I
10% Reduction	3142	Tier I
20% Reduction	3188	Tier I
30% Reduction	3234	Tier I
40% Reduction	3280	Tier II
50% Reduction	3326	Tier II
60% Reduction	3372	Tier II
70% Reduction	3419	Tier II
80% Reduction	3465	Tier II
90% Reduction	3511	Tier II
100% Reduction	3557	Tier II

Table 19: Simulated end of May Shasta Reservoir storage and the appropriate CALSIM II Tier for the different January 1 reservoir elevation scenarios.

Scenario	End of May Storage (million cubic meters)	CALSIM II Tier
***289.5 m**	2967	Tier I
300 m	3736	Tier III
310 m	4621	Tier IV
320 m	5615	Tier IV
330 m	5615	Tier IV

Reference:

USBR, US Bureau of Reclamation. 2008. Biological Assessment on the Continued Long-term Operations of the Central Valley Project and the State Water Project: Bureau of Reclamation. Mid-Pacific Region. Appendix H.

Appendix E. Explanation of DTS technology

Light can be scattered in glass in three ways: Rayleigh, Brillouin, and Raman. Rayleigh, or elastic scattering, causes a glass molecule that absorbs a photon to emit a photon with the same frequency as the incident photon, and thus results in no frequency change of the reflected light. Both Brillouin and Raman are inelastic scattering. Inelastic causes a glass molecule to emit a phonon (a quantum of energy associated with vibration of a crystal lattice) at a different frequency than the incident photon. If the emitted phonon has a lower frequency than the incident photon, it is referred to as the Stokes frequency. The glass molecule is left slightly warmer. If the emitted phonon has a higher frequency than the incident photon, it is referred to as the anti-Stokes frequency and the glass molecule is left slightly cooler (Selker et al. 2006, Hausner personal communication 2017).

The DTS instrument uses Raman inelastic scattering, in which phonons are emitted with a predictable wavelength, to determine temperature along the cable. The natural log of the ratio between the power of the Stokes frequency and the power of the anti-Stokes frequency is proportional to the temperature of the glass at the location of backscatter. This relationship is because the incident photon is more likely to strike pre-excited molecules in warmer glass, (yielding anti-Stokes phonons) than in cooler glass where there are fewer pre-excited molecules to strike. Thus, the anti-Stokes scattering happens less often in cooler glass. The location of backscatter can be determined by measuring the time it takes light to travel out from the DTS instrument to a given molecule and return (Selker et al. 2006, Hausner personal communication 2017).

References:

Selker, J. S., L. The, H. Huwald, A. Mallet, W. Luxemburg, N. Van De Giesen, M. Stejskal, J. Zeman, M. Westhoff, and M. B. Parlange. 2006b. Distributed fiber-optic temperature sensing for hydrologic systems. Water Resources Research 42:W12202.

Hausner, M.B. 2017. Desert Reserch Institute, Las Vegas. Personal Communication on May 4, 2017.

Appendix F. DTS temperature profiles and sonde data profiles for 2015 – 2016.

Table 20. Statistics for measured sonde temperature profiles compared to the calibrated DTS temperature profiles. Positive % bias indicates warmer sonde temperatures than DTS temperatures.

Date	R-Squared	% Bias	RMSE (°C)	Number of Observations
8/26/2015	0.997	5.828	0.917	11
9/2/2015	0.997	5.495	0.862	11
9/9/2015	0.993	6.250	1.174	11
9/15/2015	0.994	5.289	1.074	12
9/30/2015	0.994	4.530	0.864	12
10/6/2015	0.996	3.321	0.672	12
10/14/2015	0.997	3.622	0.694	13
10/20/2015	0.997	4.121	0.703	11
10/28/2015	0.996	4.304	0.743	11
11/10/2015	0.994	3.071	0.564	12
11/24/2015	0.999	0.812	0.138	12
12/8/2015	0.999	2.195	0.279	11
1/20/2016	0.995	3.037	0.276	12
2/9/2016	0.998	3.877	0.339	11
3/8/2016	0.983	3.643	0.366	11
3/15/2016	0.994	4.090	0.366	11
4/7/2016	0.991	2.490	0.512	7
5/2/2016	0.999	3.109	0.357	12
5/16/2016	0.996	3.918	0.517	12
5/31/2016	0.999	5.003	0.598	12
6/14/2016	0.999	4.260	0.482	11
6/20/2016	0.998	3.096	0.409	11
Average	**0.996**	**3.880**	**0.587**	

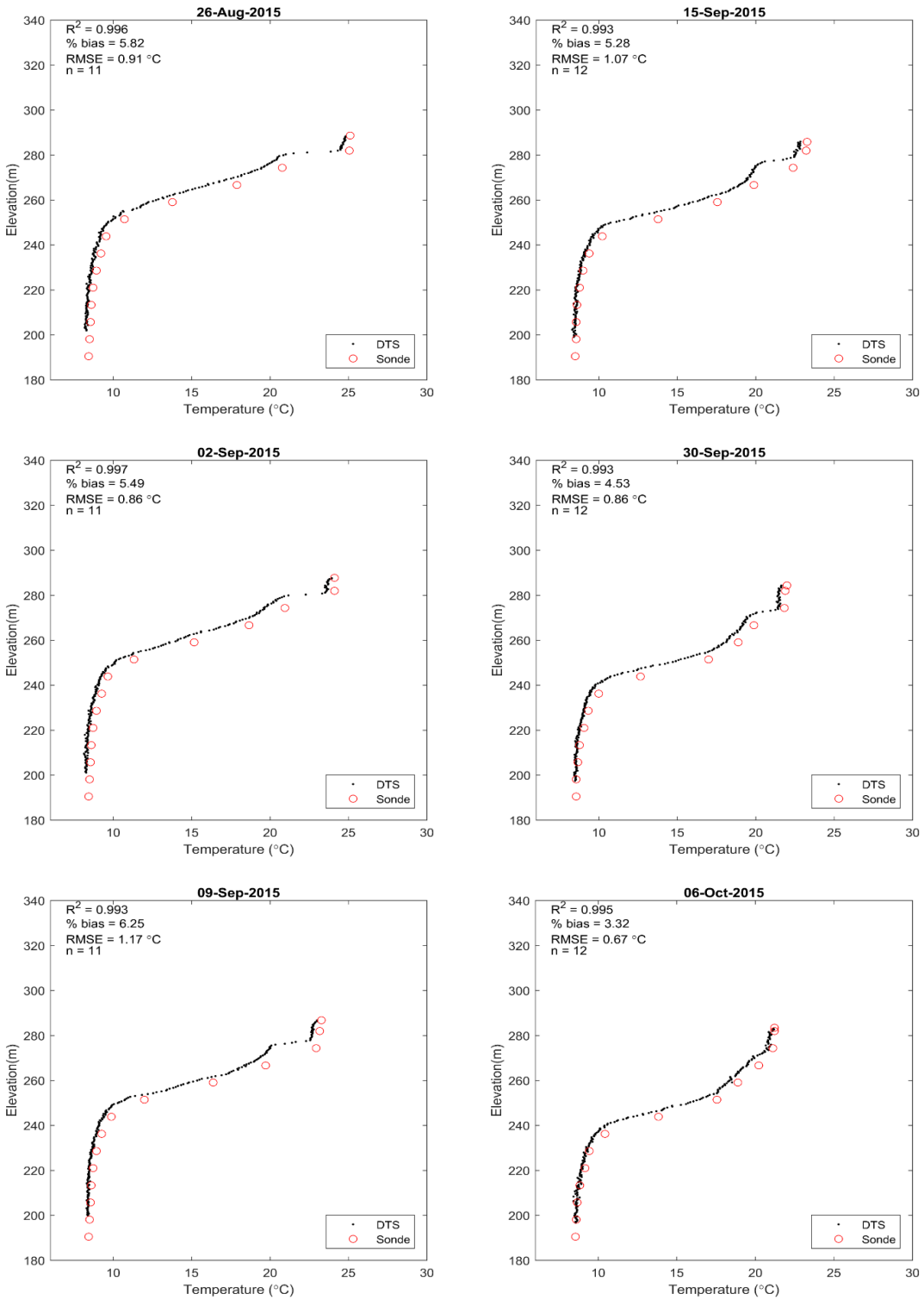

Figure 34. Distributed temperature sensing data collected just upstream of Shasta Dam plotted against sonde data profiles taken by the USBR at the same location between August and October 2015. Positive % bias indicates warmer sonde temperatures than DTS temperatures.

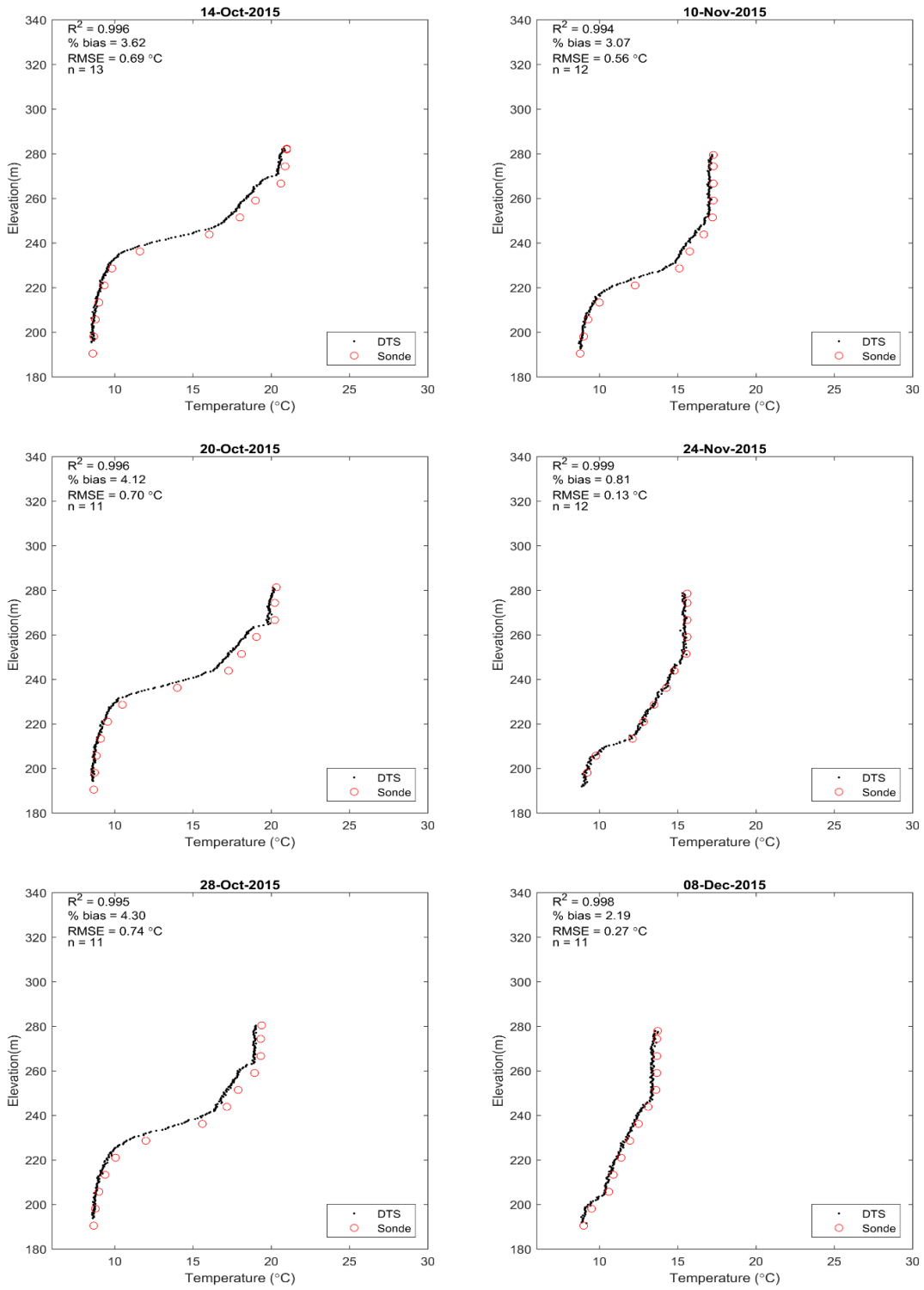

Figure 35. Distributed temperature sensing data collected just upstream of Shasta Dam plotted against sonde data profiles taken by the USBR at the same location between October and December 2015. Positive % bias indicates warmer sonde temperatures than DTS temperatures.

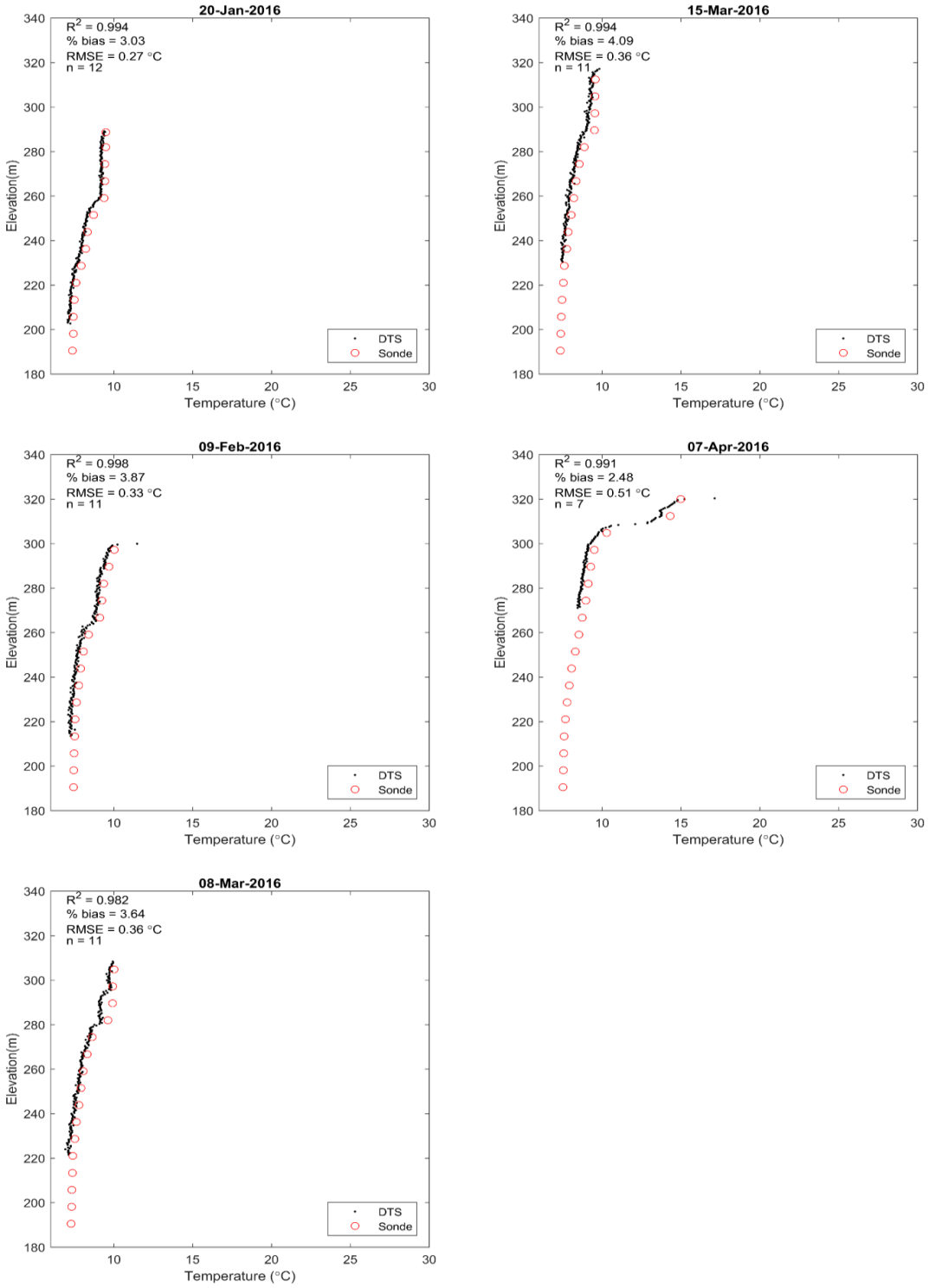

Figure 36. Distributed temperature sensing data collected just upstream of Shasta Dam plotted against sonde data profiles taken by the USBR at the same location between January and April 2016. Positive % bias indicates warmer sonde temperatures than DTS temperatures.

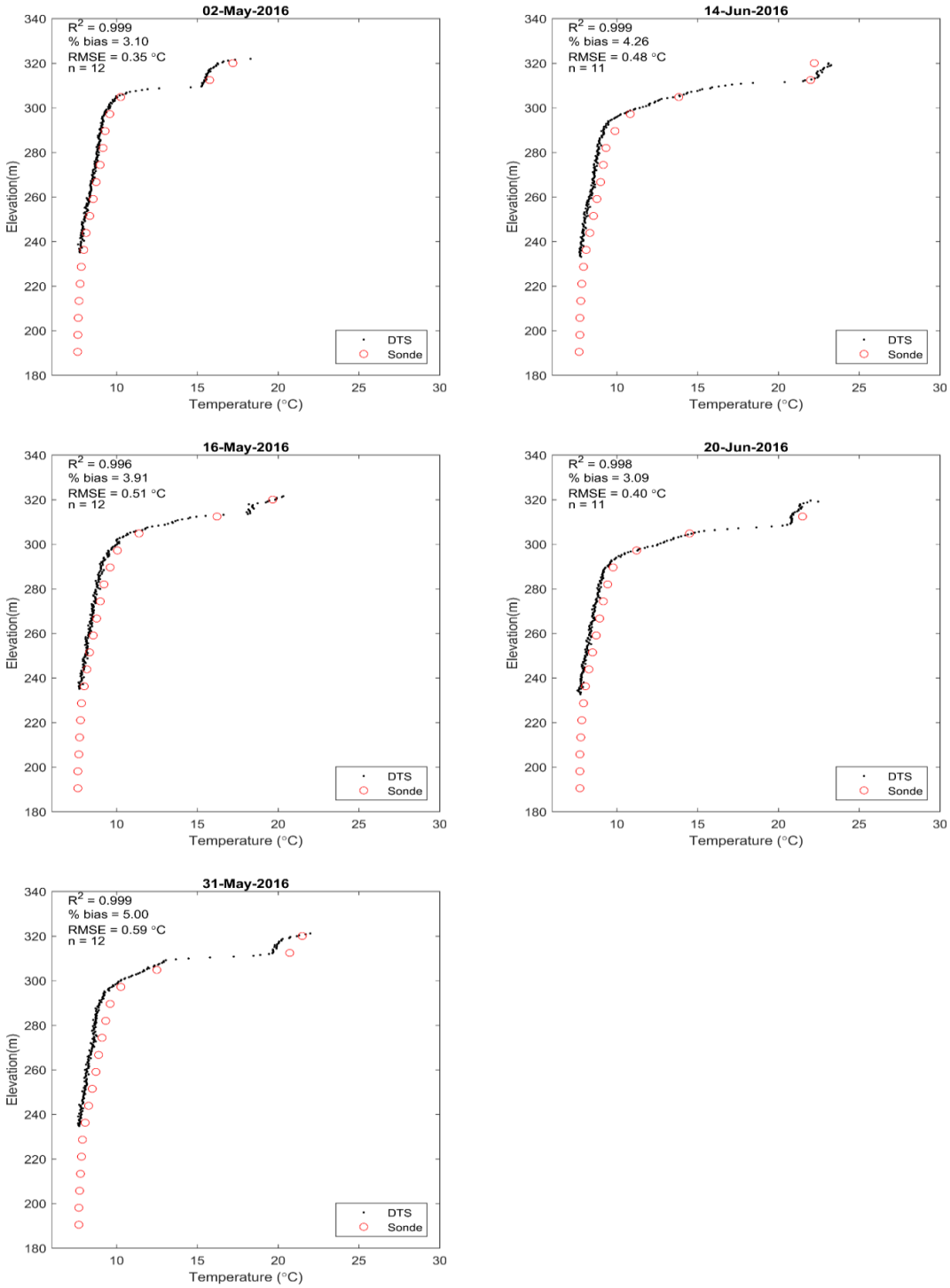

Figure 37. Distributed temperature sensing data collected just upstream of Shasta Dam plotted against sonde data profiles taken by the USBR at the same location between May and June 2016. Positive % bias indicates warmer sonde temperatures than DTS temperatures.

Appendix G. Layer depth and elevation for the CE-QUAL-W2 model of Lake Shasta

Table 21. Layer thickness and corresponding top elevation of each layer in original 60-layer CE-QUAL-W2 model.

Layer #	Layer Depth (m)	Top Elevation (m)	Layer #	Layer Depth (m)	Top Elevation (m)
1	1.5	336.81	31	3	292.56
2	1.5	335.31	32	3	289.56
3	1.5	333.81	33	3	286.56
4	1.5	332.31	34	3	283.56
5	1.5	330.81	35	3	280.56
6	1.5	329.31	36	3	277.56
7	1.5	327.81	37	3	274.56
8	1.5	326.31	38	3	271.56
9	1.5	324.81	39	3	268.56
10	1.5	323.31	40	3	265.56
11	1.5	321.81	41	3	262.56
12	1.5	320.31	42	3	259.56
13	1.5	318.81	43	3	256.56
14	1.5	317.31	44	3	253.56
15	1.5	315.81	45	3	250.56
16	1.5	314.31	46	3	247.56
17	1.5	312.81	47	3	244.56
18	1.5	311.31	48	3	241.56
19	1.5	309.81	49	3	238.56
20	1.5	308.31	50	6	235.56
21	1.5	306.81	51	6	229.56
22	1.5	305.31	52	6	223.56
23	1.5	303.81	53	6	217.56
24	1.5	302.31	54	6	211.56
25	1.5	300.81	55	6	205.56
26	1.5	299.31	56	6	199.56
27	1.5	297.81	57	6	193.56
28	1.5	296.31	58	6	187.56
29	1.5	294.81	59	6	181.56
30	1.5	293.31	60	6	175.56

Appendix H. Methods for determining CE-QUAL-W2 layer widths

Two different methods for updating the widths of each layer (i.e. length of each layer longitudinally within the reservoir) were tested on the 109-layer W2 model with 1.5-meter-deep layers: (1) linear interpolation and (2) no change from the original layer width (Table 22). The first method resulted in large deviations of the modeled reservoir volume from the USBR storage-elevation relationships (USBR 1998), with a RMSE value of approximately 50,530 million cubic meters, which is 0.73% of the full reservoir volume. The second method resulted in less deviation from the USBR storage-elevation relationships (USBR 1998), with an RMSE of 889 million cubic meters, which is only 0.01% of the total reservoir volume.

The 109-layer W2 model has more volume discrepancy than the 60-layer model because more comparison points exist. The total discrepancy and RMSE are based on the volume discrepancy between each model layer and the USBR storage-elevation curve. Thus 109 comparisons result in more total volume discrepancy than 60 comparisons. Based on these results, breaking the model layers up into smaller layers with the same total volume as the original model produced a better match to the USBR storage estimates (USBR 1998). Therefore, both the 90-layer W2 model bathymetry and the 109-layer W2 model bathymetry were updated with no width changes applied to model layers or segments. The control file and other necessary input files for CE-QUAL-W2 were modified for each bathymetric resolution to accommodate the additional layers included in the bathymetry.

Table 22. Summary of statistics comparing the USBR storage – elevation relationships for Lake Shasta with modeled storage for the 60-layer W2 model and the 109-layer W2 model with linear interpolation and no width changes.

		109-layer W2 model	
	60-layer W2 model	**Linear Interpolation**	**No Width Change**
RMSE (million cubic meters)	57	50530	889
R^2	1.00	0.999	0.999

Reference:

USBR, US Bureau of Reclamation. 1998. Shasta Dam and Reservoir Enlargement. Bureau of Reclamation. Mid-Pacific Region.

Appendix I. Calibration Statistics for W2

Table 23. Summary of statistics for the original 60-layer W2 model calibration using 1995 temperature profile data with segment 19 highlighted in grey. Segment 19 is the location of 1995 temperature measurements closest to Shasta Dam. Positive % bias indicates warmer modeled temperatures than DTS temperatures. JD stands for Julian Day.

	Segment	May JD 131	Jun JD 171	Jul JD 207	Aug JD 242	Sep JD 265	Oct JD 292	Nov JD 318	1995 all JD
RMSE (°C)	**13**	0.623	0.702	0.878	0.856	1.070	1.196	1.132	0.922
	16	0.647	0.708	0.792	0.843	1.020	1.197	1.076	0.908
	19		0.647	0.805	0.685	1.017	1.112	1.224	0.945
	41	0.512	0.916	0.699	0.883	1.151	1.285	1.087	0.964
	53/54	0.562	0.511	0.830	1.082	1.263	1.371	1.142	0.996
% Bias	**13**	5.116	3.542	0.673	-2.522	-4.208	-6.139	-4.281	-1.174
	16	5.651	2.101	-0.354	-2.110	-4.139	-6.755	-4.897	-1.810
	19		2.466	0.011	-1.744	-4.084	-6.177	-5.913	-2.656
	41	3.866	0.394	-0.106	-2.768	-5.379	-7.277	-4.823	-2.669
	53/54	3.494	-0.051	-1.720	-4.601	-5.948	-7.650	-4.961	-3.336
R-Squared	**13**	0.984	0.988	0.979	0.979	0.979	0.974	0.851	0.964
	16	0.989	0.983	0.986	0.979	0.975	0.968	0.914	0.969
	19		0.981	0.981	0.984	0.976	0.971	0.900	0.965
	41	0.982	0.966	0.991	0.981	0.975	0.990	0.866	0.968
	53/54	0.965	0.991	0.978	0.979	0.976	0.989	0.941	0.964
Number of Observations	**13**	31	32	29	25	24	25	22	188
	16	29	31	32	28	28	29	23	200
	19		32	30	24	31	31	29	177
	41	24	29	28	25	27	25	23	181
	53/54	27	30	29	25	26	24	24	185

Table 24. Summary of statistics for the 90-layer W2 model calibration using 1995 temperature profile data with segment 19 highlighted. Segment 19 is the location of 1995 temperature measurements closest to Shasta Dam. Positive % bias indicates warmer modeled temperatures than DTS temperatures.

	Segment	May JD 131	Jun JD 171	Jul JD 207	Aug JD 242	Sep JD 265	Oct JD 292	Nov JD 318	1995 all JD
RMSE (°C)	13	0.504	0.641	1.587	1.220	1.110	0.943	0.908	1.031
	16	0.572	0.591	1.540	1.168	1.056	0.972	0.869	1.030
	19		0.593	1.339	1.325	0.984	1.028	0.978	0.702
	41	0.357	0.682	1.482	1.339	1.214	1.119	0.970	1.108
	53/54	0.497	0.815	1.544	1.547	1.356	1.198	0.967	1.197
% Bias	13	2.751	0.329	-3.144	-2.699	-2.529	-3.326	-1.979	-1.663
	16	3.349	-0.380	-3.783	-2.882	-2.895	-3.826	-2.605	-2.208
	19		-0.649	-3.646	-3.945	-2.883	-4.440	-3.538	-3.228
	41	1.396	-1.184	-3.641	-3.693	-3.737	-4.483	-2.761	-2.978
	53/54	1.707	-3.236	-5.033	-4.949	-4.082	-4.419	-2.904	-3.609
R-Squared	13	0.982	0.989	0.957	0.969	0.968	0.974	0.838	0.966
	16	0.989	0.994	0.972	0.975	0.974	0.976	0.928	0.973
	19		0.982	0.974	0.973	0.982	0.985	0.951	0.974
	41	0.989	0.987	0.981	0.974	0.972	0.990	0.903	0.975
	53/54	0.972	0.988	0.977	0.973	0.963	0.981	0.930	0.968
Number of Observations	13	21	21	19	16	14	17	13	121
	16	18	19	21	15	18	20	13	124
	19		21	20	14	21	22	17	115
	41	12	17	16	16	18	17	11	107
	53/54	15	19	19	15	17	13	14	112

Table 25. Summary of statistics for the 109-layer W2 model calibration using 1995 temperature profile data with segment 19 highlighted. Segment 19 is the location of 1995 temperature measurements closest to Shasta Dam. Positive % bias indicates warmer modeled temperatures than DTS temperatures.

	Segment	May JD 131	Jun JD 171	Jul JD 207	Aug JD 242	Sep JD 265	Oct JD 292	Nov JD 318	1995 all JD
RMSE (°C)	13	0.542	0.649	1.432	2.623	0.751	2.658	2.258	1.751
	16	0.603	0.597	1.447	2.477	0.809	2.538	2.204	1.708
	19		0.585	1.116	2.721	0.827	2.332	2.179	0.702
	41	0.423	0.650	1.330	2.605	0.988	2.831	2.284	1.851
	53/54	0.482	0.760	1.404	2.222	0.754	2.824	2.414	1.728
% Bias	13	3.648	1.253	-2.762	11.653	1.349	-10.782	-12.115	-0.764
	16	4.328	0.412	-3.609	10.812	1.361	-9.680	-11.900	-1.293
	19		0.035	-2.841	12.119	1.831	-8.959	-12.517	-1.568
	41	2.545	-0.433	-3.348	11.635	0.428	-11.773	-12.519	-1.640
	53/54	2.416	-2.602	-4.910	10.599	-0.546	-12.420	-13.536	-2.732
R-Squared	13	0.984	0.990	0.963	0.911	0.987	0.932	0.971	0.888
	16	0.987	0.994	0.973	0.923	0.988	0.937	0.990	0.901
	19		0.984	0.978	0.903	0.986	0.929	0.990	0.880
	41	0.987	0.989	0.983	0.907	0.983	0.912	0.978	0.881
	53/54	0.975	0.989	0.980	0.942	0.990	0.938	0.982	0.888
Number of Observations	13	25	26	24	23	20	23	16	157
	16	22	23	25	21	25	26	17	159
	19		21	20	14	21	22	17	115
	41	16	21	20	23	25	23	15	143
	53/54	19	23	23	22	24	19	18	148

Appendix J. Statistics and figures for DTS data versus the W2 models

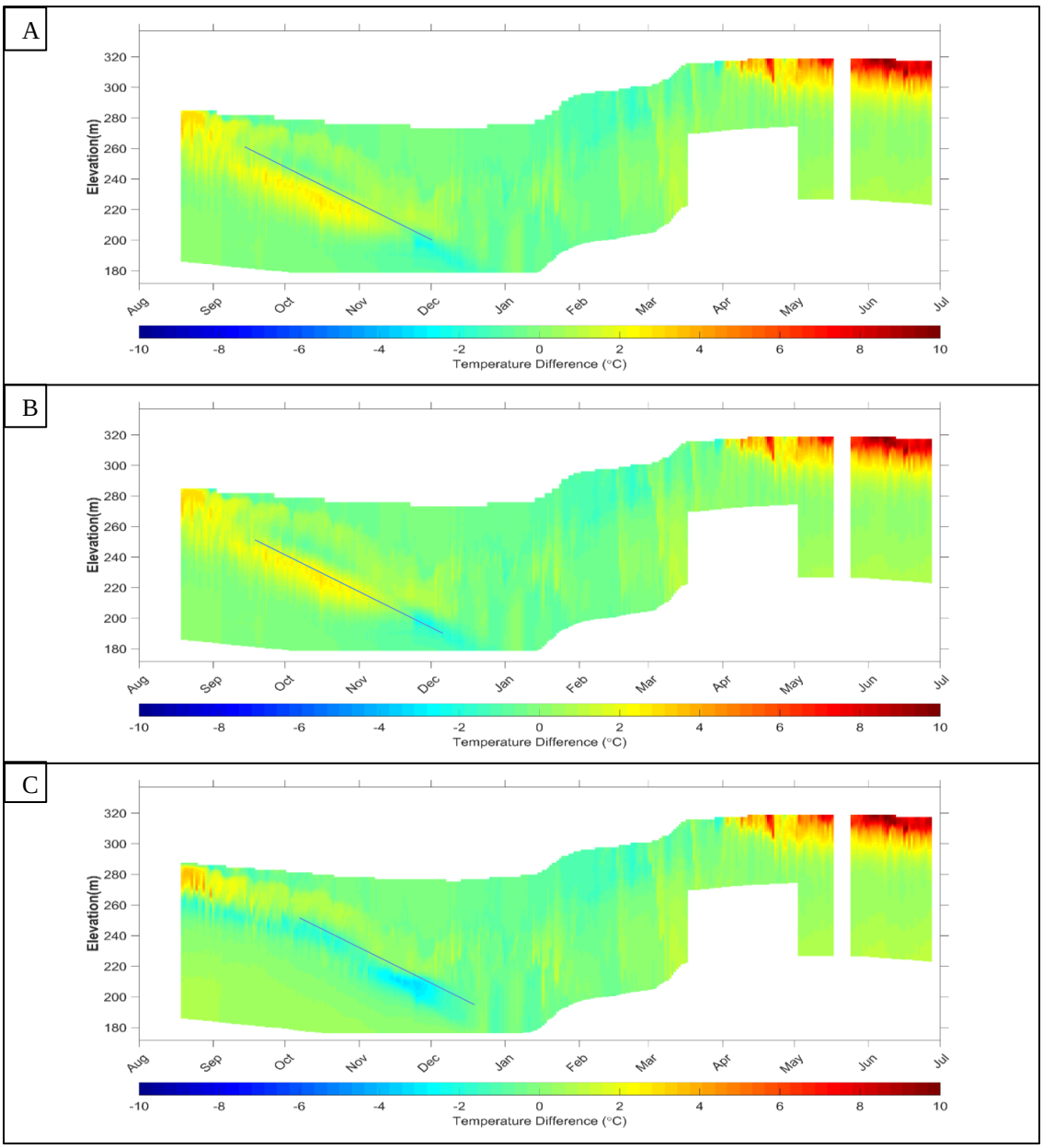

Figure 38. Temperature difference between the DTS temperatures and simulated temperatures from (A) the 60-layer W2 model, (B) the 90-layer W2 model, and (C) the 109-layer W2 model. Blue spectrum colors indicate that the modeled temperature is less than the DTS, and red/yellow spectrum colors indicate that the modeled temperature is higher than the DTS. The general location of a somewhat linear threshold where simulated temperatures deviate from DTS data for all three models is marked with a blue line.

Table 26. Statistics for measured DTS temperature profiles compared to modeled temperature profiles of segment 21 from the 60-layer W2 model. Segment 21 is the segment directly upstream of Shasta Dam. Positive % bias indicates warmer modeled temperatures than measured DTS temperatures.

Date	R-Squared	% Bias	RMSE (°C)	Number of Observations
8/26/2015	0.988	6.966	1.293	23
9/2/2015	0.984	8.028	1.465	22
9/9/2015	0.978	8.516	1.655	22
9/15/2015	0.976	7.342	1.576	22
9/30/2015	0.967	7.734	1.783	21
10/6/2015	0.955	7.308	1.895	21
10/14/2015	0.957	7.396	1.829	22
10/20/2015	0.946	6.766	1.869	21
10/28/2015	0.941	6.625	1.807	21
11/10/2015	0.885	4.665	1.662	21
11/24/2015	0.906	2.077	0.984	20
12/8/2015	0.971	1.812	0.607	20
1/20/2016	0.912	-5.669	0.546	22
2/9/2016	0.946	-11.102	0.970	27
3/8/2016	0.910	-3.067	0.752	30
3/15/2016	0.394	-0.776	0.626	35
4/7/2016	0.956	-4.775	1.224	24
5/2/2016	0.921	5.166	1.209	37
5/16/2016	0.962	5.289	1.098	37
5/31/2016	0.979	6.511	1.144	37
6/14/2016	0.992	2.463	0.736	36
6/20/2016	0.985	2.487	0.906	36
Average	**0.928**	**3.262**	**1.256**	

Table 27. Statistics for measured DTS temperature profiles compared to modeled temperature profiles of segment 21 from the 90-layer W2 model. Segment 21 is the segment directly upstream of Shasta Dam. Positive % bias indicates warmer modeled temperatures than measured DTS temperatures.

Date	R-Squared	% Bias	RMSE (°C)	Number of Observations
8/26/2015	0.993	5.371	0.870	39
9/2/2015	0.992	5.842	0.958	39
9/9/2015	0.996	5.370	0.868	40
9/15/2015	0.993	3.977	0.723	40
9/30/2015	0.996	4.111	0.651	40
10/6/2015	0.994	3.531	0.655	41
10/14/2015	0.992	5.152	0.870	42
10/20/2015	0.978	6.250	1.193	41
10/28/2015	0.973	6.611	1.257	42
11/10/2015	0.942	5.697	1.358	43
11/24/2015	0.968	1.562	0.657	42
12/8/2015	0.958	2.140	0.484	42
1/20/2016	0.926	-5.557	0.516	39
2/9/2016	0.964	-8.479	0.799	38
3/8/2016	0.919	-0.203	0.746	37
3/15/2016	0.405	0.537	0.647	37
4/7/2016	0.957	-4.418	1.232	24
5/2/2016	0.922	5.747	1.241	37
5/16/2016	0.961	5.830	1.143	37
5/31/2016	0.981	7.127	1.156	38
6/14/2016	0.994	3.277	0.745	38
6/20/2016	0.986	3.252	0.945	38
Average	**0.945**	**2.851**	**0.896**	

Table 28. Statistics for measured DTS temperature profiles compared to modeled temperature profiles of segment 21 from the 109-layer W2 model. Segment 21 is the segment directly upstream of Shasta Dam. Positive % bias indicates warmer modeled temperatures than measured DTS temperatures.

Date	R-Squared	% Bias	RMSE (°C)	Number of Observations
8/26/2015	0.992	4.262	0.846	56
9/2/2015	0.986	4.413	1.042	57
9/9/2015	0.995	4.346	0.785	57
9/15/2015	0.992	3.142	0.839	57
9/30/2015	0.995	3.814	0.732	57
10/6/2015	0.994	3.258	0.726	57
10/14/2015	0.996	3.664	0.660	57
10/20/2015	0.988	3.887	0.918	57
10/28/2015	0.983	4.500	1.016	57
11/10/2015	0.962	3.445	1.039	57
11/24/2015	0.966	0.139	0.593	57
12/8/2015	0.959	0.946	0.443	56
1/20/2016	0.916	-3.709	0.485	57
2/9/2016	0.941	-9.048	0.841	57
3/8/2016	0.900	0.394	0.679	56
3/15/2016	0.422	2.114	0.641	56
4/7/2016	0.957	-3.328	1.107	31
5/2/2016	0.932	5.512	1.041	56
5/16/2016	0.964	5.639	0.981	56
5/31/2016	0.984	6.895	0.987	57
6/14/2016	0.995	3.703	0.657	57
6/20/2016	0.986	4.300	0.885	57
Average	**0.946**	**2.377**	**0.816**	